

EDM II

— Cryogenic Approach —

Fundamental Neutron Summer School
June 16, 2015

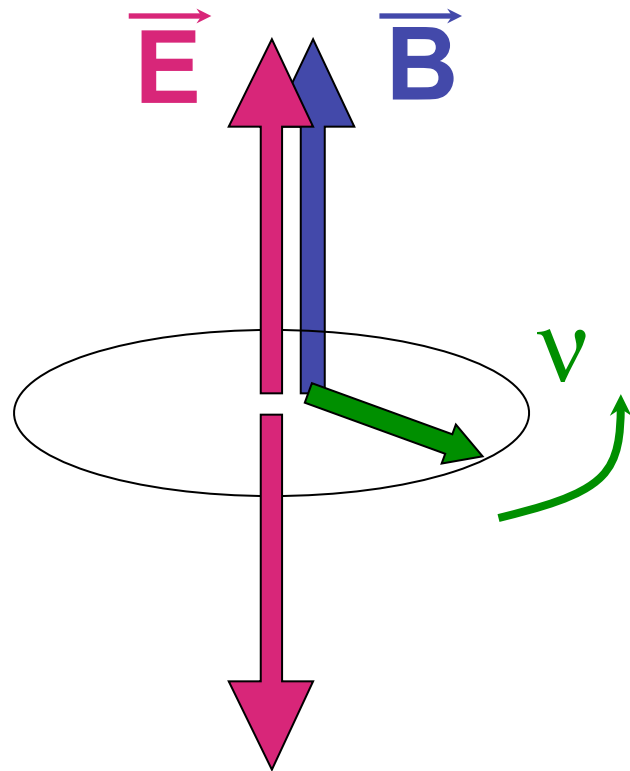
Takeyasu Ito*
Los Alamos National Laboratory

* With contributions from W. Korsch (U. Kentucky), K. Leung (NSCU), W. C. Griffith (U. Sussex)

Outline

- Why perform an nEDM experiment in LHe?
- UCN production
- UCN storage
- Electric field
- Examples
 - CryoEDM
 - New cryogenic experiment in Europe
 - SNS nEDM
- Summary

nEDM measurement principle



$$\nu = (2\mu_n B \pm 2d_n E) / h$$

$$\Delta\nu = 4d_n E / h$$

$$\delta d_n = h \frac{\delta\Delta\nu}{4E}$$

For $B \sim 10$ mG, $\nu = 30$ Hz.

For $E = 10$ kV/cm and $d_n = 3 \times 10^{-27}$ e-cm,
 $\Delta\nu = 0.03$ μ Hz. \rightarrow comagnetometer essential

For each measurement, the statistical sensitivity goes as

$$\delta d_n \propto \frac{1}{ET\sqrt{N}}$$

Sussex-ILL experiment

Baker et al. Phys. Rev. Lett. **97**, 131801 (2006).

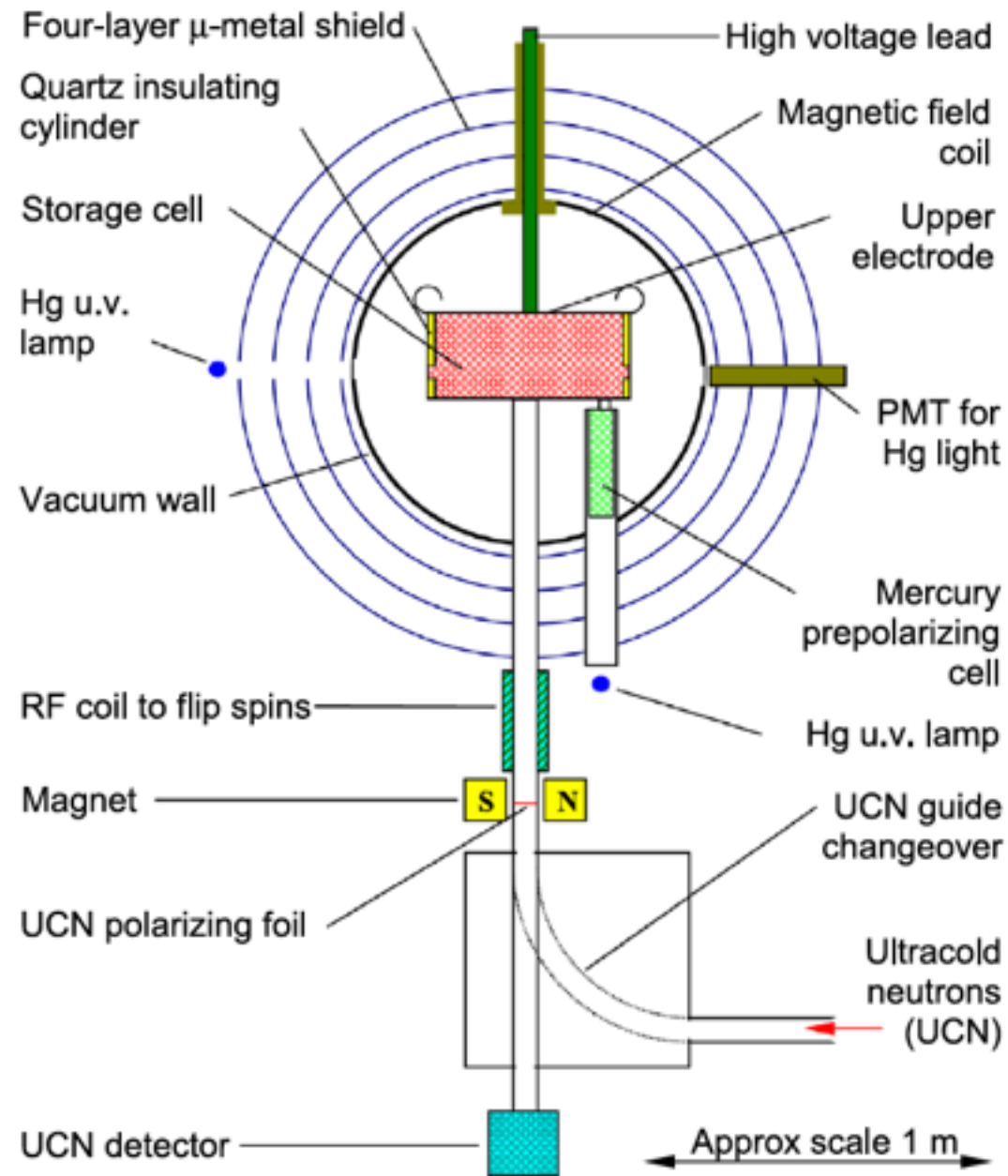


Fig. 6. The neutron EDM experimental apparatus.

- Precession measurement
 - Ramsey's separated oscillatory field magnetic resonance method
- Magnetometry
 - ^{199}Hg comagnetometer
- Selected parameters
 - $E \sim 10 \text{ kV/cm}$
 - $N \sim 14,000$
 - $T \sim 130 \text{ s}$
- Results
 - $d_n < 2.9 \times 10^{-26} \text{ e-cm}$

Sussex-ILL experiment

Baker et al. Phys. Rev. Lett. **97**, 131801 (2006).

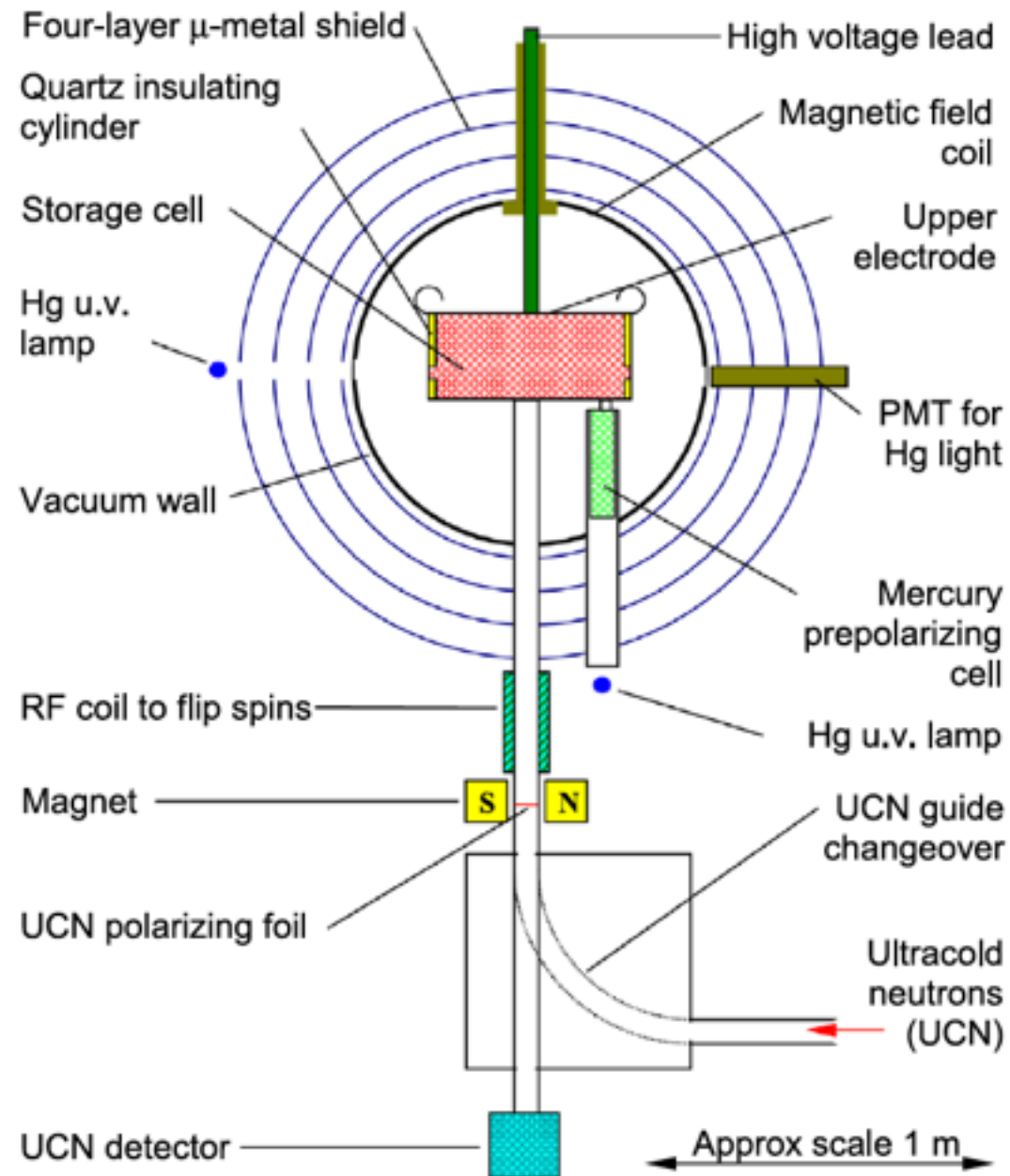


Fig. 6. The neutron EDM experimental apparatus.

- Precession measurement
 - Ramsey's separated oscillatory field magnetic resonance method
- Magnetometry
 - ^{199}Hg comagnetometer
- Selected parameters
 - $E \sim 10 \text{ kV/cm}$
 - $N \sim 14,000$
 - $T \sim 130 \text{ s}$
- Results
 - $d_n < 2.9 \times 10^{-26} \text{ e-cm}$

Experimental considerations

- Statistical sensitivity:

$$\delta d_n \propto \frac{1}{ET\sqrt{N}}$$

- Therefore we need:

- Higher E
- Longer T
- Larger N

- Systematics

- $v \times E$ (motional magnetic field) effect
- Leakage currents
- Non-uniformity and instability of magnetic field
- Geometric phase effects

Experimental considerations

- Statistical sensitivity:

$$\delta d_n \propto \frac{1}{ET\sqrt{N}}$$

- Therefore we need:

- Higher E

- Longer T

- Larger N

Performing an experiment in LHe can increase E , T , and N

- Systematics

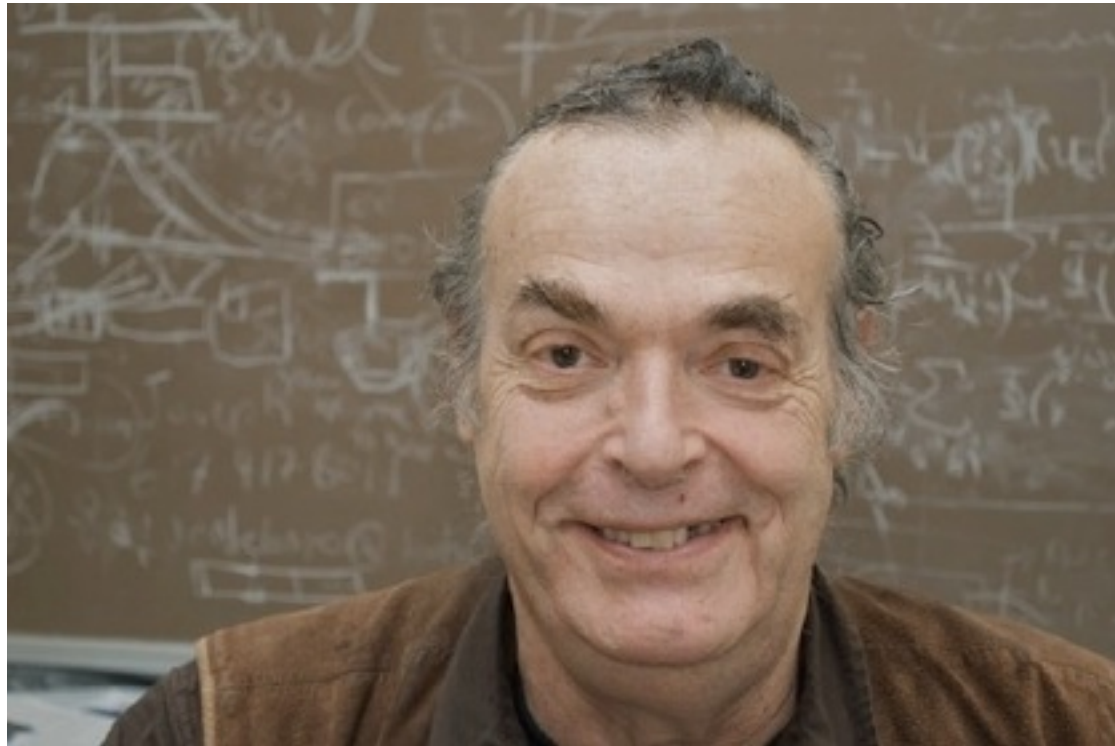
- $v \times E$ (motional magnetic field) effect

- Leakage currents

- Non-uniformity and instability of magnetic field

- Geometric phase effects

Idea of performing an nEDM search in the liquid helium of a superthermal source



R. Golub

Tome 44

N° 9

1^{er} MAI 1983

LE JOURNAL DE PHYSIQUE-LETTRES

J. Physique — LETTRES 44 (1983) L-321 - L-326

1^{er} MAI 1983, PAGE L-321

Classification

Physics Abstracts

13.40F — 14.20 — 29.25

New application of the superthermal Ultra-Cold Neutron source. I — The search for the neutron electric dipole moment

R. Golub

Physics Dept. E21, Technische Universität München, 8046 Garching, F.R.G.

(Reçu le 13 décembre 1982, révisé le 21 février 1983, accepté le 15 mars 1983)

Résumé. — Une source « super-thermique » de neutrons ultra-froids qui contient une solution diluée d'hélium 3 dans l'hélium 4 peut permettre la recherche du moment dipolaire électrique du neutron sans limiter l'angle solide des neutrons incidents. De même, on peut ainsi éviter des pertes de neutrons dues à différentes causes.

Abstract. — A superthermal Ultra-Cold Neutron source containing a dilute solution of polarized ³He in ⁴He can provide a method for carrying out the search for the neutron electric dipole moment which will not place any limits on the solid angle of the incoming neutrons and eliminate losses due to several causes.

As recent experiments [1-3] have confirmed the principles of the superthermal source of Ultra-Cold Neutrons [4-6] it now seems appropriate to consider some new techniques for applying the extremely high UCN densities [7] made available by this source. In this paper we discuss a new method for searching for the neutron electric dipole moment (edm) using UCN.

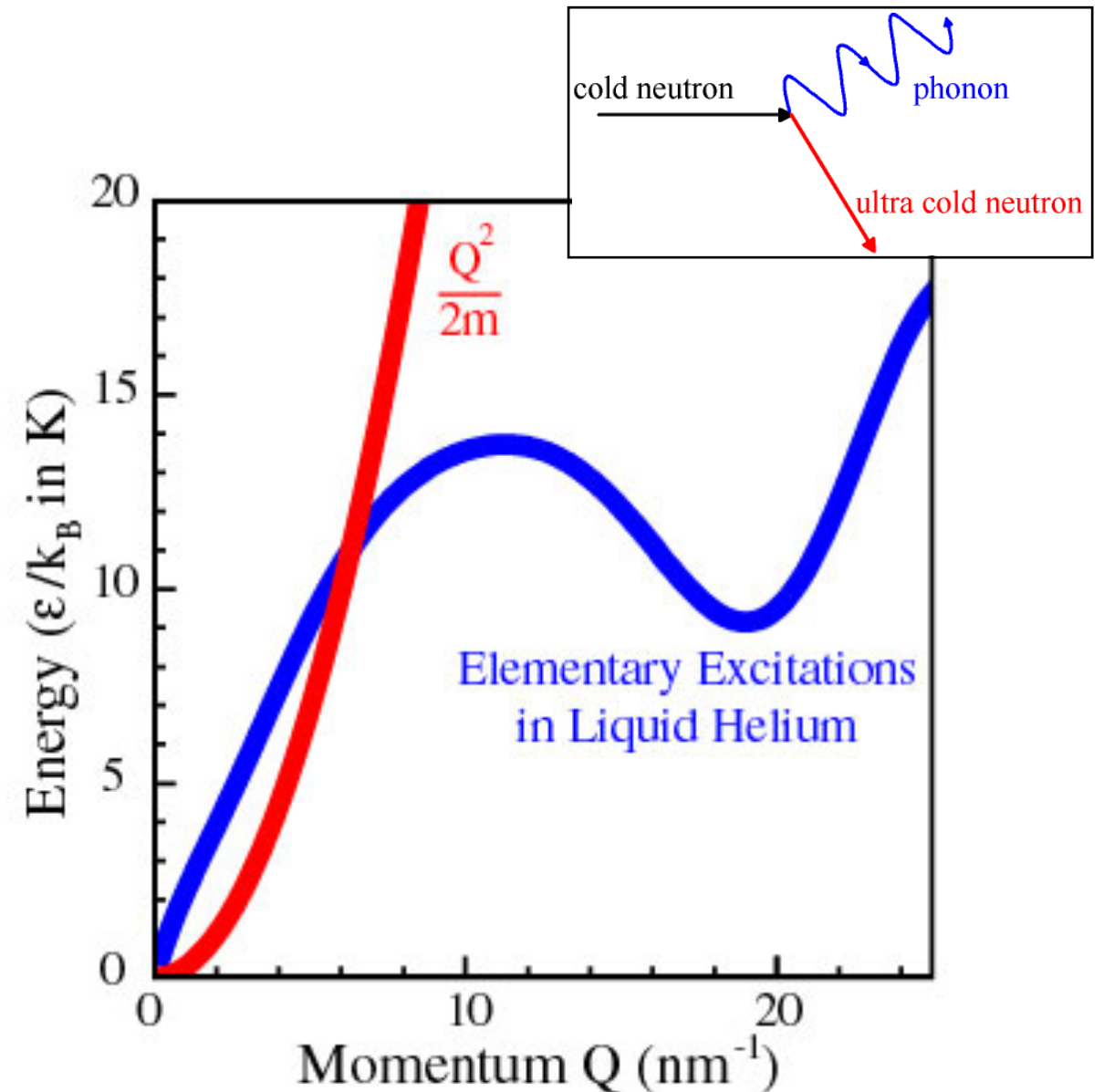
UCN are neutrons with energies so low ($\sim 10^{-3}$ K) that they are totally reflected from many materials at any angle of incidence and hence can be stored in material bottles for times approach-

Superthermal production of UCN



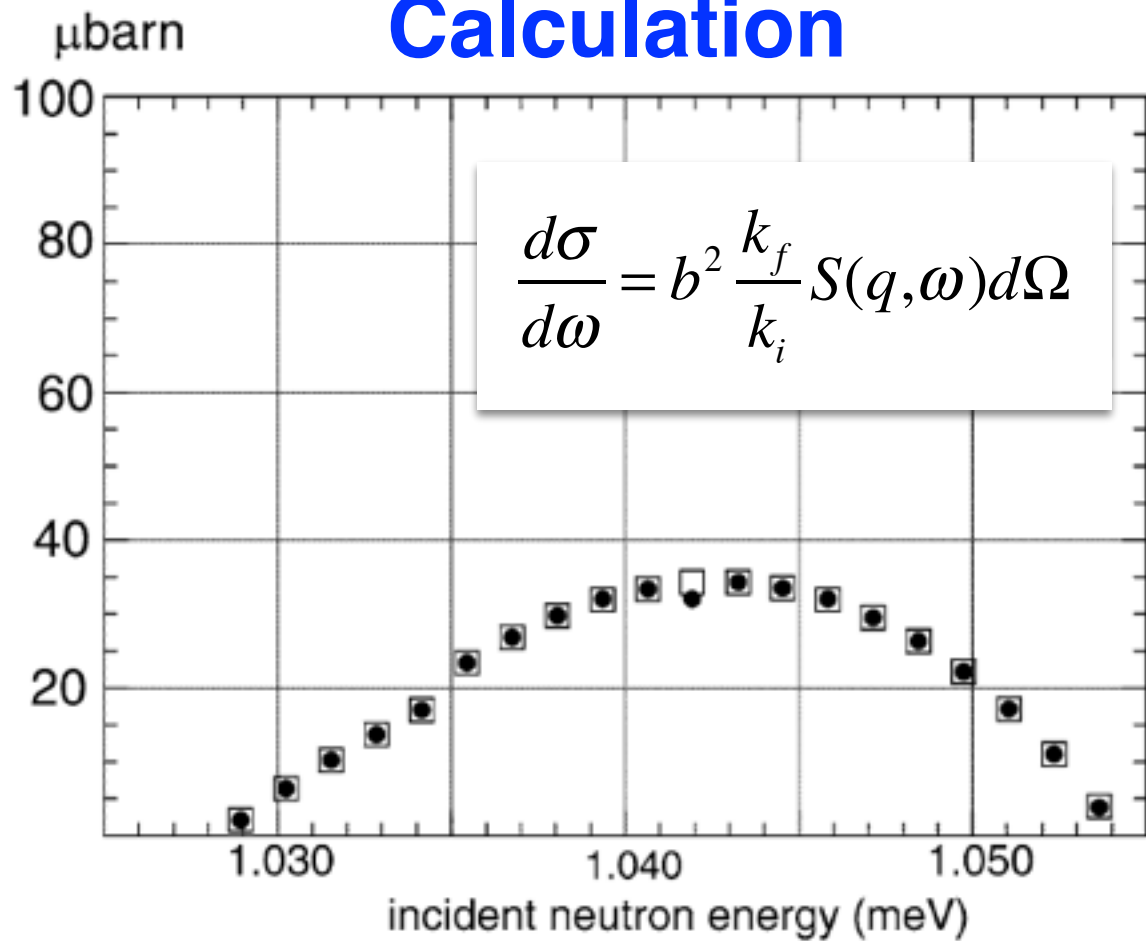
R. Golub and J. M. Pendlebury, Phys. Lett. A 62, 337 (1977)

- 8.9 Å cold neutrons get down-scattered in superfluid ^4He by exciting elementary excitation
- Up-scattering process is suppressed by a large Boltzmann factor
 - $\exp(-E/kT)$, where $E/k = 12 \text{ K}$ and $T = 0.4 \text{ K}$
- There is no nuclear absorption



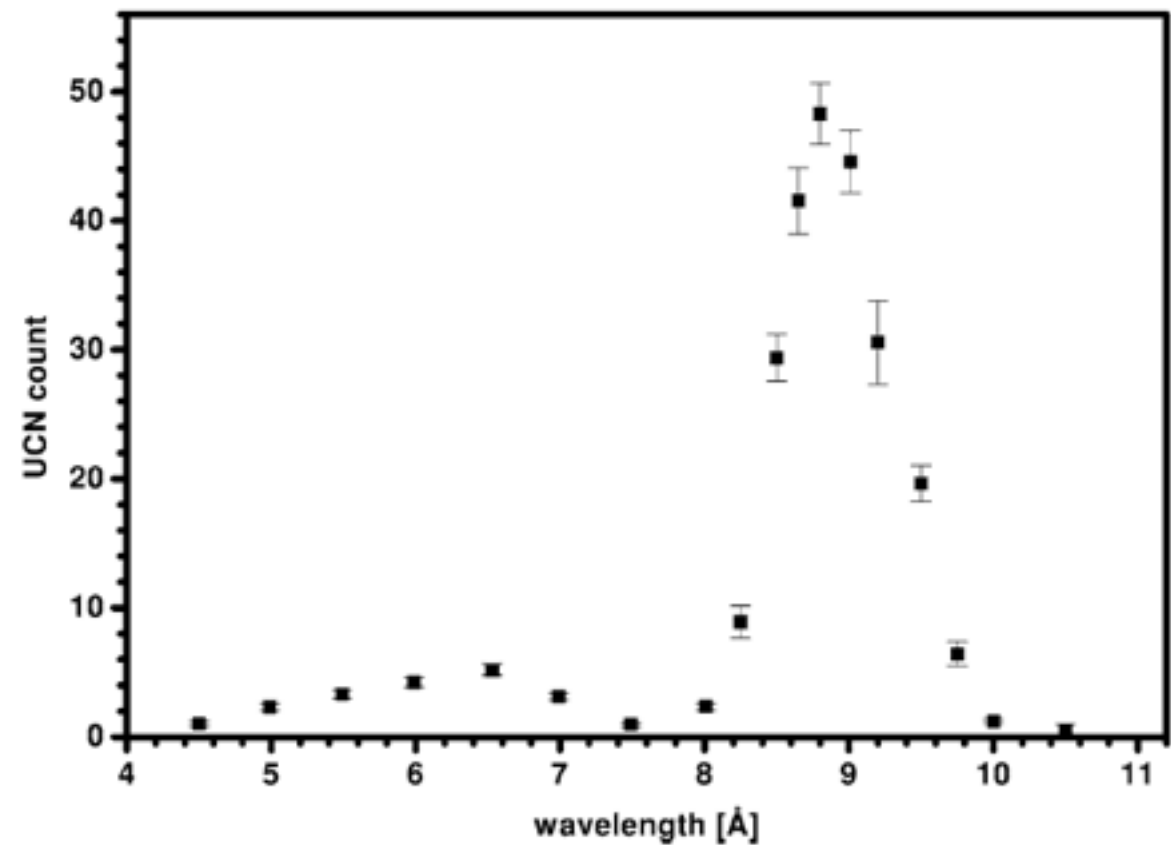
Superthermal production of UCN

Calculation



H. Yoshiki, Compt. Phys. Commun. **151**, 141 (2003)

Measurement



C.A. Baker et al. Phys. Lett. A **308**, 67 (2003)

Measured UCN production rate ($V_F = 252$ neV): $P = (4.55 \pm 0.25) \times 10^{-8} d\Phi/d\lambda|_{\lambda^*} \text{ cm}^{-3} \text{ s}^{-1}$
 ($d\Phi/d\lambda|_{\lambda^*}$ is the differential flux in neutrons $\text{cm}^{-2} \text{ s}^{-1} \text{ \AA}^{-1}$.)

Achievable UCN density

$$\frac{d\rho}{dt} = P - \frac{\rho}{\tau}$$

$$\rightarrow \rho = P\tau \text{ for } \frac{d\rho}{dt} = 0$$

ρ : UCN density

P : UCN production rate

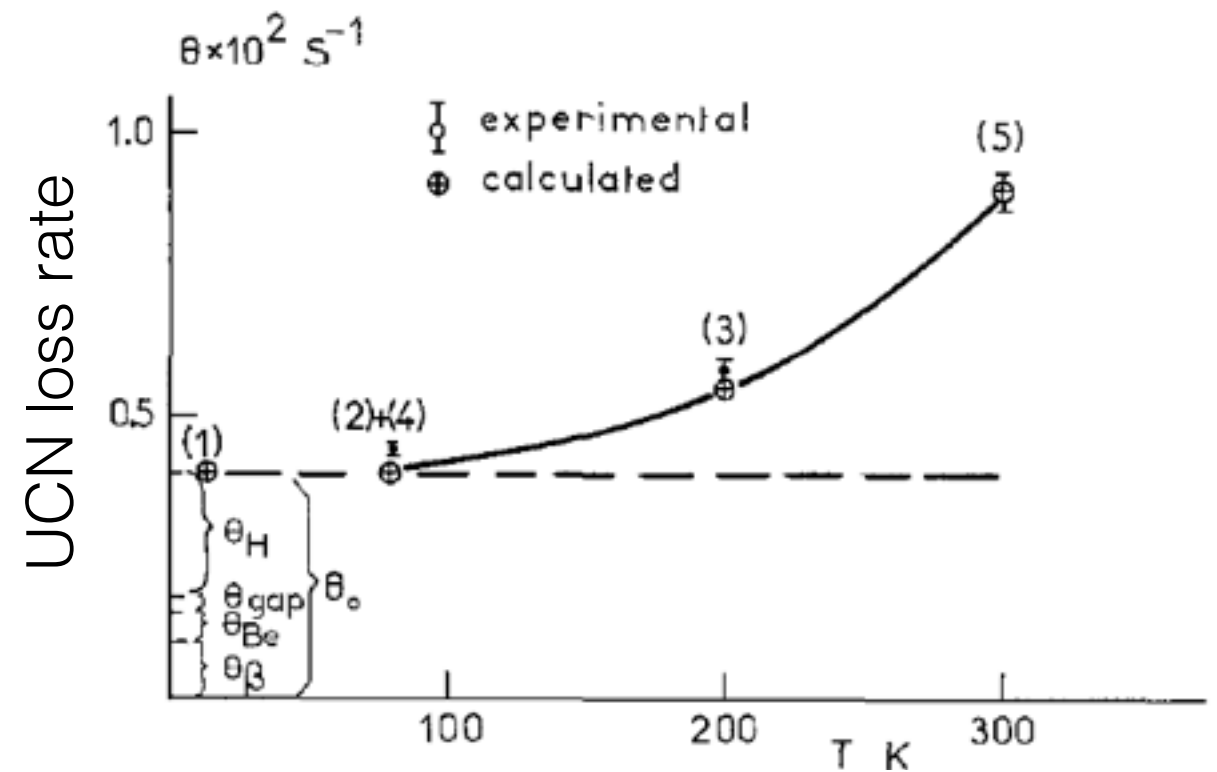
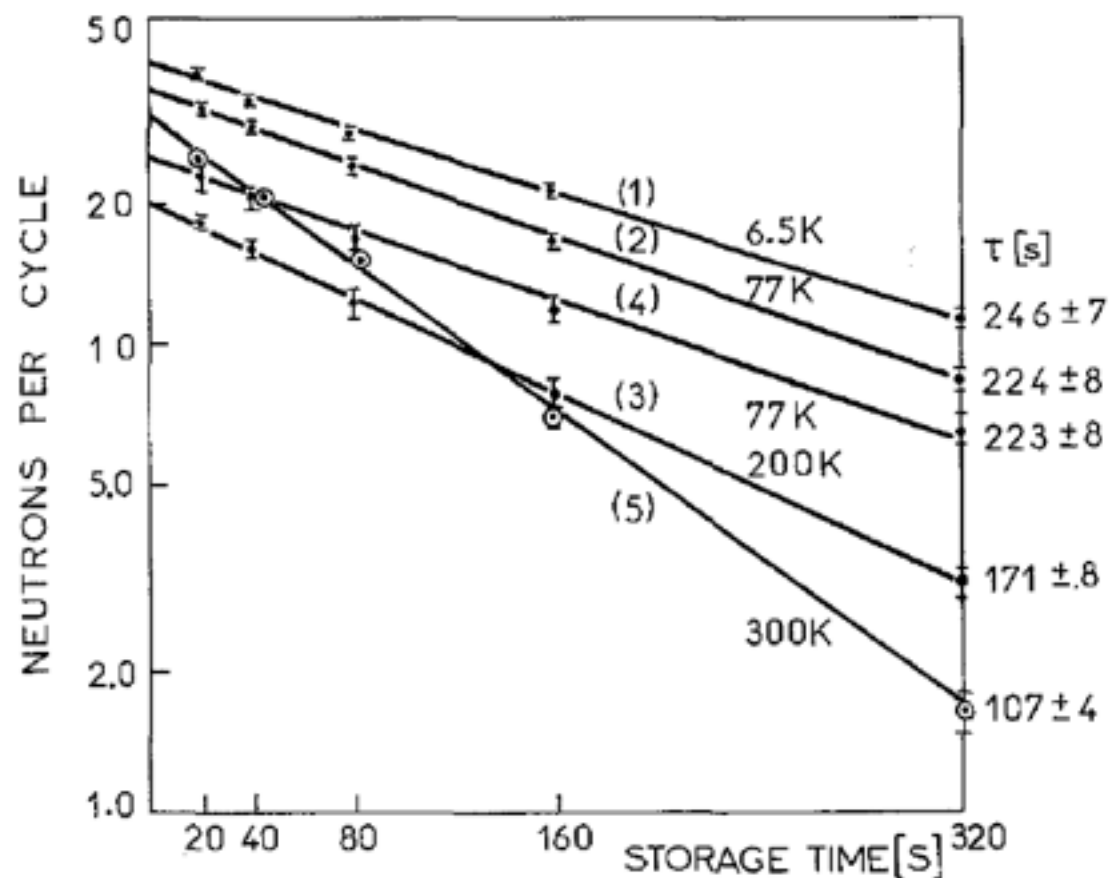
τ : UCN lifetime

- Example:
 - At SNS FNPB, the expected UCN production rate is $P \sim 0.3 \text{ UCN/cm}^3/\text{s}$. This gives, with $\tau \sim 500\text{s}$, $\rho \sim 150 \text{ UCN/cm}^3$.
 - At ILL, at the position where the cryoEDM was installed, the neutron flux was $3 \times 10^7 \text{ cm}^{-2} \text{ s}^{-1} \text{ \AA}^{-1}$, which gives a UCN production rate of $1.4 \text{ UCN/cm}^3/\text{s}$. The measured UCN storage time in the UCN source was 90 s . A stored UCN density of 10 UCN/cm^3 was observed. 29 UCN/cm^3 was expected with a various factors reducing the expected UCN density taken into account. With no such factors, a stored UCN density of 220 UCN/cm^3 would be expected, with a projected source lifetime of 160 s .

UCN storage

- Up-scattering from surface hydrogen contamination makes an important contribution to the wall loss.
- This effect is suppressed at low temperatures.

P. Ageron, W. Mampe, and A. L. Kilvington, Z. Phys. B **59**, 261 (1985)

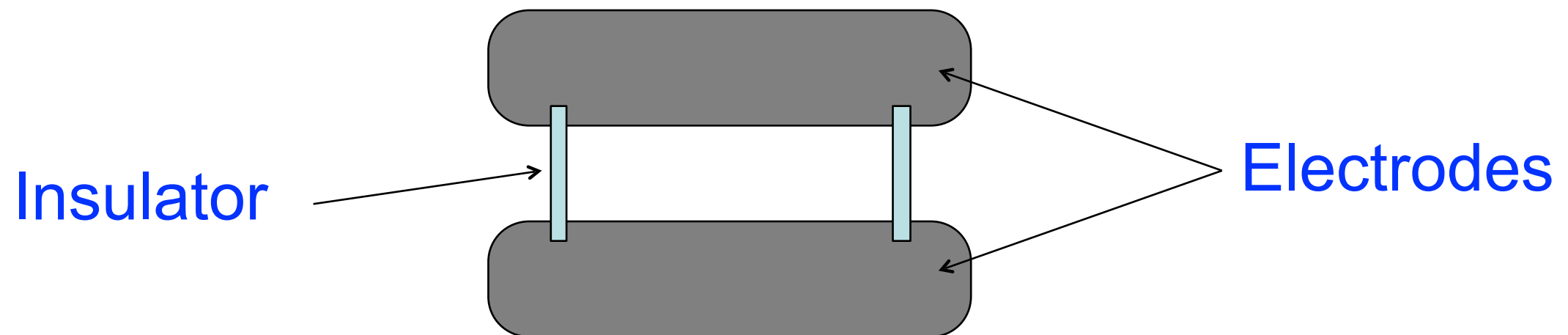


See also E. Korobkina et al. Phys. Rev. B **70**, 035409 (2004).

For the history of “anomalous” UCN loss, see Golub, Richardson, Lamoreaux (1991)

Electric field for nEDM experiments

- The electric field strength for room temperature EDM experiments with UCN has typically been limited to ~ 10 kV/cm.
 - Problem: field-emission electrons from the point of contact of insulator with the electrode.



- It is expected that a higher electric field can be used in EDM experiments in which the measurement cell is immersed in LHe.

Electrical breakdown in LHe

Electrical breakdown in dielectric fluid

- Far less well understood than breakdown in gases

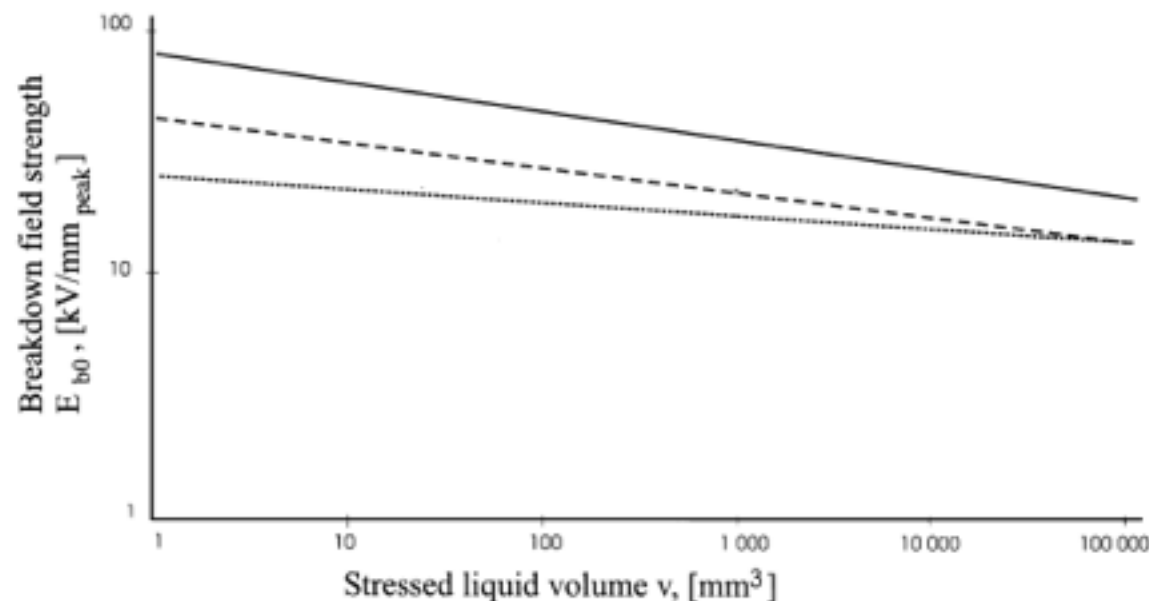
Some properties of LHe

- He ionization potential - 24.6 eV
- He atom density in liquid - 2×10^{22} /cm³
- Low energy e/He elastic scattering cross section $\sim 5 \times 10^{-16}$ cm²
- Mean free path $\sim 10^{-7}$ cm
 - In field of 10^5 V/cm gain energy of 0.01 eV between collisions
- When KE < 1 eV, electron forms bubble 19 Å radius in He 0.9 eV below conduction band electron; hydrodynamic mass $\sim 250 m_{\text{He}}$
- He⁺ ion forms snowball, $m \sim 25 m_{\text{He}}$

No intrinsic mechanism in bulk for creating breakdown below 10 MV/cm

Electrical Breakdown in LHe

- Data exist for 1.2 – 4.2 K, mostly at SVP (bulk of the data were taken at 4.2 K)
 - For varying geometries (plane-plane, sphere-plane, sphere-sphere)
 - Breakdown field values $\sim \mathcal{O}(100)$ kV/cm (depends on the size of the system)
- Note: much lower than the intrinsic bulk breakdown field



J. Gerhold, Cryogenics 38, 1063 (1998)

Figure 15 Volume effect in liquid helium breakdown. — fit from ref. ³⁶; - - - data from ref. ³¹; ... near zero breakdown probability estimation from ref. ³⁷

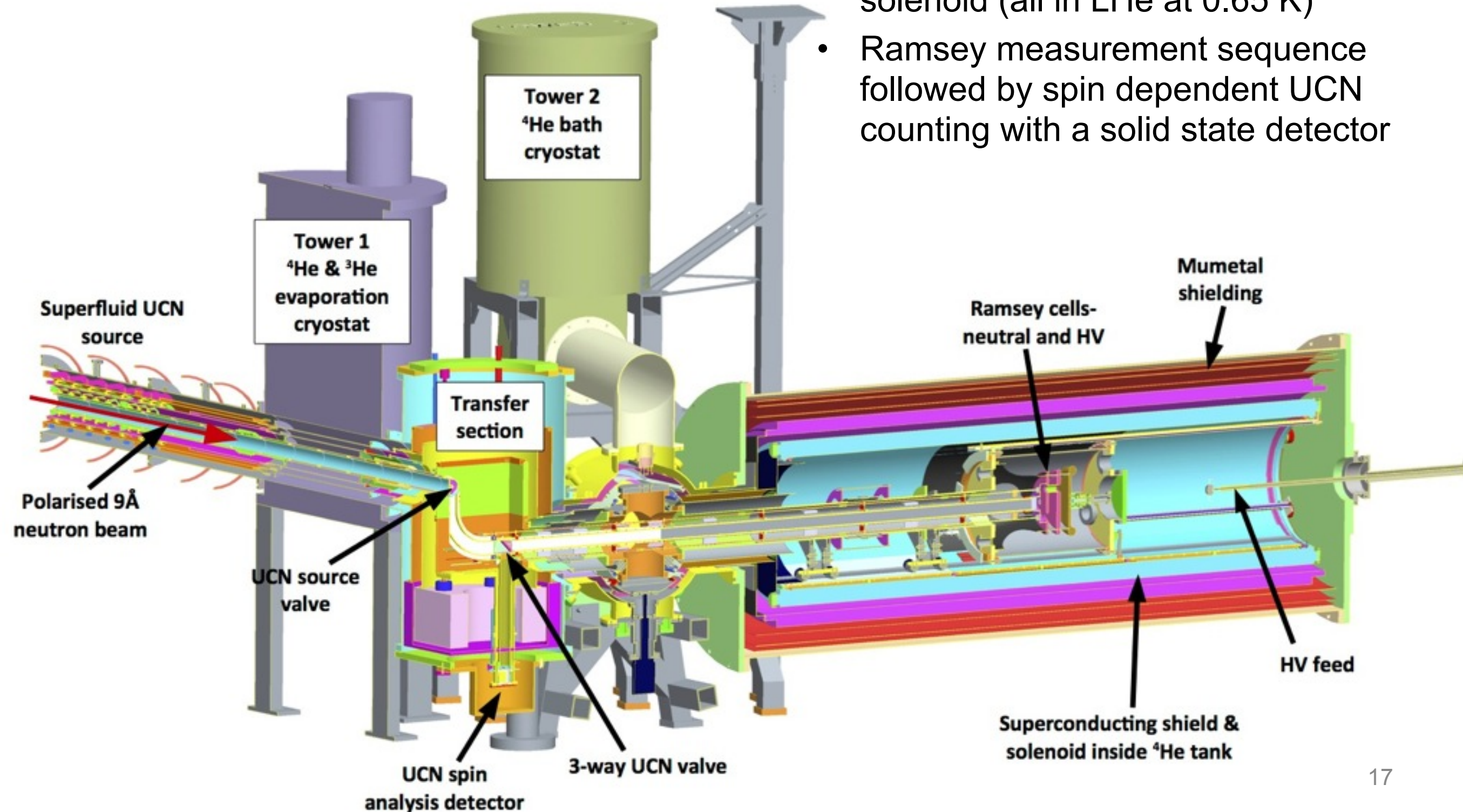
- Some of the processes responsible for breakdown initiated at the electrode-insulator junction are also expected to be suppressed at lower temperatures.

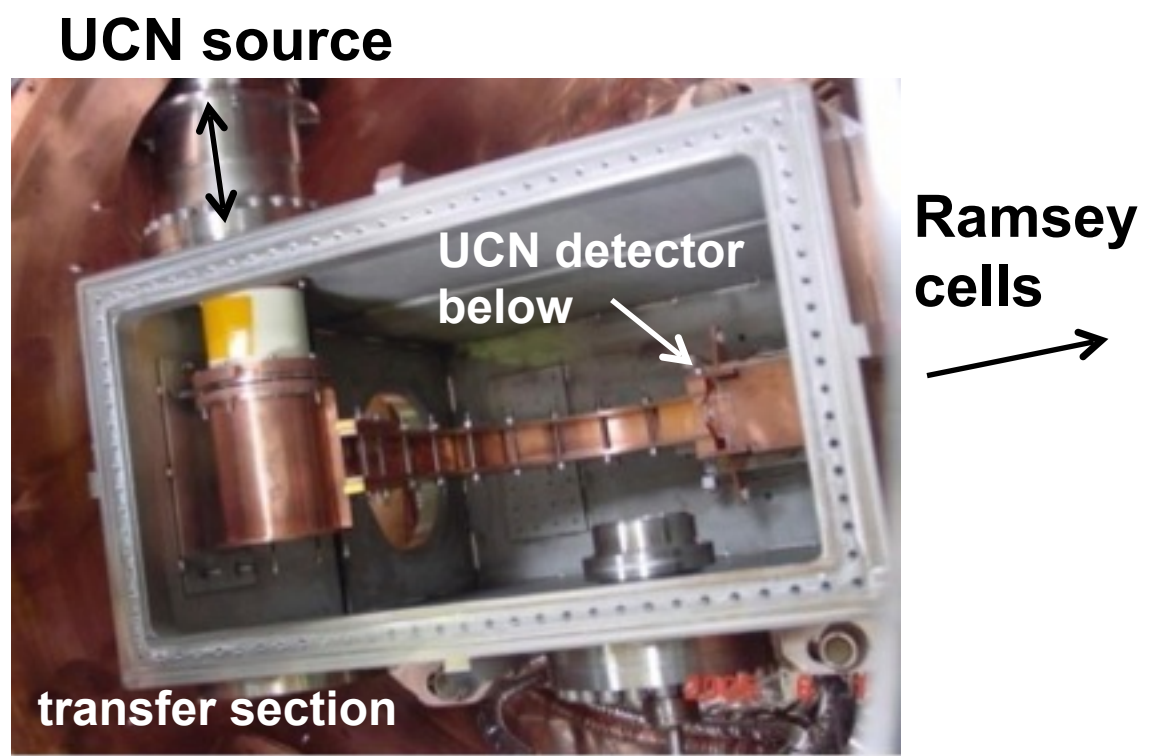
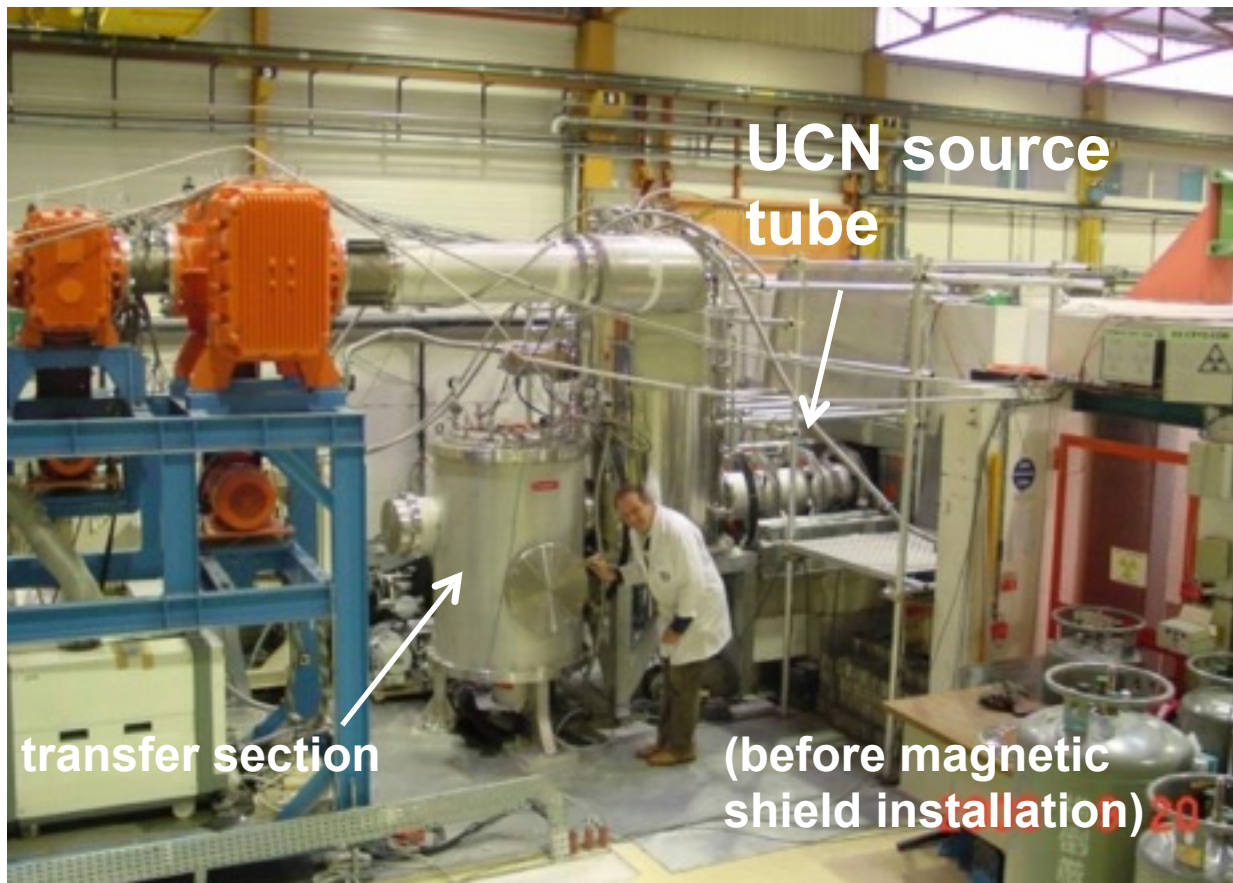
World's cryogenic nEDM experiments

Experiment	Facility	Method
CryoEDM	ILL	Ramsey's separated oscillatory fields
nEDM at ESS	ESS	Ramsey's separated oscillatory fields
nEDM at SNS	SNS @ ORNL	Golub and Lamoreaux (He-3 comagnetometer)

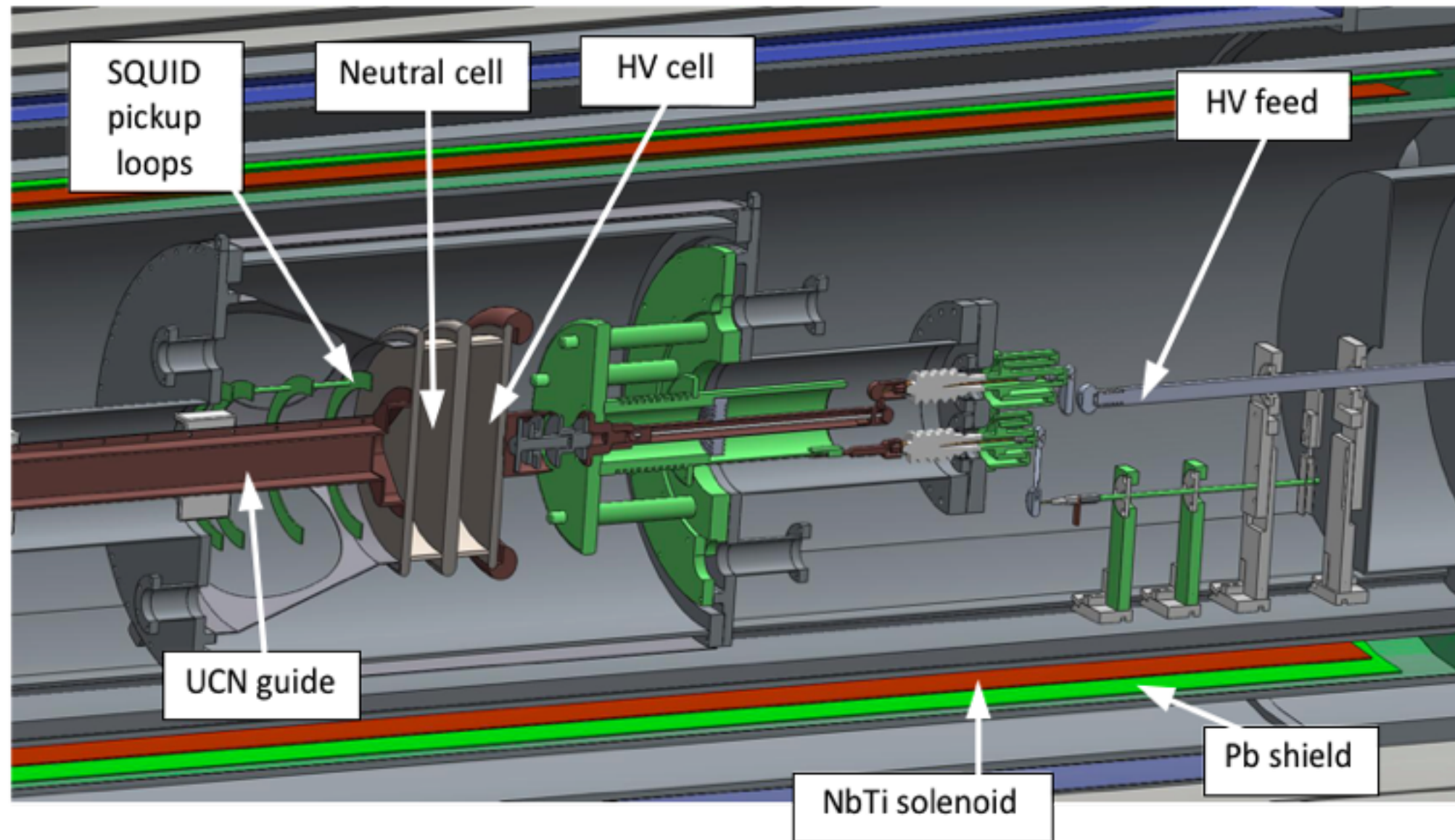
CryoEDM:

- Superthermal LHe UCN source
- UCN transferred to measurement cells within a superconducting shield solenoid (all in LHe at 0.65 K)
- Ramsey measurement sequence followed by spin dependent UCN counting with a solid state detector





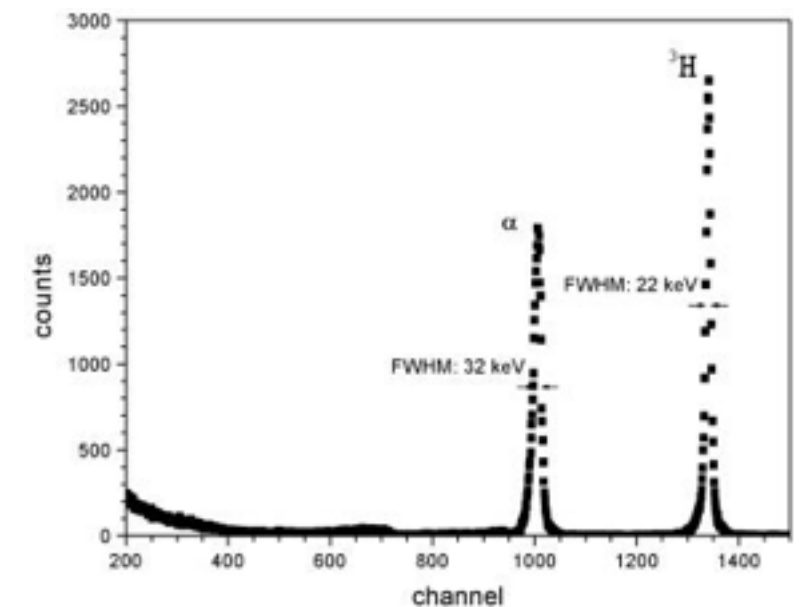
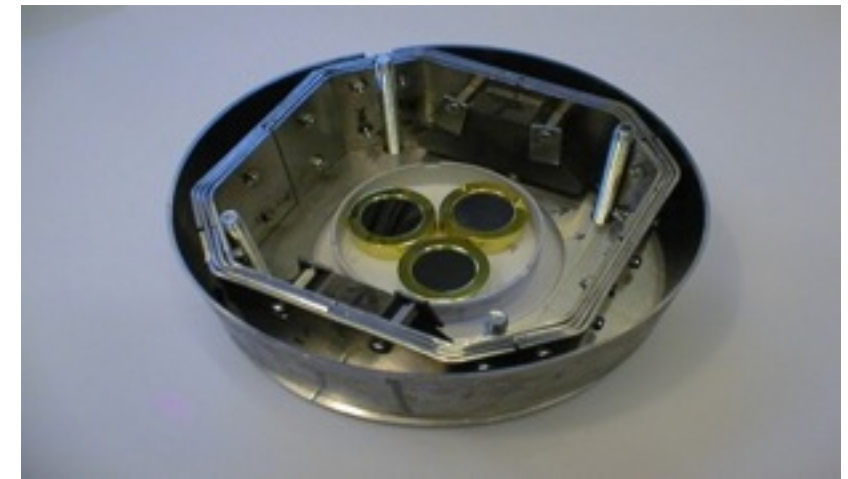
Ramsey cell detail



- HV cell provides EDM measurement, cell at zero E field gives adjacent magnetic field measurement
- SQUID pickup loops provide additional magnetic monitoring
- 10 kV/cm field achieved in HV cell (40 kV, 4 cm gap), limited by HV feed system (improved feed designed with potential for 30 kV/cm)

Detectors

- Solid-state detectors developed for use in LHe
- Thin surface film of ${}^6\text{LiF}$: $n + {}^6\text{Li} \rightarrow \alpha + {}^3\text{H}$; 82% efficient
- Fe layer for spin analysis
- Currently, α peak hidden under γ background
 - pulse-shape discrimination
- Now moving to detector with 10x area, to cover entire guide



C.A.Baker et al.,
NIM **A487** 511-520
(2002)

CryoEDM at ILL, 2003-2013

- **Achievements:**
 - regular operation of a large cryogenic system filled with 250 L of ultrapure superfluid ^4He at 0.65 K
 - 10 UCN/cm³ density in 10.5 L superthermal source (limited by cold neutron beam flux and UCN lifetime)
 - solid state ^6Li UCN detectors developed and successfully operated at low temperature
 - transported UCN from source, to Ramsey cells, and back to the detector with a system of 3 valves, all operated within superfluid He
- **Limitations:**
 - long turn around to cycle apparatus (several months)
 - large losses of UCN between source and Ramsey cells
 - very small collaboration (almost entirely UK based)
 - UK funding agency decided to pull out of project at end of 2013

Towards a new Europe based cryogenic nEDM measurement...

- LHe superthermal source development ongoing at ILL (SuperSUN)
- Couple this source first to a room temperature nEDM apparatus
- Later switch to a cryogenic measurement cell
 - larger E field, longer UCN storage times...
 - modular approach allows faster turn-around times and greater flexibility in improving the apparatus compared to CryoEDM
- Initial development at ILL, later move to ESS
 - A letter of intent (ILL/TUM/TUW/RAL) has been submitted to ESS for a superthermal UCN facility on which a cryogenic nEDM experiment will be operated

nEDM @ SNS COLLABORATION

R. Alarcon, R. Dipert

Arizona State University

G. Seidel

Brown University

E. Hazen, A. Kolarkar, J. Miller, L. Roberts

Boston University

D. Budker

UC Berkeley

M. Blatnik, R. Carr, B. Filippone, C. Osthelder, S. Slutsky,

X. Sun, C. Swank

California Institute of Technology

M. Ahmed, M. Busch, P. -H. Chu, H. Gao

Duke University

I. Silvera

Harvard University

M. Karcz, C.-Y. Liu, J. Long, H.O. Meyer, M. Snow

Indiana University

L. Bartoszek, D. Beck, C. Daurer, J.-C. Peng, T. Rao,

S. Williamson, L. Yang

University of Illinois Urbana-Champaign

C. Crawford, T. Gorringer, W. Korsch,

E. Martin, N. Nouri, B. Plaster

University of Kentucky

S. Clayton, S. Currie, T. Ito, Y. Kim, M. Makela,

J. Ramsey, W. Sondheim, Z. Tang, W. Wei

Los Alamos National Lab

K. Dow, D. Hasell, E. Ihloff, J. Kelsey, J. Maxwell, R. Milner, R. Redwine, E.

Tsentlovich, C. Vidal

Massachusetts Institute of Technology

D. Dutta, E. Leggett

Mississippi State University

R. Golub, C. Gould, D. Haase, A. Hawari, P. Huffman,

E. Korobkina, K. Leung, A. Reid, A. Young

North Carolina State University

R. Allen, V. Cianciolo, Y. Efremenko, P. Mueller,

S. Penttila, W. Yao

Oak Ridge National Lab

M. Hayden

Simon Fraser University

G. Greene, N. Fomin

University of Tennessee

S. Stanislaus

Valparaiso University

S. Baeßler

University of Virginia

S. Lamoreaux

Yale University

SNS nEDM experiment overview

Golub and Lamoreaux, Phys. Rep. 237, 1 (1994)

- Experiment performed in superfluid LHe
- In situ production of UCN from 8.9 Å cold neutron beam via superthermal process
- Higher electric field expected to be achievable in LHe
- Longer UCN storage time expected at cryogenic temperatures
- ^3He as comagnetometer and spin analyzer for UCN
- Two complementary approaches to look for the nEDM signal ($\mathbf{d} \cdot \mathbf{E}$)
 - Free precession method
 - Dressed spin method

Two techniques provide critical crosscheck of the EDM results with different challenges and systematics.

^3He as co-magnetometer

- ^3He atoms will be used as a co-magnetometer.
- A co-magnetometer is a polarized atomic species within the same storage volume as the neutrons that provides a nearly exact spatial and temporal average of the magnetic field affecting the neutrons over the storage period.
- Requirements for a comagnetometer:
 - It does not have an EDM of its own.
 - Short diffusion time (rapid sampling of the entire cell).
- ^3He as used in this experiment meets both requirements:
 - ^3He atomic EDM: $d_{\text{atm}}(^3\text{He}) \sim d_{\text{atm}}(^{199}\text{Hg})/3000 < 10^{-32}$ e-cm, Dzuba et al. PRA 76, 034501 (2007). (See also Stetcu et al. PLB 665, 168 (2008).)
 - ^3He diffusion in SFL ^4He : Lamoreaux, et al. EPL 58, 781 (2002).

^3He as spin analyzer

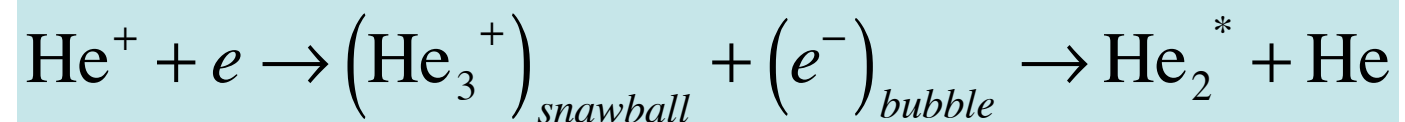
- ^3He 's gyromagnetic ratio is larger than neutron's by $\sim 10\%$ ($\gamma_3/\gamma_n \sim 1.1$)
- ^3He -n absorption reaction: $n + ^3\text{He} \rightarrow p + t$
 - $\sigma_{\uparrow\downarrow} \sim 10^4$ b and $\sigma_{\uparrow\uparrow} < 10^2$ b at 2200 m/s
- The neutron absorption rate is proportional to:

$$1 - \vec{p}_3 \cdot \vec{p}_n = 1 - p_3 p_n \cos [(\gamma_n - \gamma_3) B t]$$

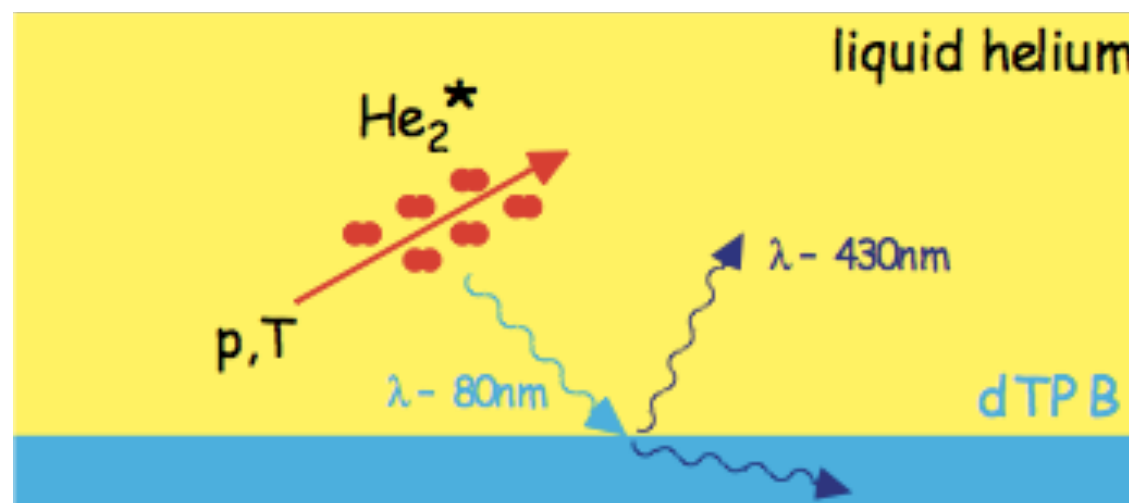
- ^3He -n absorption occurs every time ^3He and neutron spins become anti-parallel.
- By measuring the frequency at which ^3He -n absorption occurs, difference between the neutron and ^3He precession frequencies can be determined.
- The sensitivity to change in magnetic field is reduced by a factor 10.

LHe as detector

- Reaction productions of $n + {}^3\text{He} \rightarrow p + t$ generate UV scintillation light (80 nm) in LHe
 - Ionizing radiation in helium produces excited helium dimers.

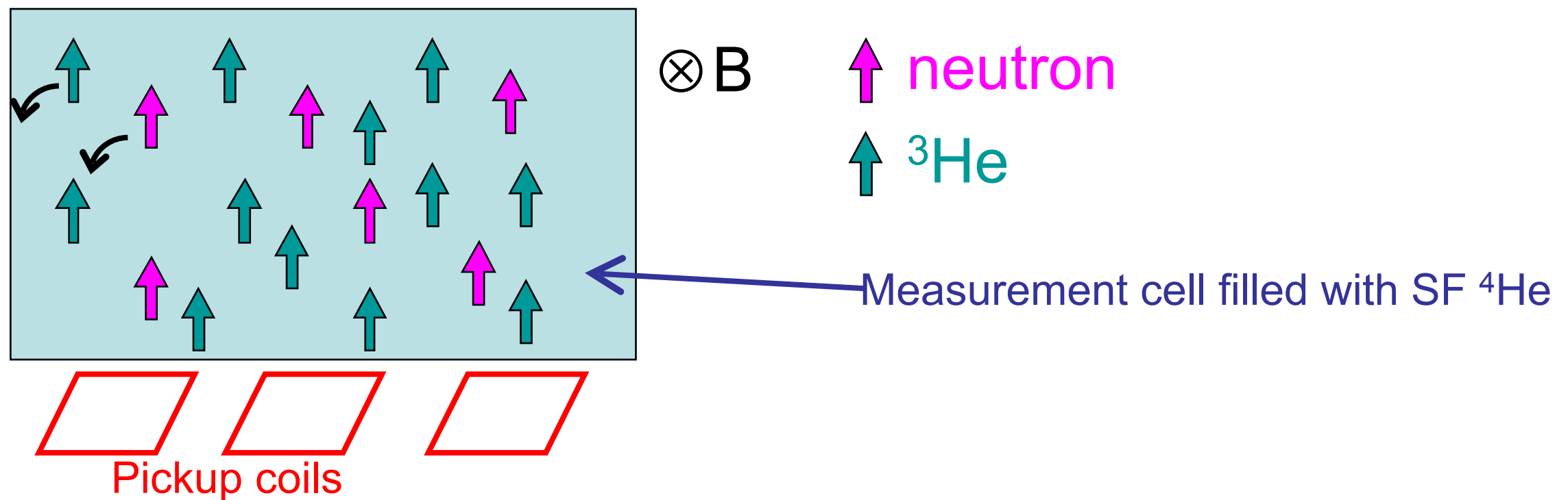


- LHe scintillation is generated when excited helium dimers decays to the unbound ground level.
- The UV light will be down-converted by a wavelength shifter and detected by PMTs.



Free precession method

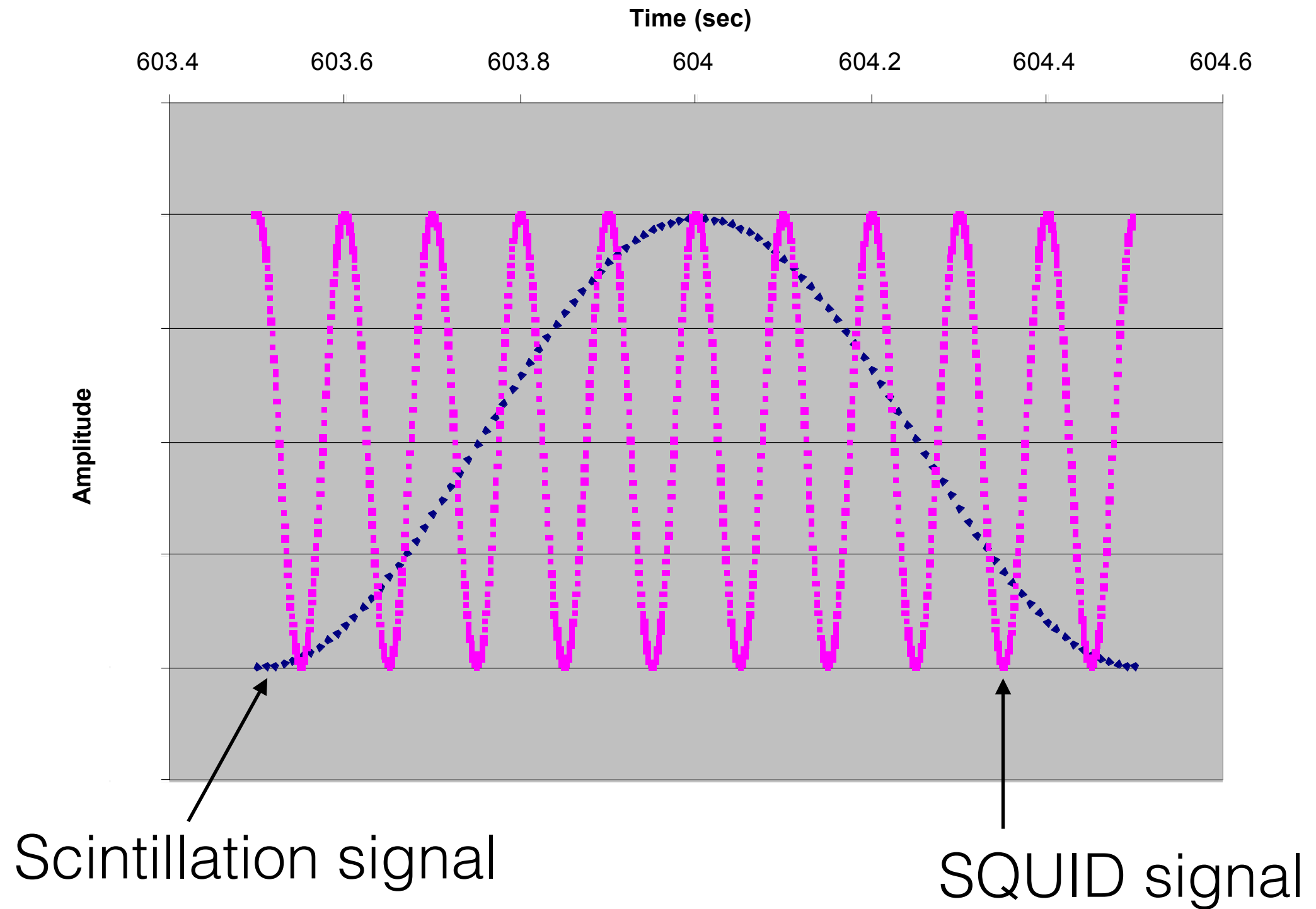
A dilute admixture of polarized ^3He atoms is introduced to the bath of SF ^4He ($x = N_3/N_4 \sim 10^{-10}$ or $\rho_{^3\text{He}} \sim 10^{12}/\text{cc}$) as comagnetometer



Change in magnetic field due to the rotating magnetization of ^3He by SQUID magnetometers

Signature of EDM appears as a shift in $\omega_3 - \omega_n$ corresponding to the reversal of \mathbf{E} with respect to \mathbf{B} with no change in ω_3

Signals



^3He density and neutron storage time

$$\frac{1}{\tau_{\pm}} = \frac{1}{\tau_{\beta}} + \frac{1}{\tau_w} + (1 \mp P_3) N_3 \sigma_0 v_n$$

τ_{\pm} τ_{β} τ_w $(1 \mp P_3)$ N_3 σ_0 v_n

β decay (PDG: 880.3 ± 1.1 s) wall loss (goal: 2000 s) ^3He polarization ^3He density cross section velocity

- Because $\sigma_0 \propto 1/v_n$, $\sigma_0 v_n$ is independent of velocity.
- $\sigma_0 = 5333$ b at $v_n = 2200$ m/s.
- $N_3 \sigma_0 v_n = 1/500$ s gives $x = N_3/N_4 \sim 10^{-10}$.
- Note: $x \sim 10^{-6}$ for natural helium.

Dressed spin method

- In the free precession method with a ^3He co-magnetometer, the sensitivity to change in magnetic field is reduced by a factor 10 due to $\gamma_3/\gamma_n \sim 1.1$.
- If the species used for the co-magnetometer had the same gyromagnetic ratio as the neutron, an experiment insensitive to magnetic field change would be possible.

Spin dressing

C. Cohen-Tannoudji and S. Haroche, J. Physique 30, 153 (1969).

- The spin is initially pointing along the z-axis
- A strong non-resonant alternating field is applied.

$$B_x(t) = B_{\text{rf}} \sin \omega_{\text{rf}} t$$

- The spin starts to precess in the y-z plane with a frequency

$$\omega(t) = \dot{\theta}(t) = \gamma B_x(t)$$

- The angle θ is given by:

$$\theta(t) = \gamma (B_{\text{rf}} / \omega_{\text{rf}}) \cos \omega_{\text{rf}} t$$

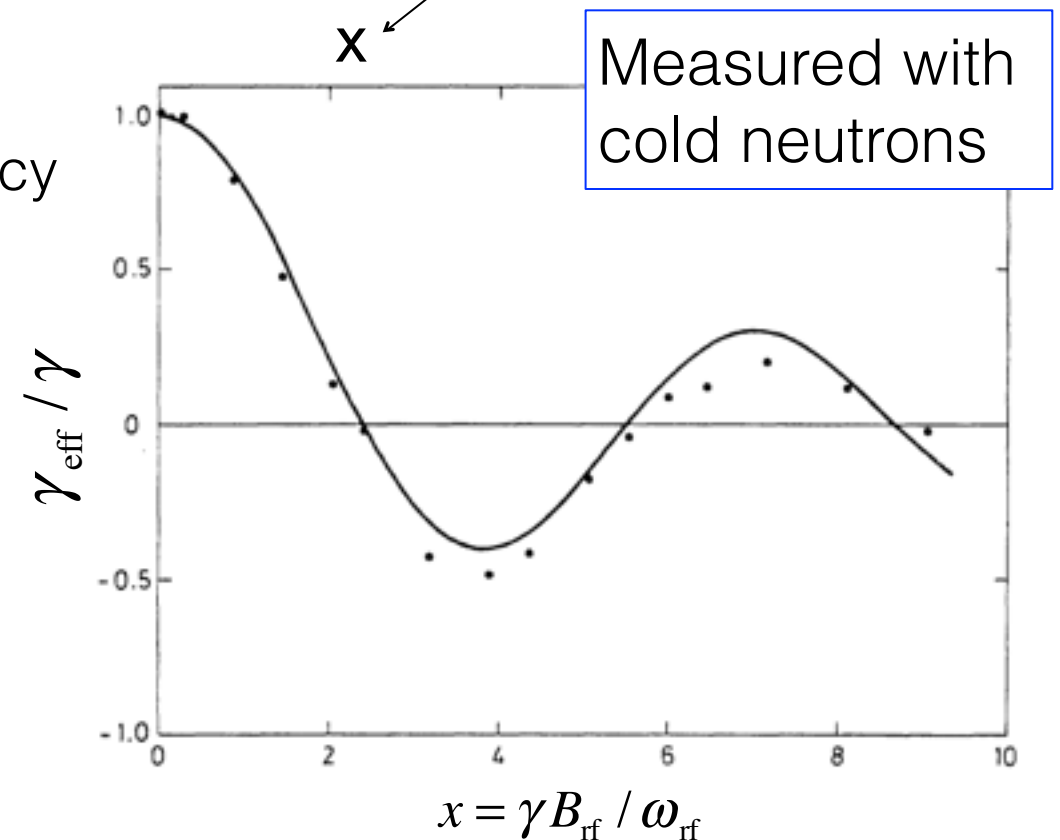
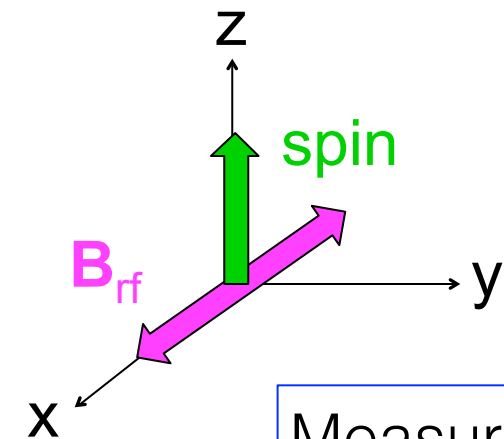
- The time average of the z component of the spin is

$$\langle \cos \theta(t) \rangle_T = \frac{1}{T} \int dt \cos \left[(\gamma B_{\text{rf}} / \omega_{\text{rf}}) \cos \omega_{\text{rf}} t \right]$$

$$= J_0(\gamma B_{\text{rf}} / \omega_{\text{rf}}) \equiv J_0(x)$$

- The effective gyromagnetic ratio

$$\gamma_{\text{eff}} = \gamma_0 J_0(x)$$



Muscat et al., PRL **58**, 2047 (1987)

cf. Measurements with ^3He

- Esler et al., PRC 76, 051302 (2007)
- Chu et al., PRC 84, 022501 (2011).
- Eckel et al., PRA 85, 032124 (2012)

Critical spin dressing

- Relative precession

$$\omega_{rel} = (\gamma_n^{eff} - \gamma_3^{eff}) B_0; \quad \gamma_i^{eff} = J_0(x_i) \gamma_i;$$

$$x_i = \gamma_i B_{rf} / \omega_{rf}; \quad i = \text{UCN}, {}^3\text{He}$$

- The effect of B field can be eliminated if

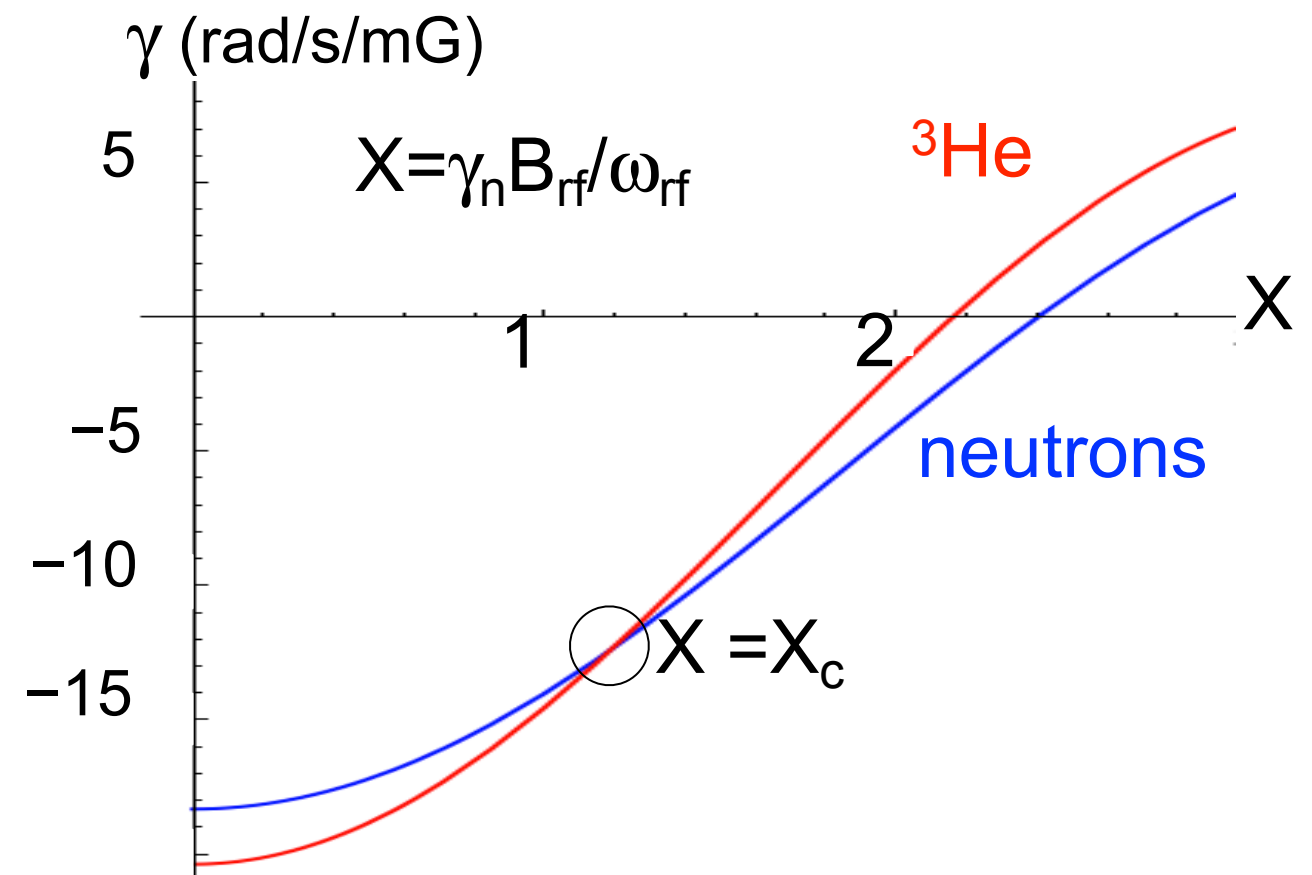
$$\gamma_n J_0(x_n) - \gamma_3 J_0(x_3) = 0$$

- This means

$$\alpha J_0(\alpha x_c) = J_0(x_c); \quad \alpha = \gamma_3 / \gamma_n = x_3 / x_n$$

- Solution: “critical dressing”

$$x_c \approx 1.19, \quad J_0(x_c) = 0.65$$



Detection of nEDM with a dressed spin method

- In the presence of nEDM

$$\omega_{rel} = (\gamma_n^{eff} - \gamma_3^{eff}) B_0 + 2ed_n E J_0(x) / \hbar$$

- At critical dressing

$$\omega_{rel} = 2ed_n E J_0(x) / \hbar$$

$$\theta_{n3} = \omega_{rel} t = 2ed_n E J_0(x_c) t / \hbar$$

- If we modulate the dressing field so that

$$x(t) = x_c + \varepsilon \cos \omega_m t + kd_n E$$

$$\delta\theta \sim (\varepsilon / \omega_m) \sin \omega_m t + kd_n E t = \delta\theta_0 + kd_n E t$$

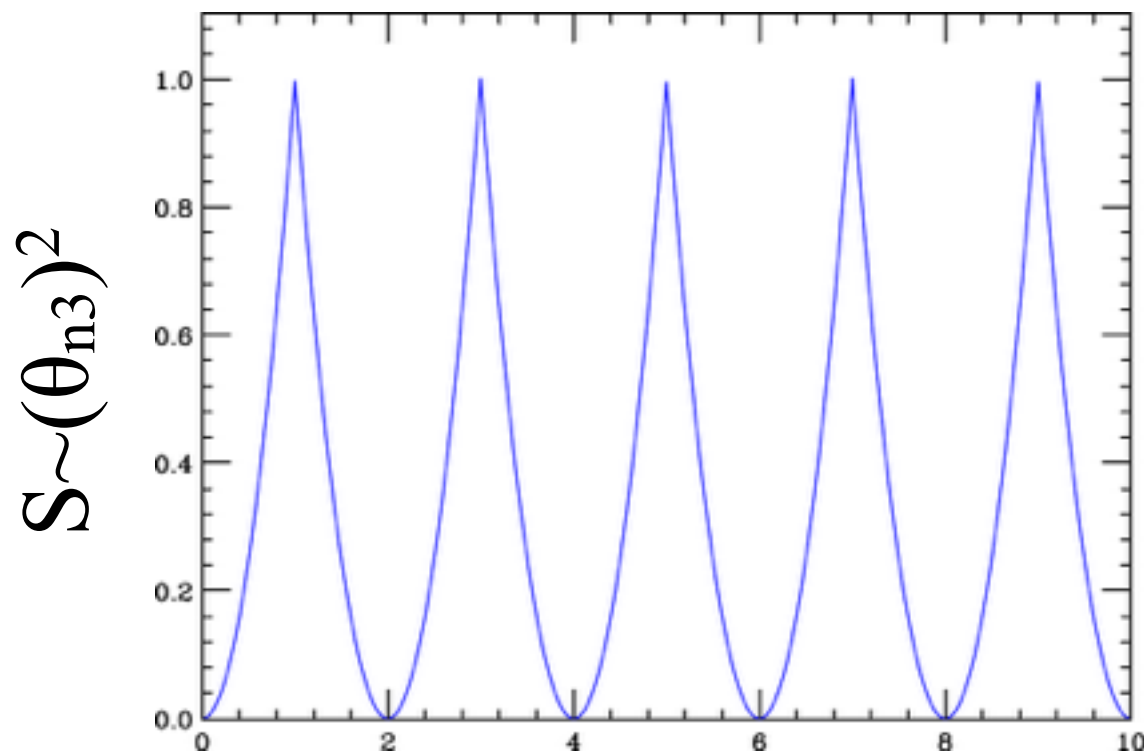
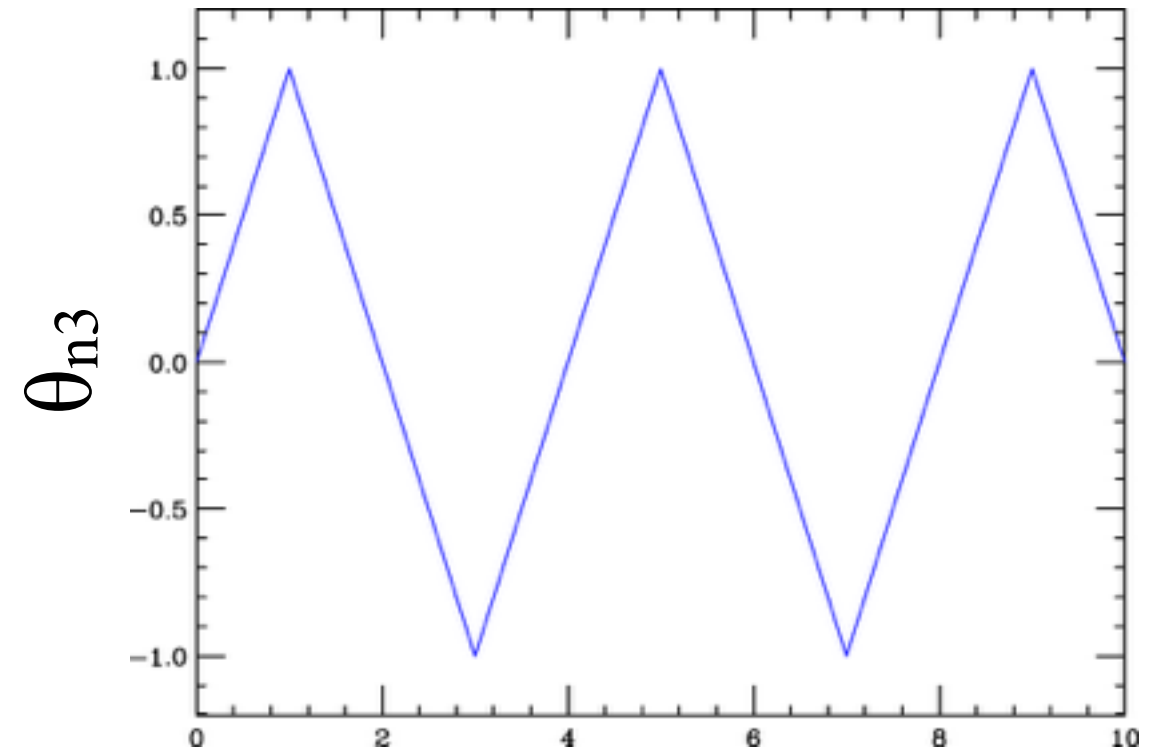
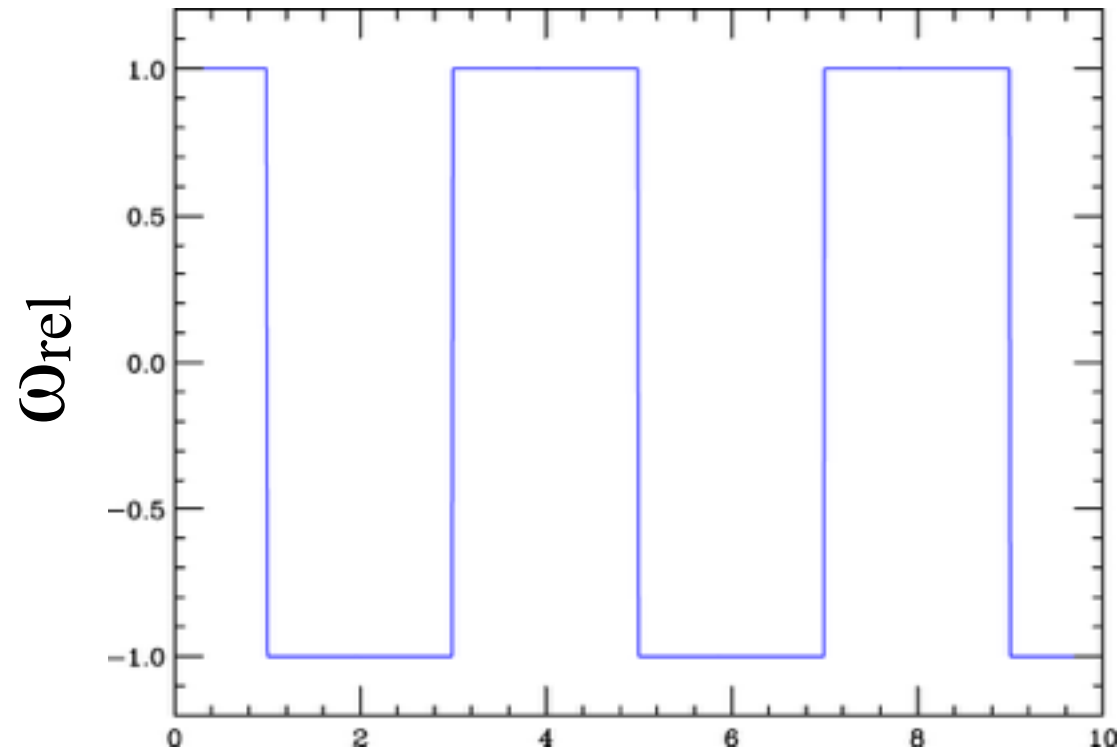
- Scintillation rate is

$$S \propto (\delta\theta_0)^2 \quad \text{No nEDM}$$

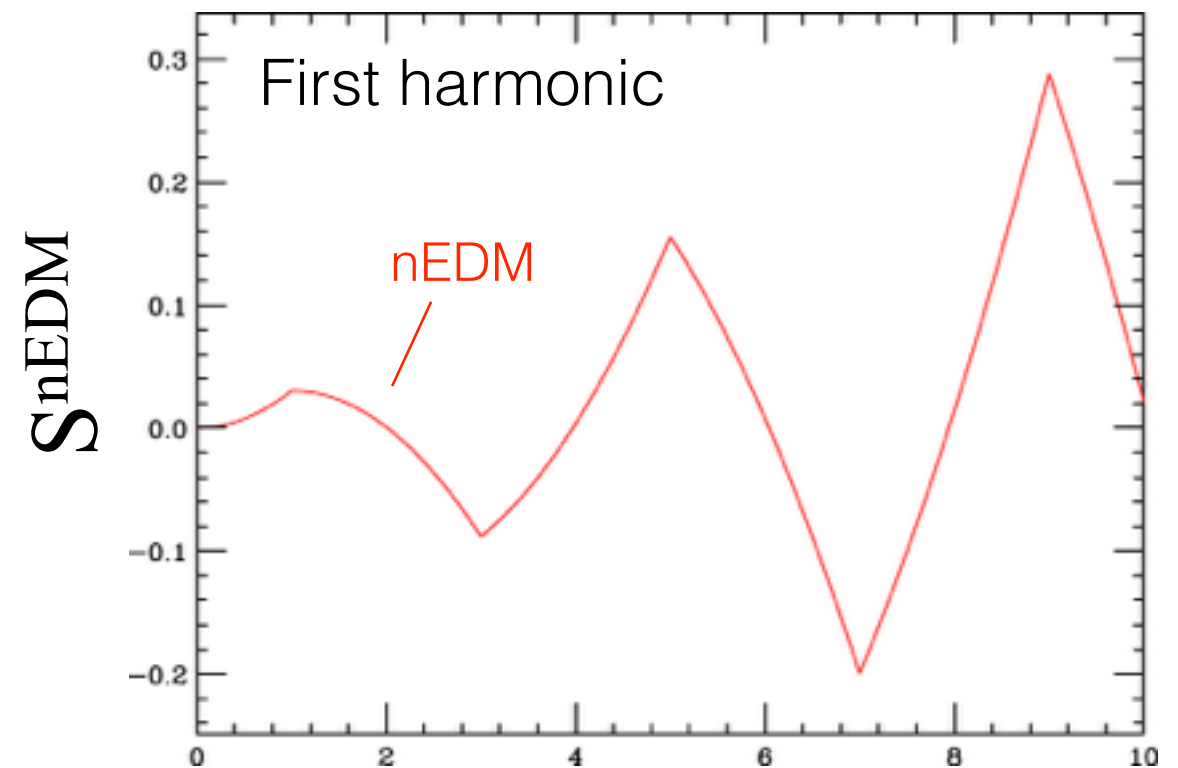
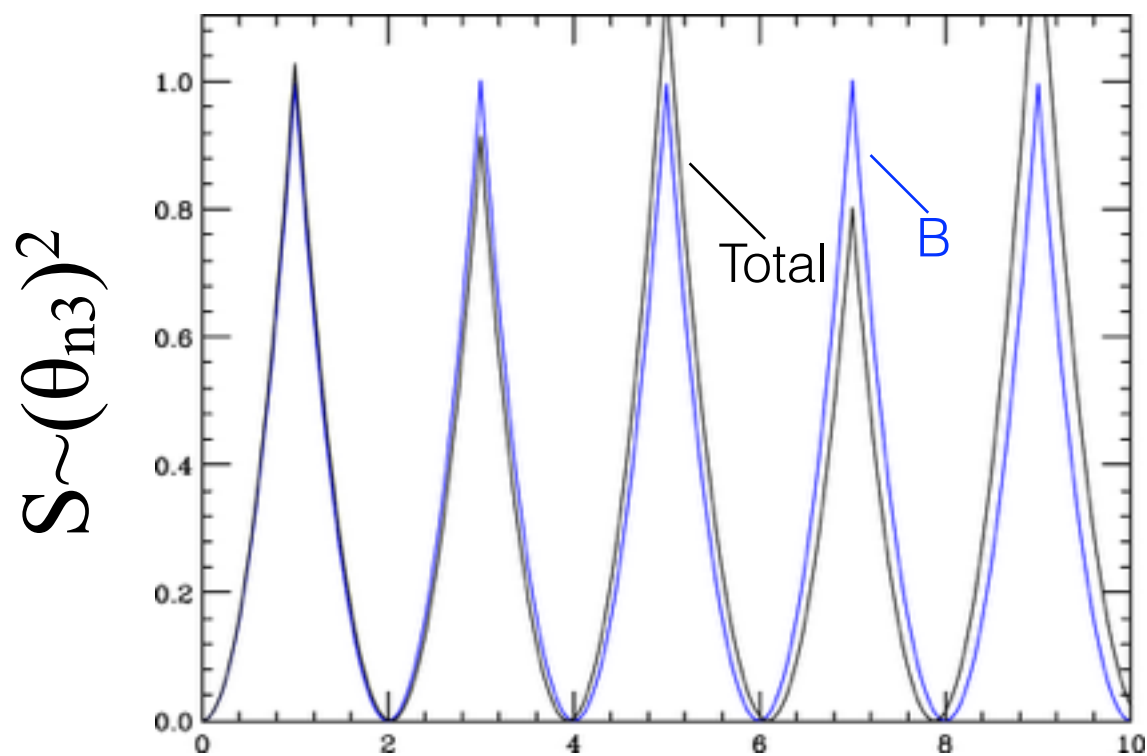
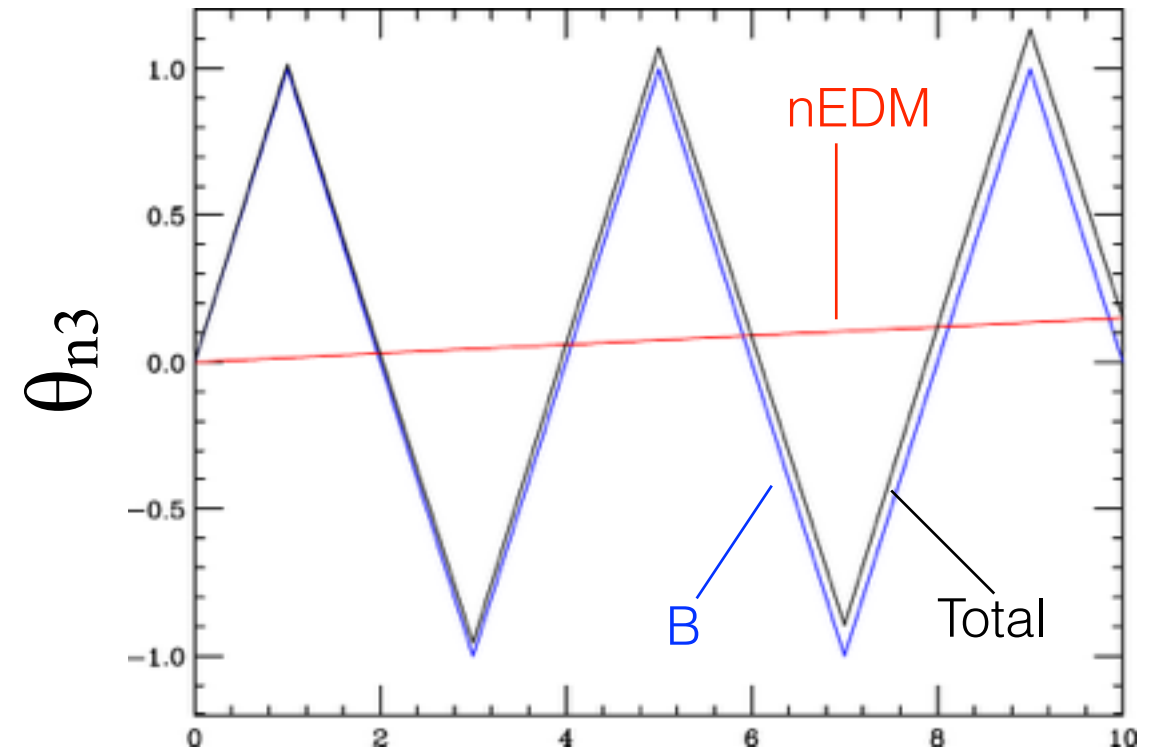
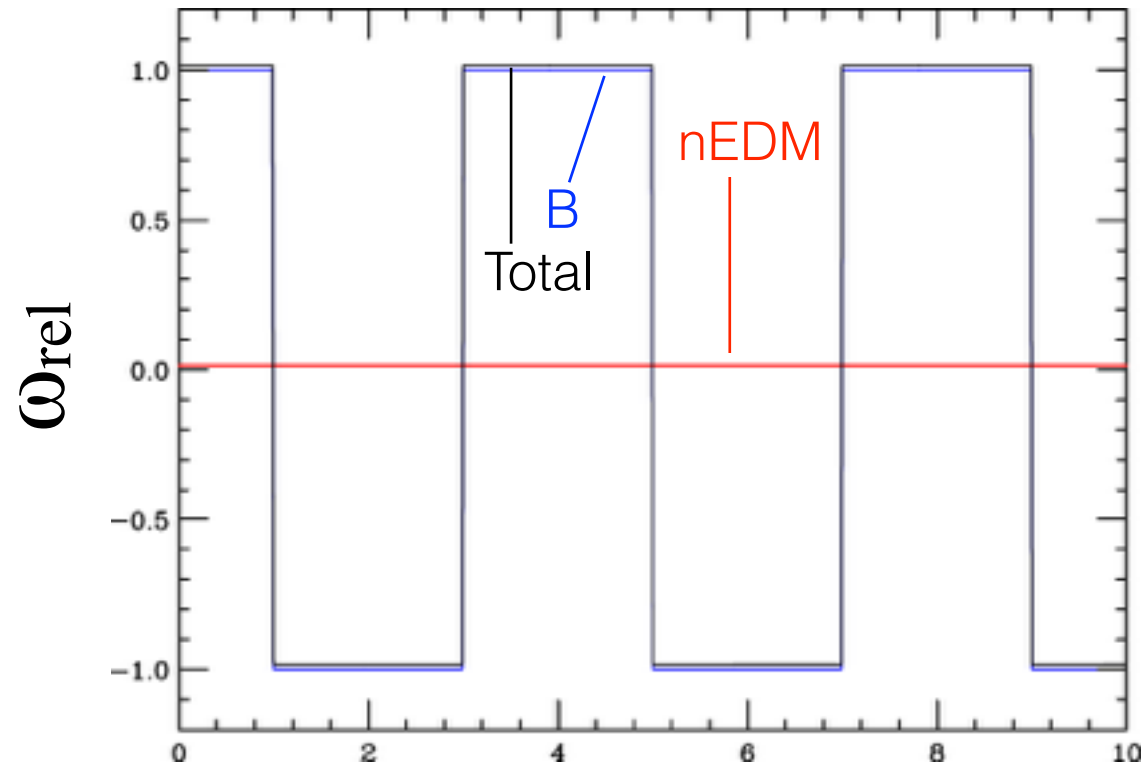
$$S \propto (\delta\theta)^2 = (\delta\theta_0)^2 + 2\delta\theta_0 kd_n E t \quad \text{With nEDM}$$

In the absence of nEDM, the scintillation rate will only show a second harmonic $(\delta\theta_0)^2$. An nEDM will produce a first harmonic term increasing linearly in time.

Without nEDM (with square modulation)

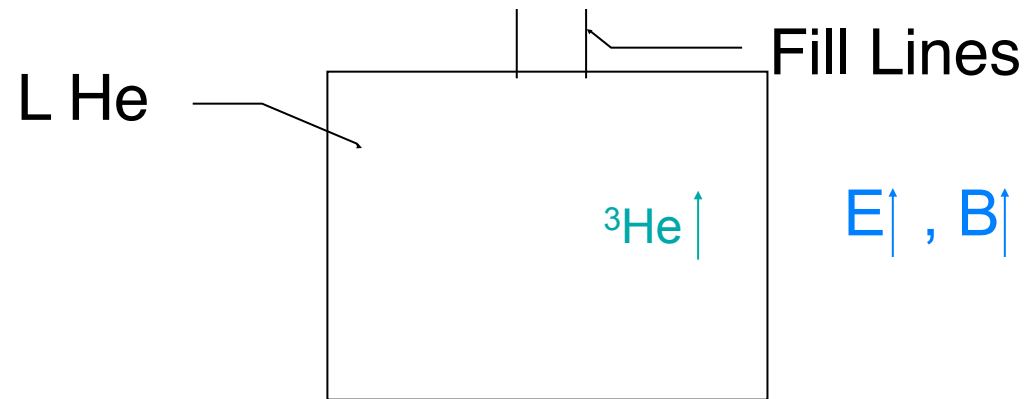


With nEDM (with square modulation)

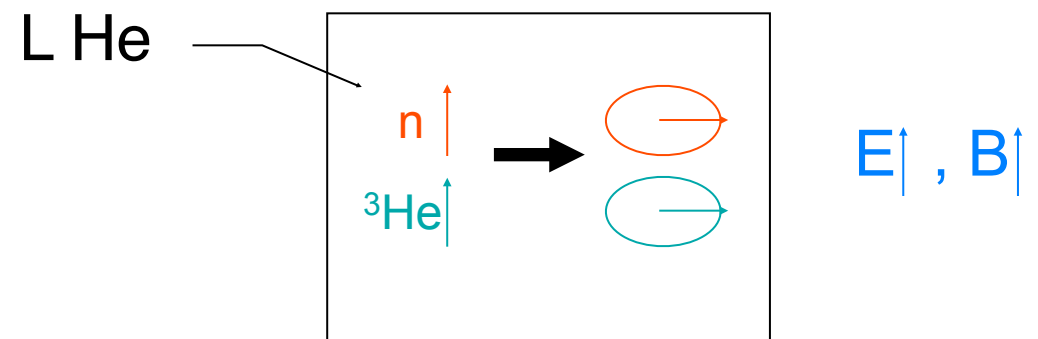


Experiment Cycle

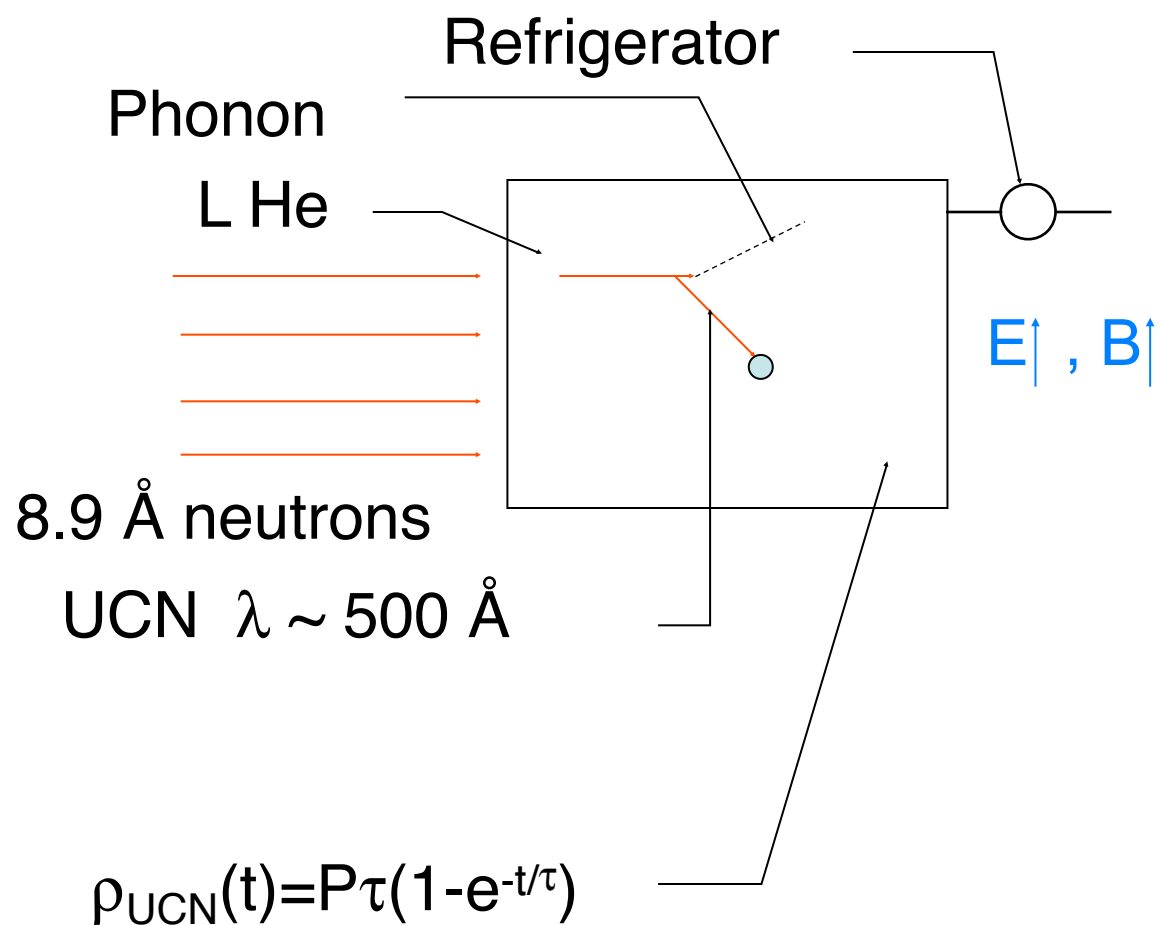
$T = 0 - 40$ s Fill ${}^4\text{He}$ with ${}^3\text{He}$



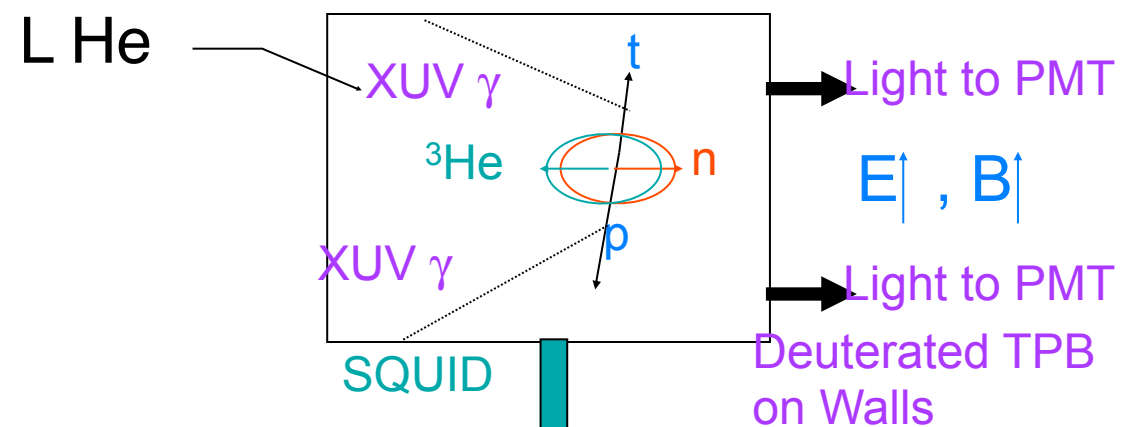
$T = 1040 - 1041$ s $\pi/2$ pulse



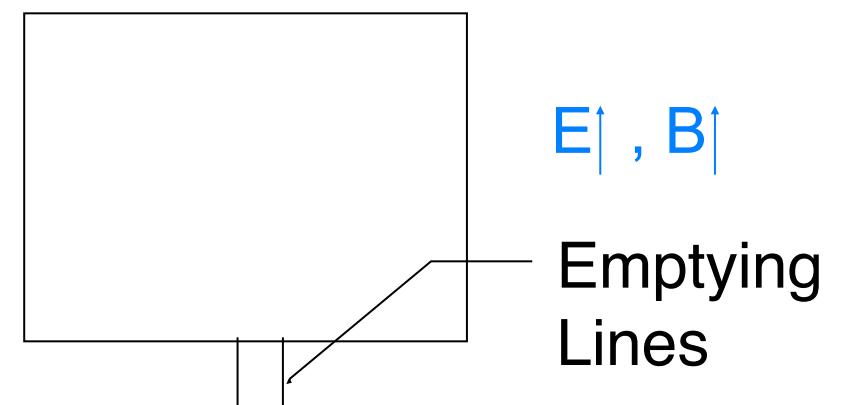
$T = 40 - 1040$ s $\overline{\text{UCN}}$ from Cold \bar{n}



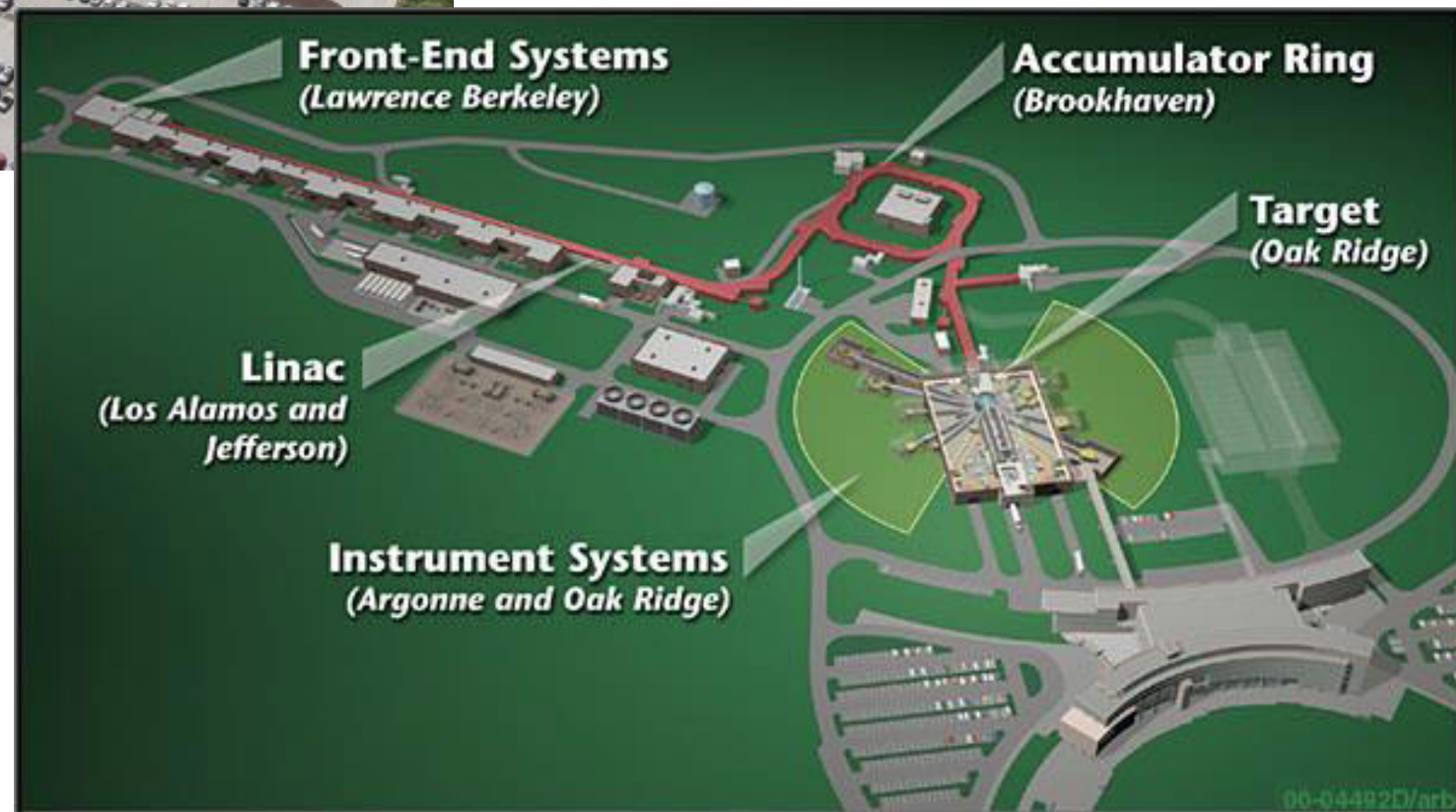
$T = 1041 - 2041$ s Precession about \vec{E} & \vec{B}



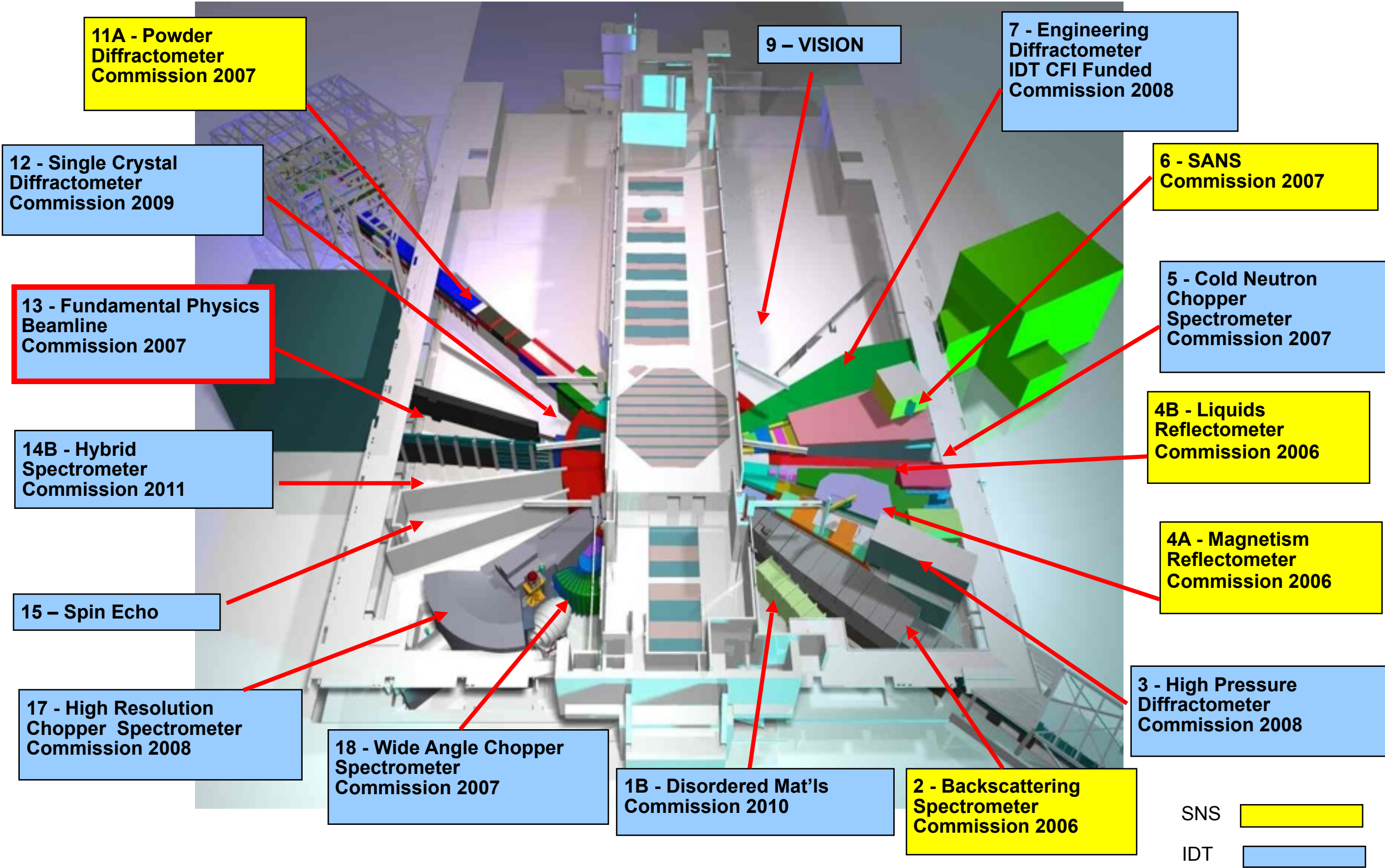
$T = 2041 - 2421$ s Remove ${}^3\text{He}$



Spallation Neutron Source (SNS)



SNS Target Hall



SNS nEDM Experiment Apparatus

Magnetically shielded house

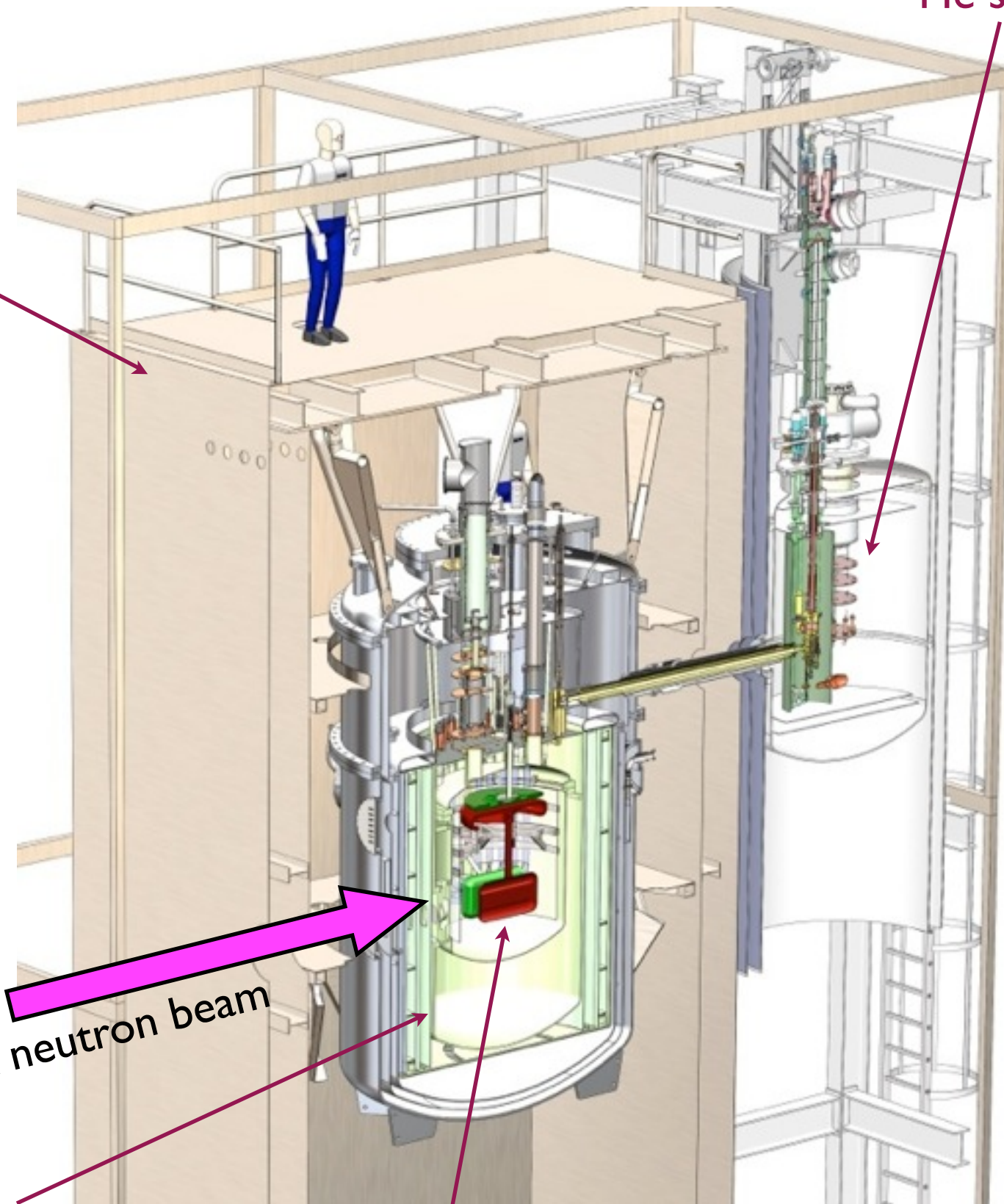
^3He services

Goal: $\delta d_n \sim 3 \times 10^{-28} \text{ e}\cdot\text{cm}$

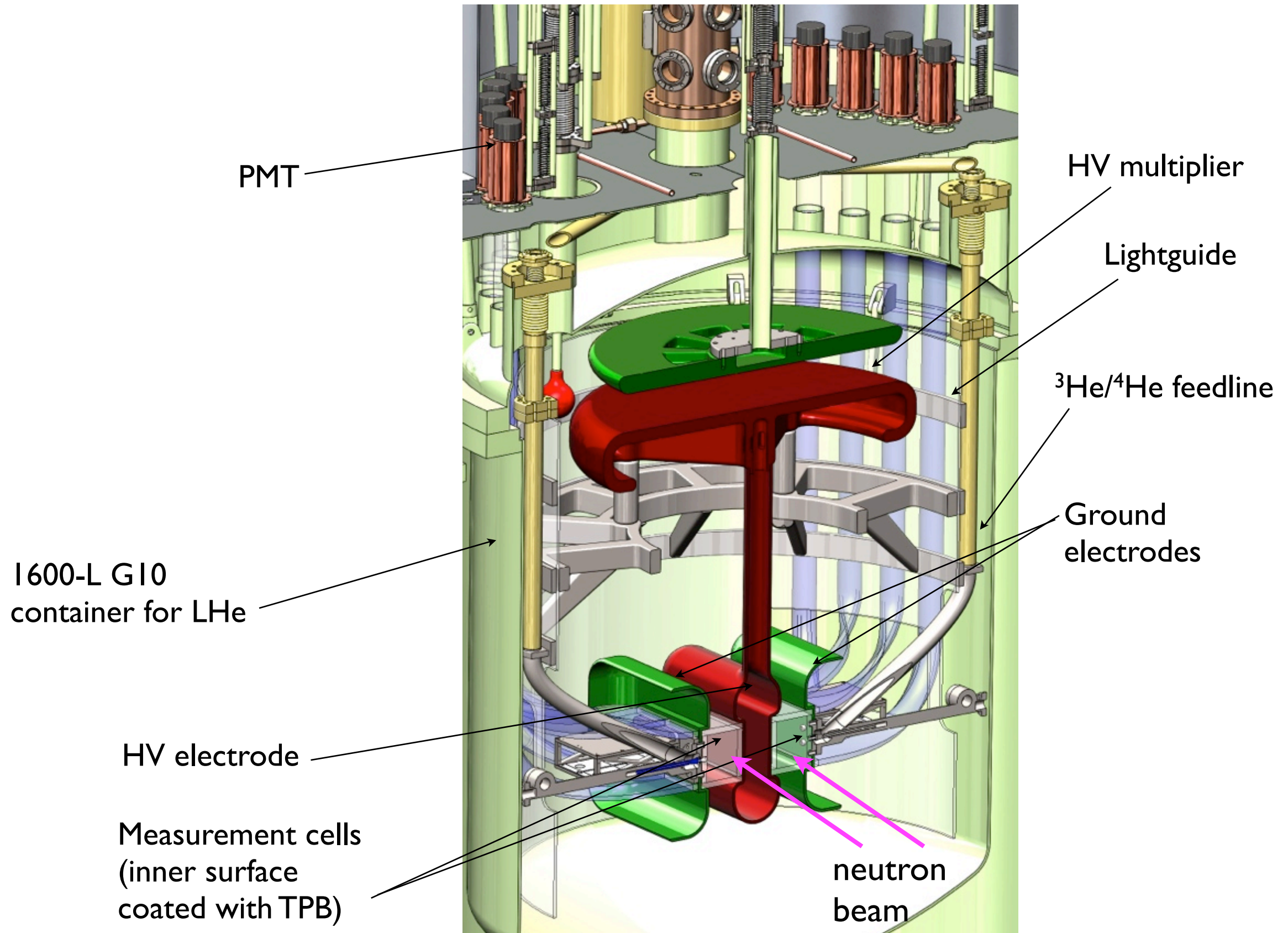
8.9 Å neutron beam

Magnet and shielding package

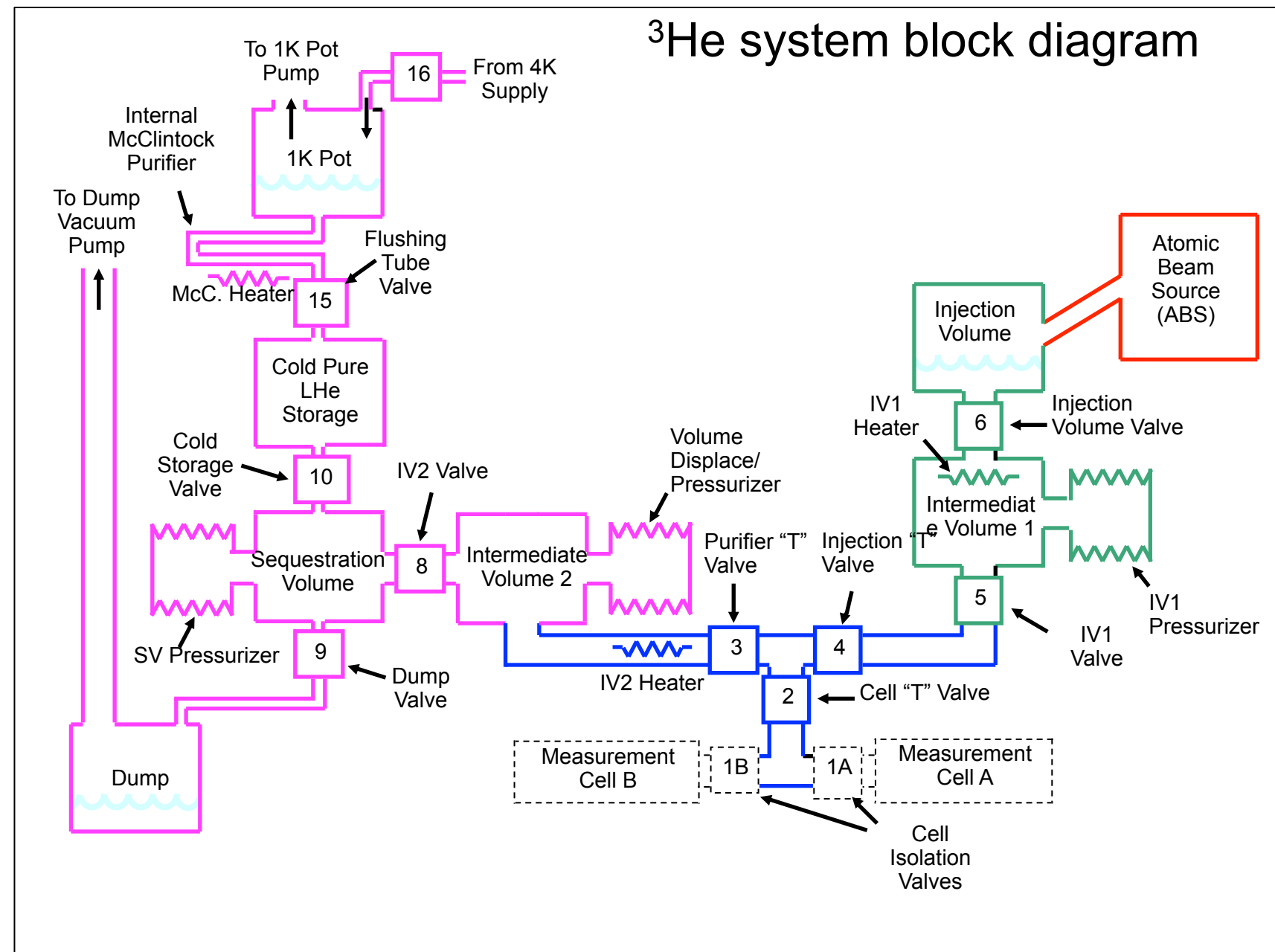
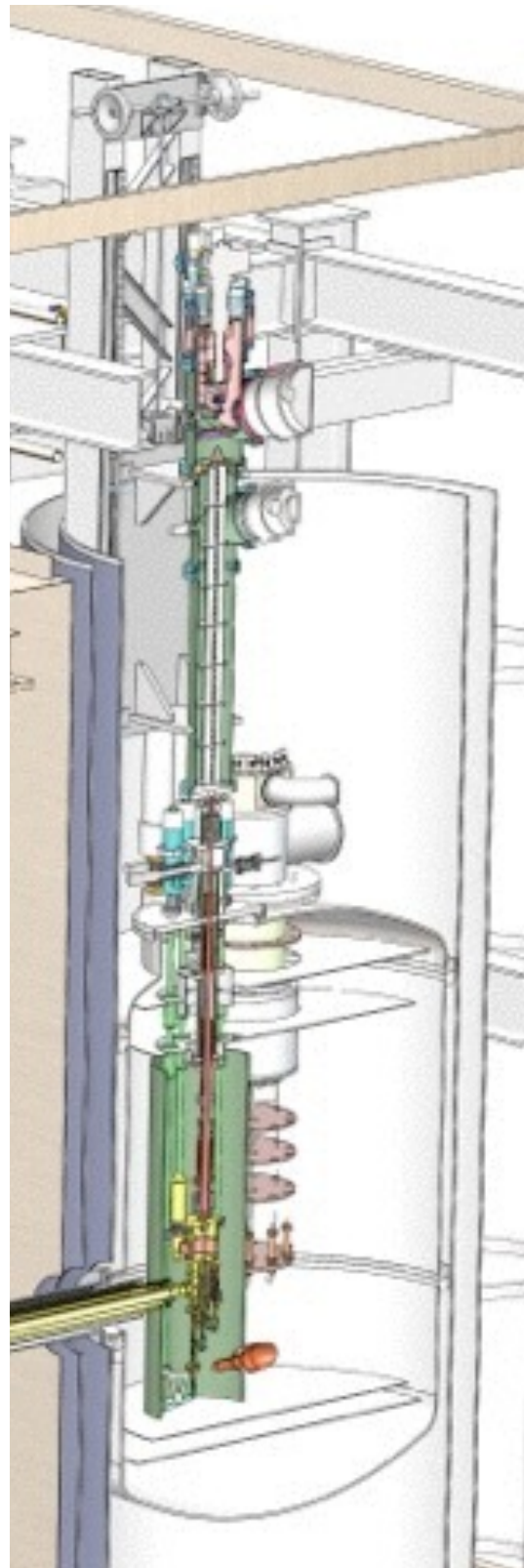
Central LHe volume (400 mK, 1600 liters)



Central Detector System



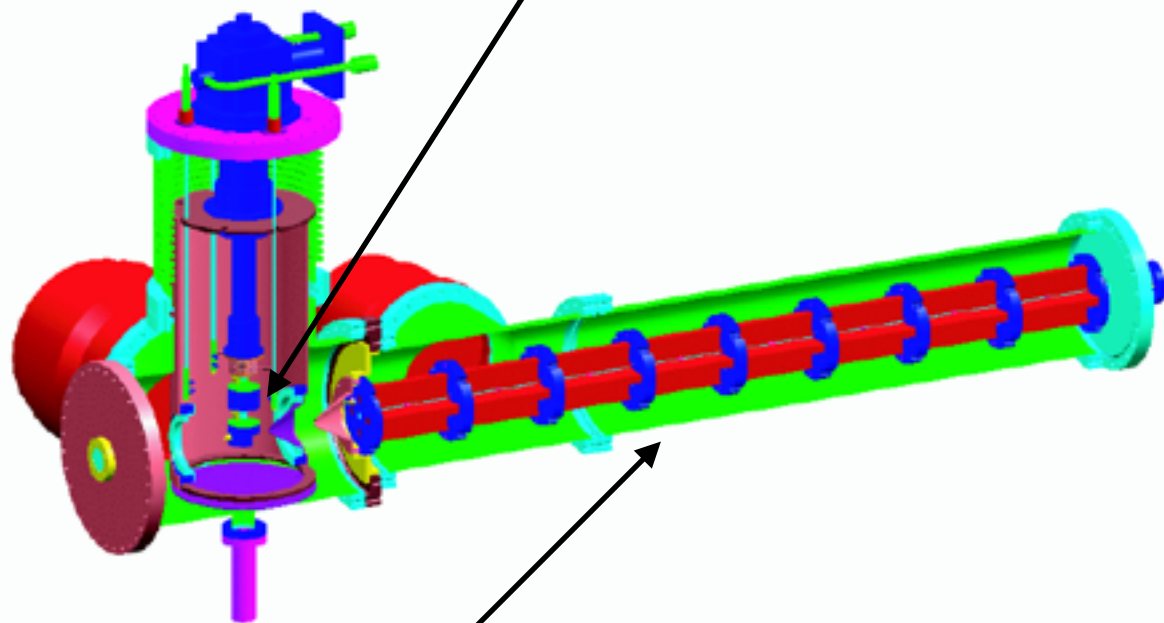
^3He Services



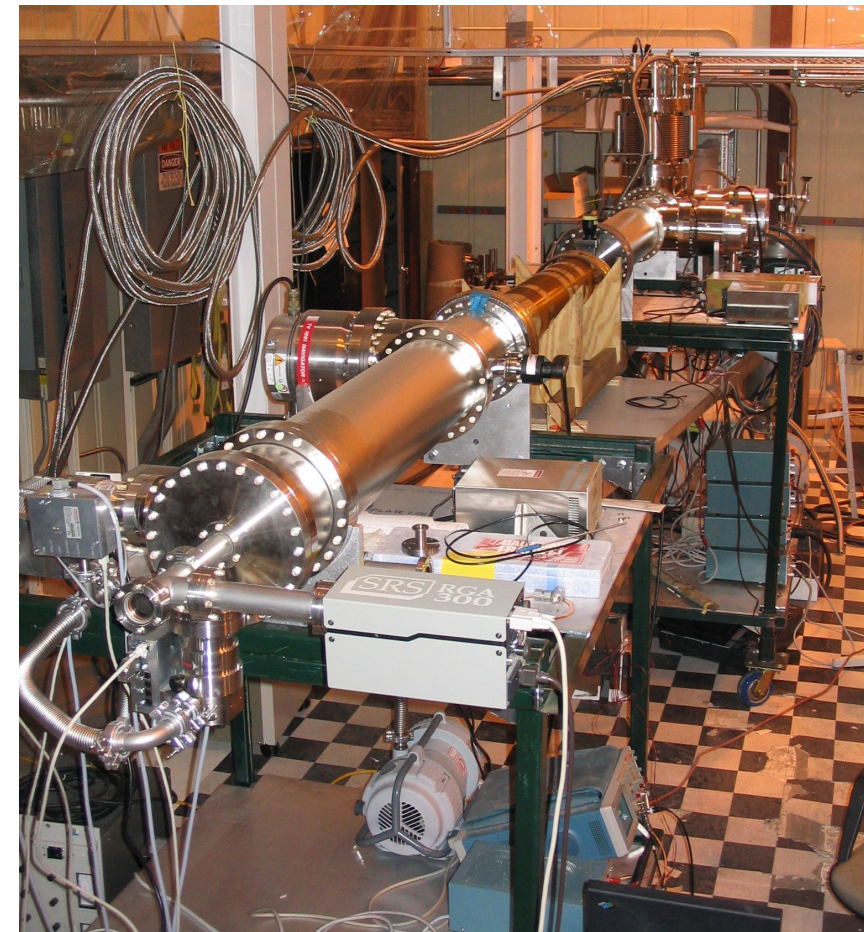
- Heat flush and diffusion methods is used to move ^3He
- ^3He flow is controlled by heaters, valves, and pressurizers.

^3He atomic beam source

^3He gas is delivered to a nozzle held at 1.4 K cooled by a cryocooler



1 m long quadrupole-spin-state selector constructed from NdFeB permanent magnets (filed at pole surface 7.5 kG)



^3He Atomic Beam Source
($P=99.6\pm 0.25\%$, flux= 10^{14} atoms/s)

Brief description available in
S. Eckel, et al. PRA 85, 032124 (2012)

Heat flush

- Two-fluid model

Mass $\rho = \rho_n + \rho_s$

Momentum $j = \rho_n v_n + \rho_s v_s$

Normal fluid $\rho_n \quad \eta = \eta_n \quad S_n = S_{\text{He}}$

Superfluid $\rho_s \quad \eta = 0 \quad S_s = 0$

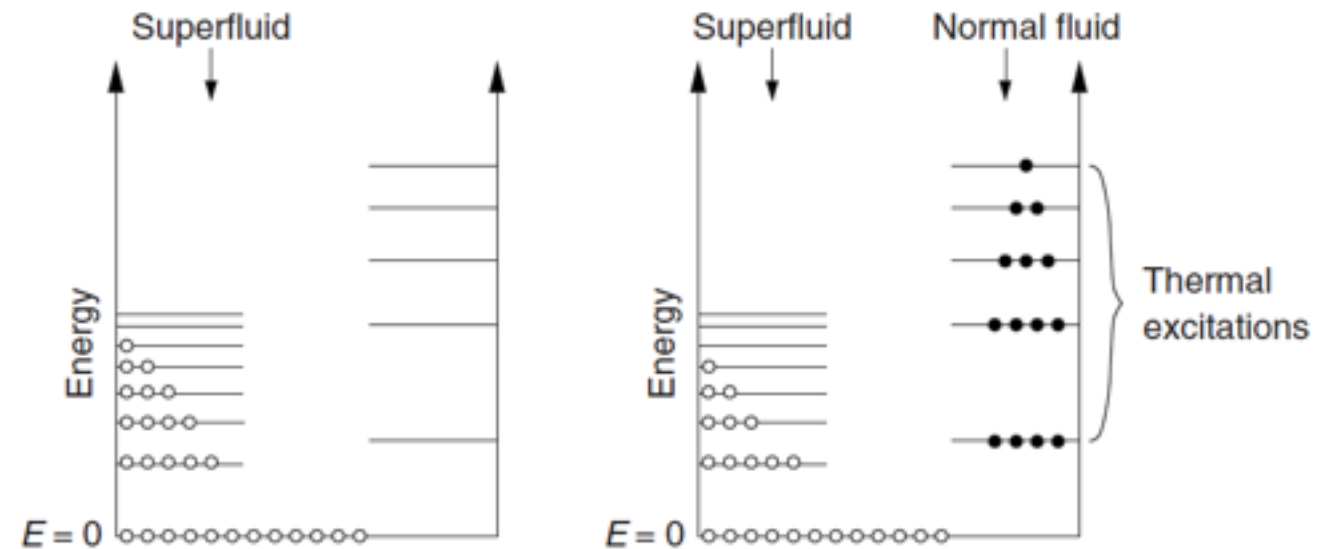
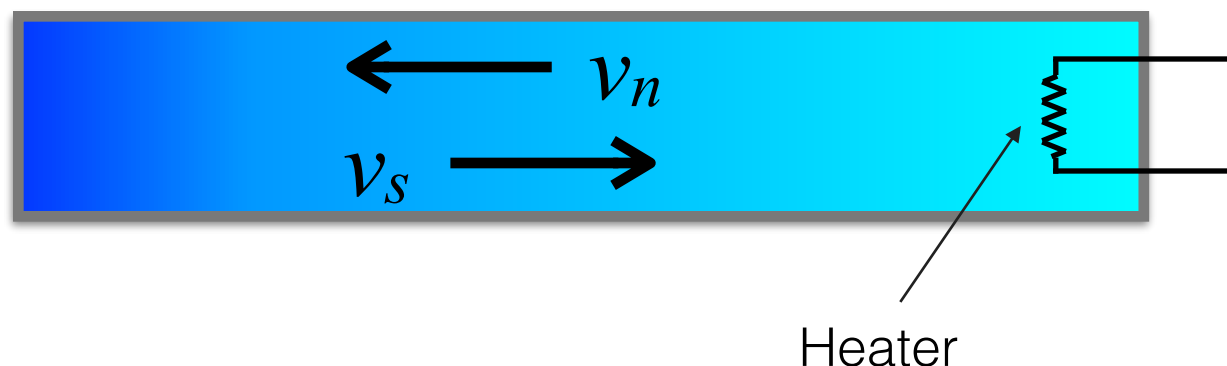


Fig. 2.32. Schematic illustration of the population of the superfluid and normal-fluid component in helium II. (a) At $T = 0$, all helium atoms belong to the superfluid component. Due to interaction, however, some atoms are scattered into virtual states with $E > 0$. (b) At finite temperatures, thermal excitations also occur, which are identical to longitudinal phonons at very low temperatures. As we shall see later, these thermal excitations form the normal-fluid component

Figure taken from C. Enss "Low-Temperature Physics", Springer 2005

- Heat flush



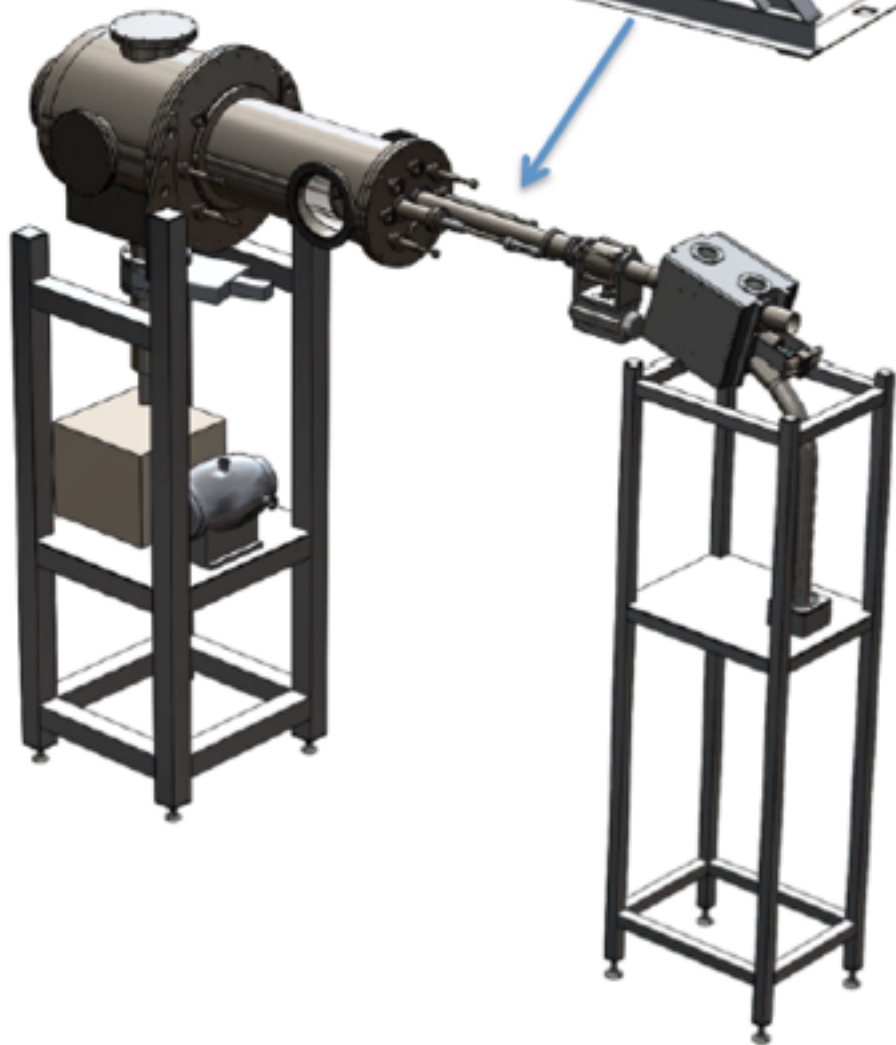
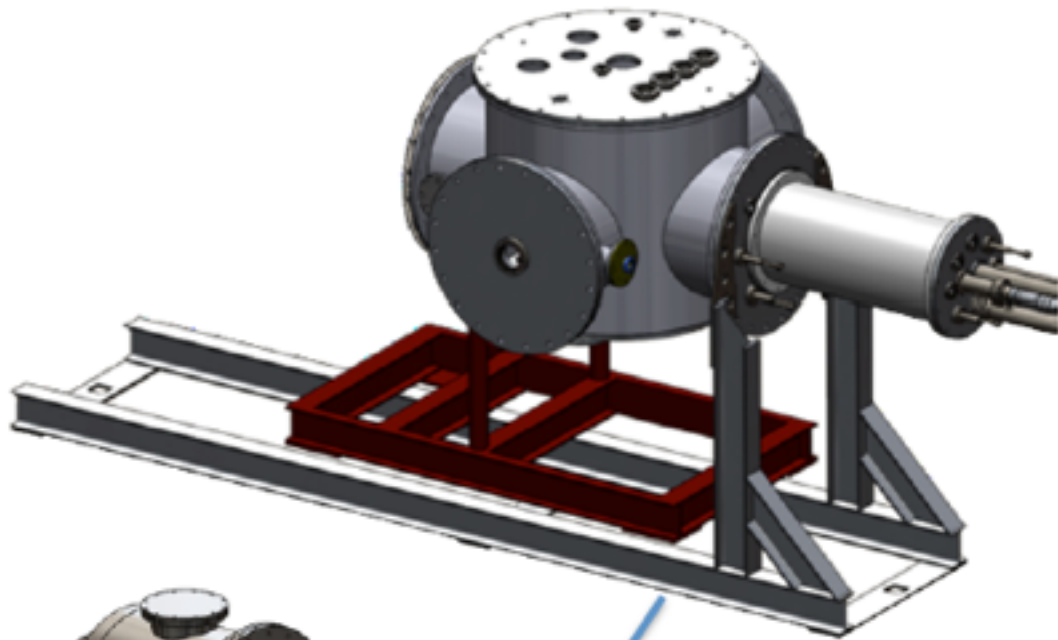
Normal fluid flows away from the heater at velocity v_n , carrying with it the impurities, which are unaffected by the fact that the superfluid component is simultaneously flowing at velocity v_s toward the heater.

McClintock, Cryogenics **18**, 201 (1978)

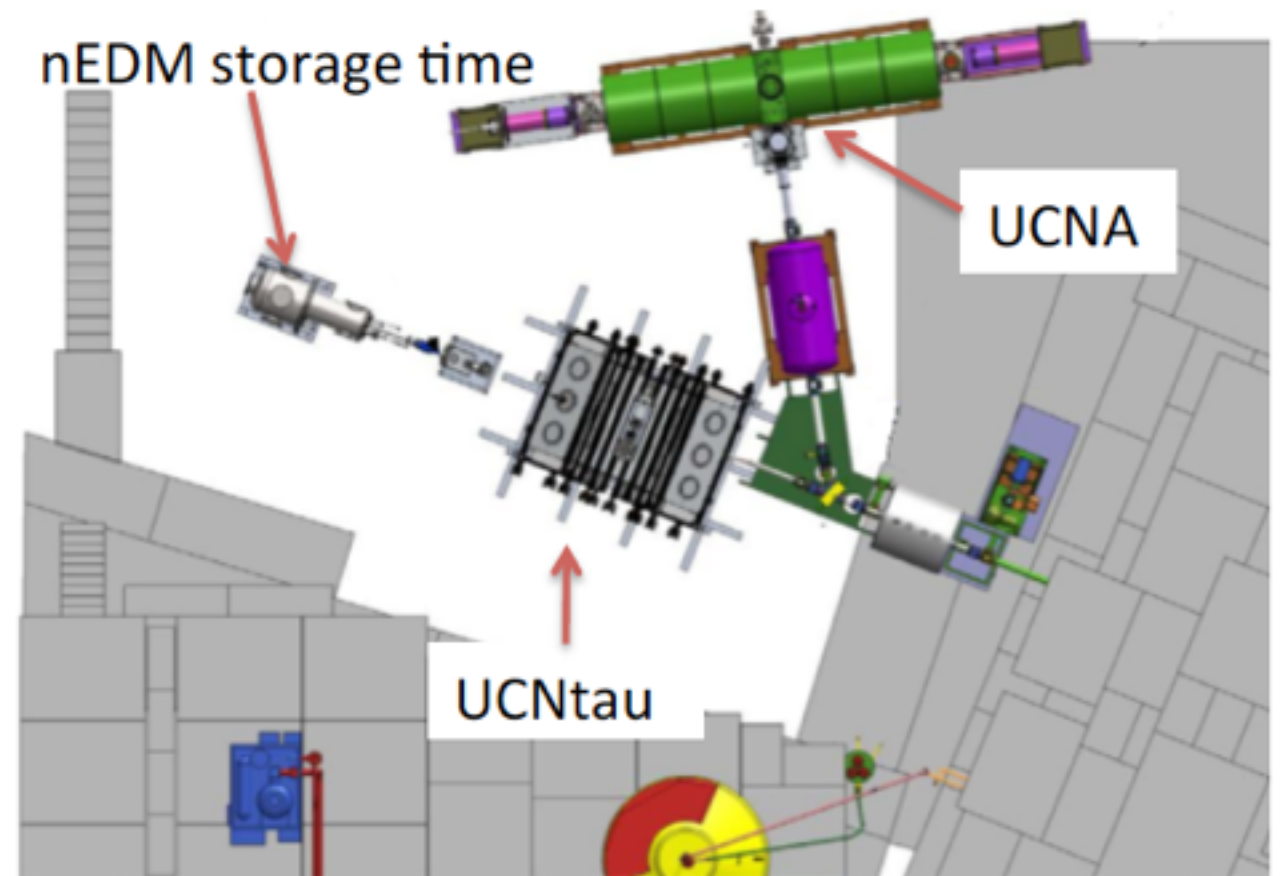
SNS nEDM R&D

- Cold neutron beam transport
- Cryogenics
- ^3He injection, transport, and removal
- Electric field
- Magnetic field and shielding
- UCN storage
- Detectors (SQUID, light detection)
- Systematics test apparatus

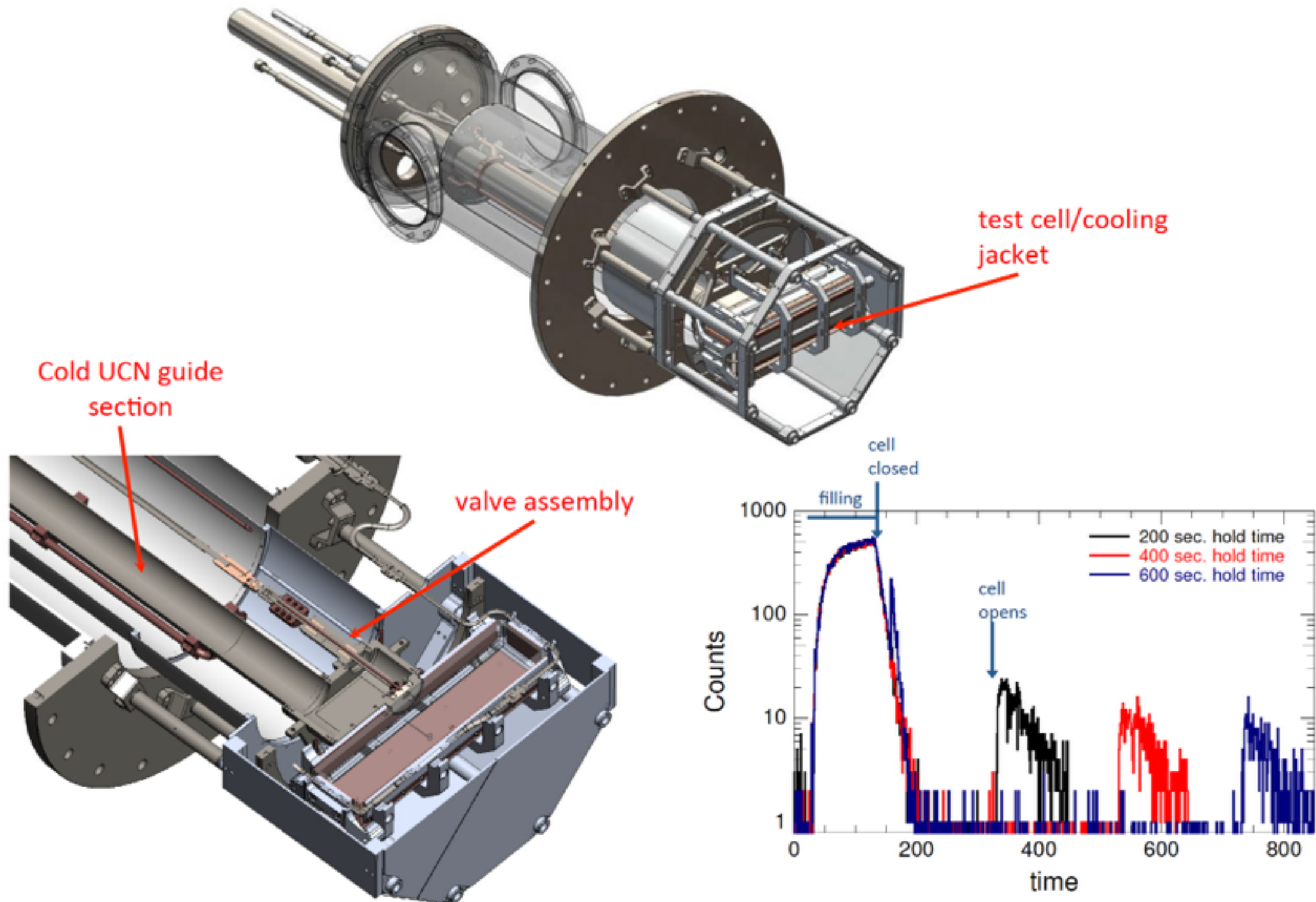
UCN storage R&D



Layout at Area B, LANL:

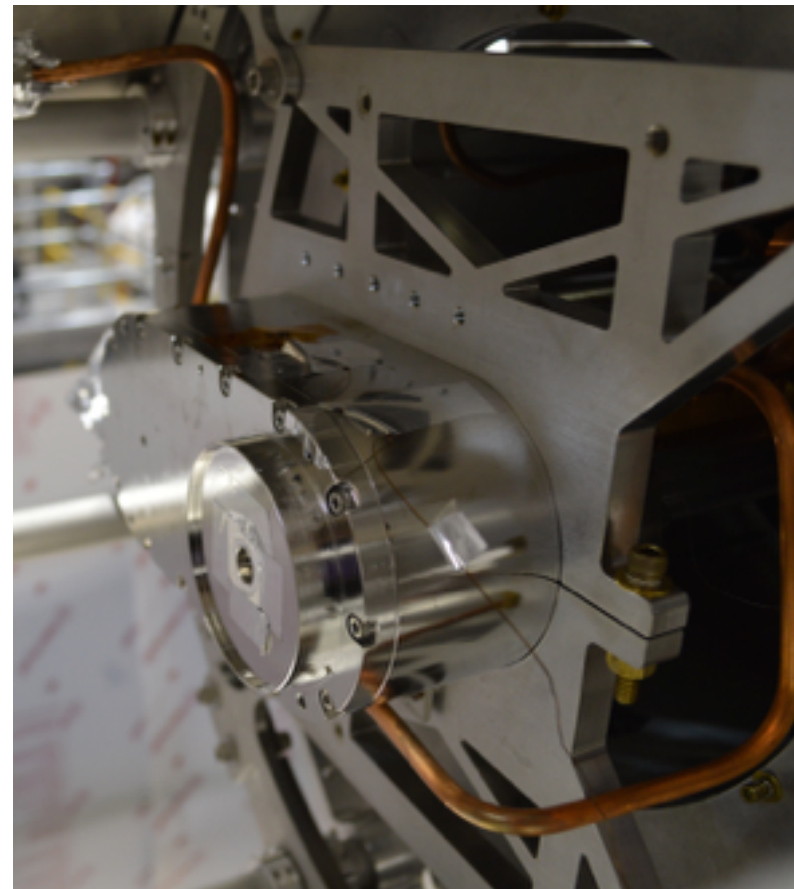
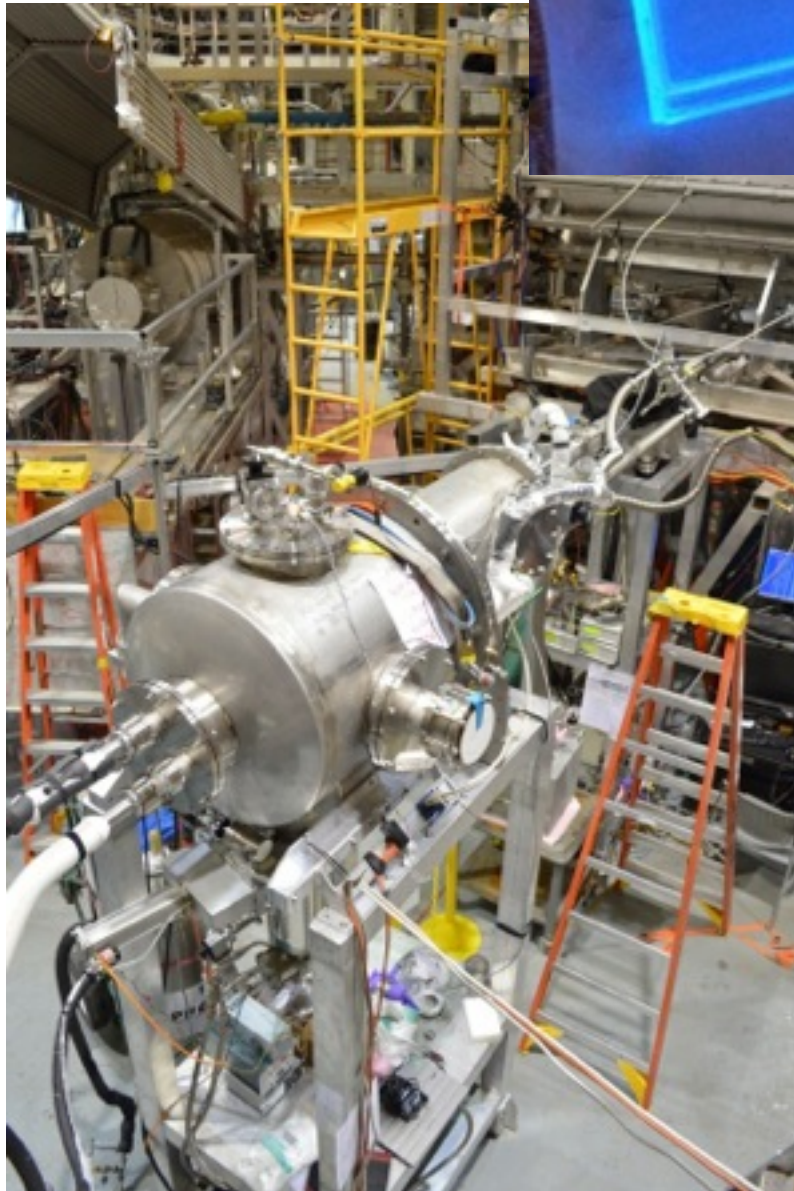
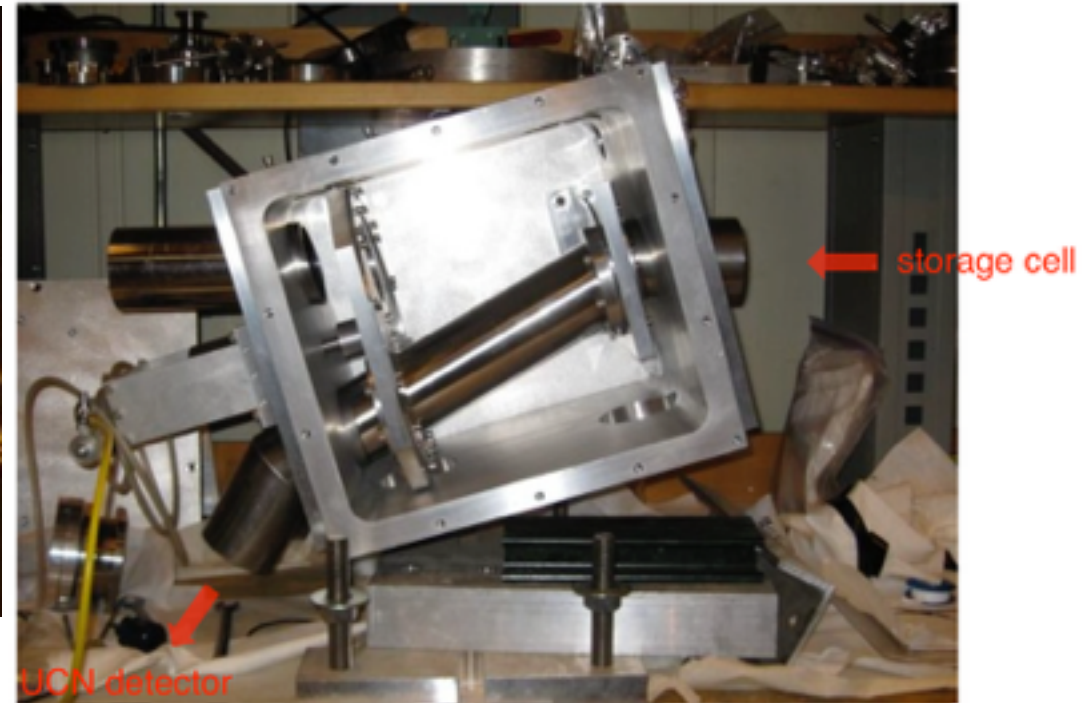
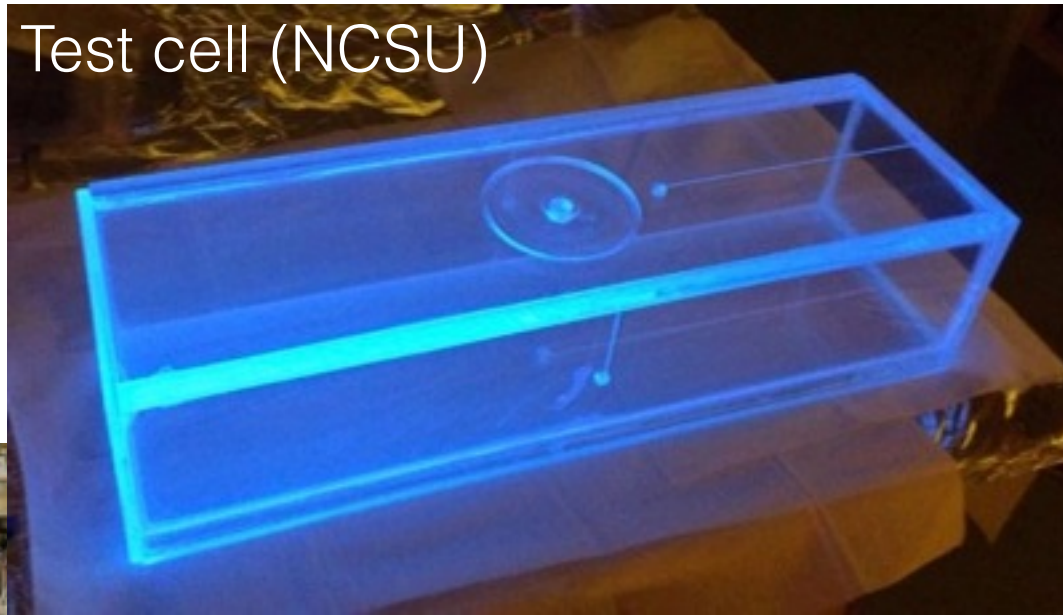


UCN storage time apparatus

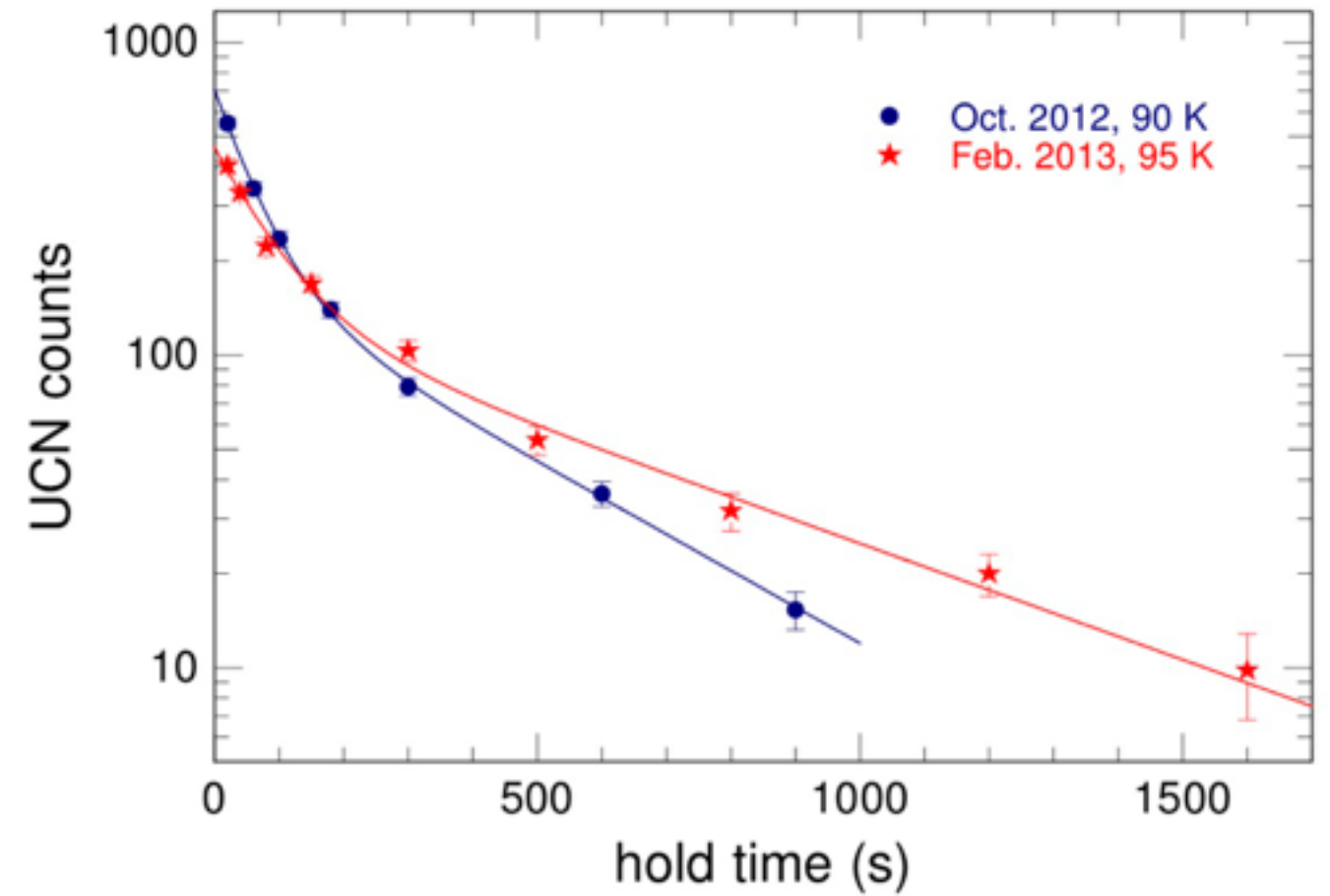
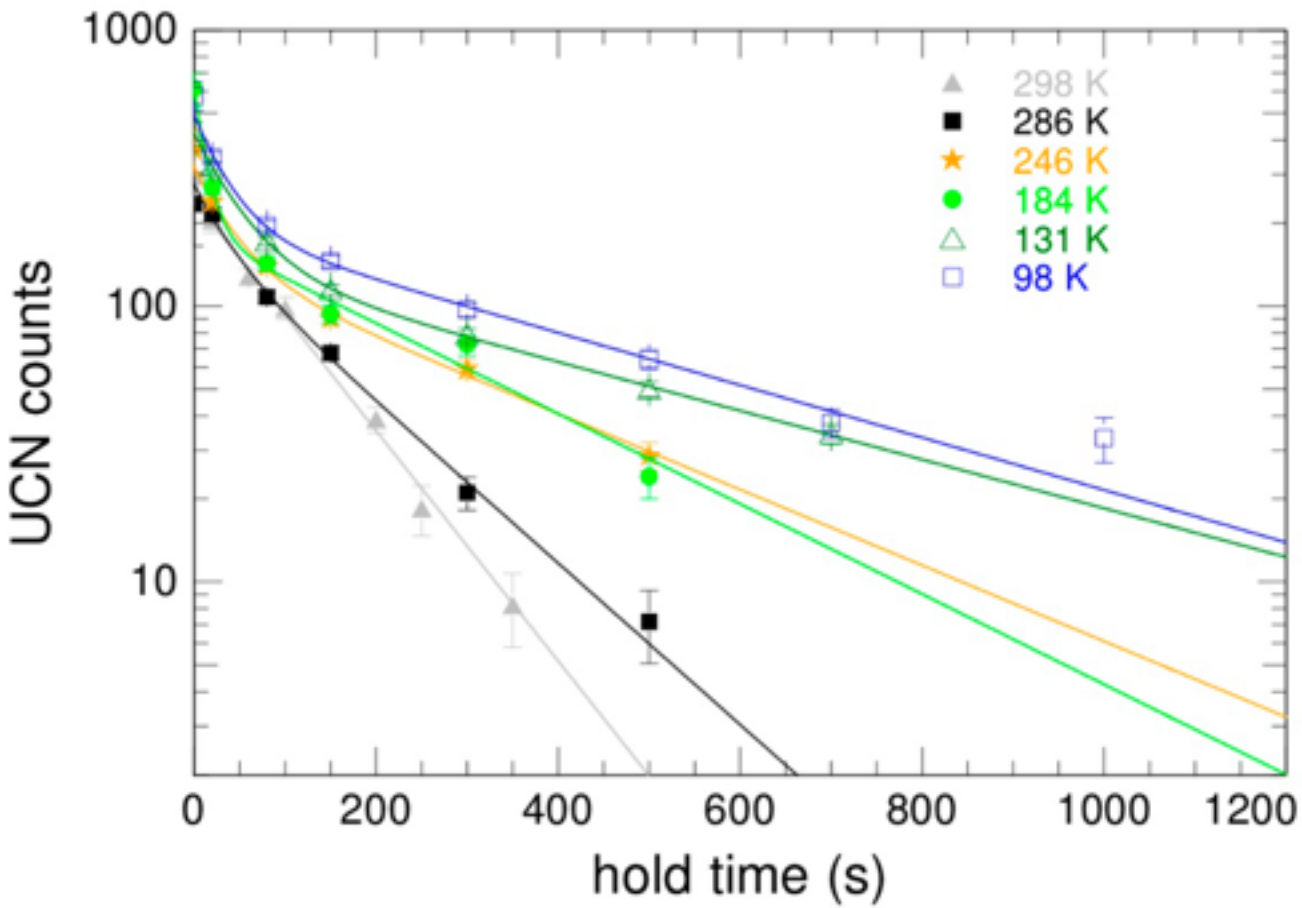


UCN storage test apparatus

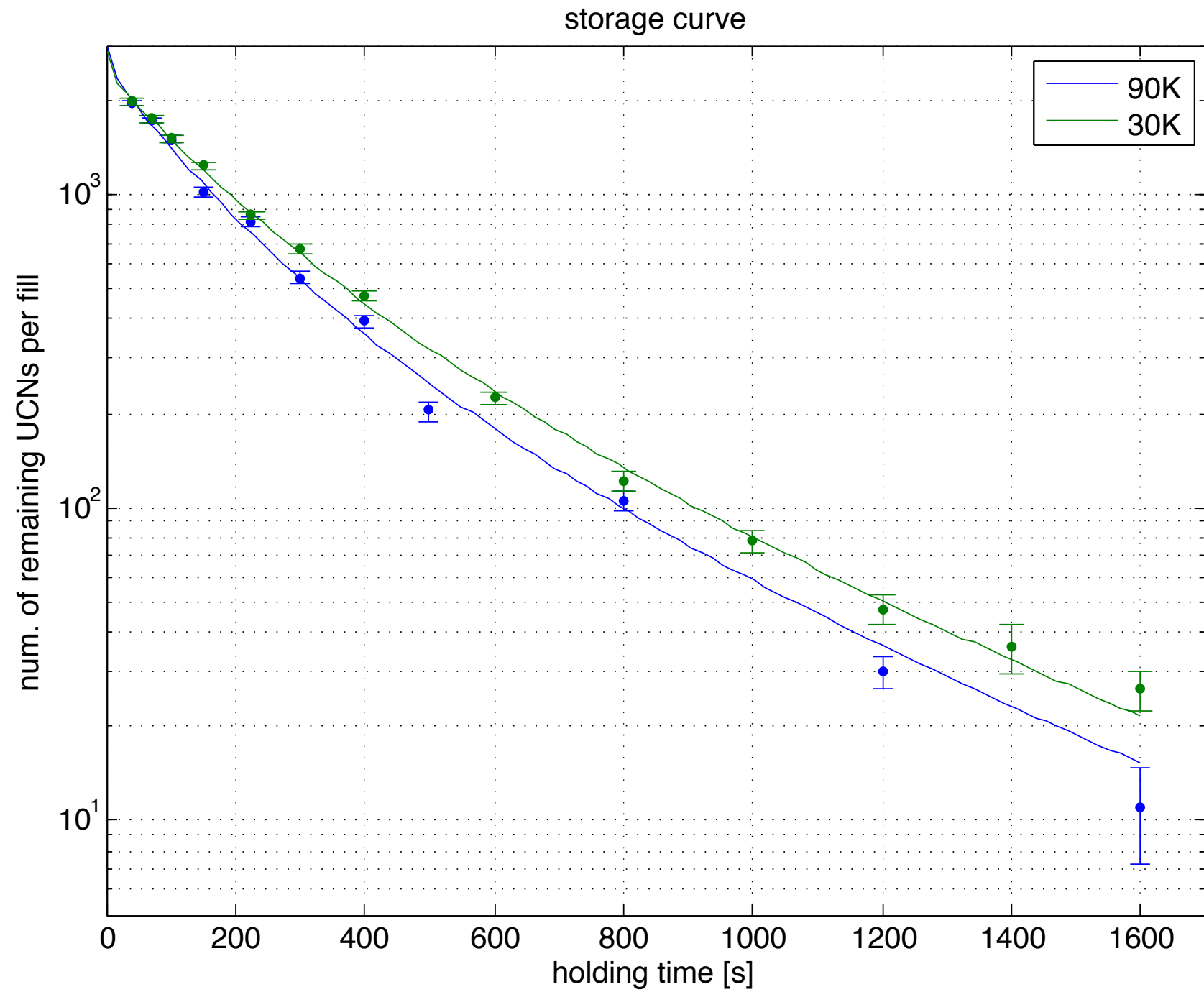
Test cell (NCSU)



Previous UCN storage time data



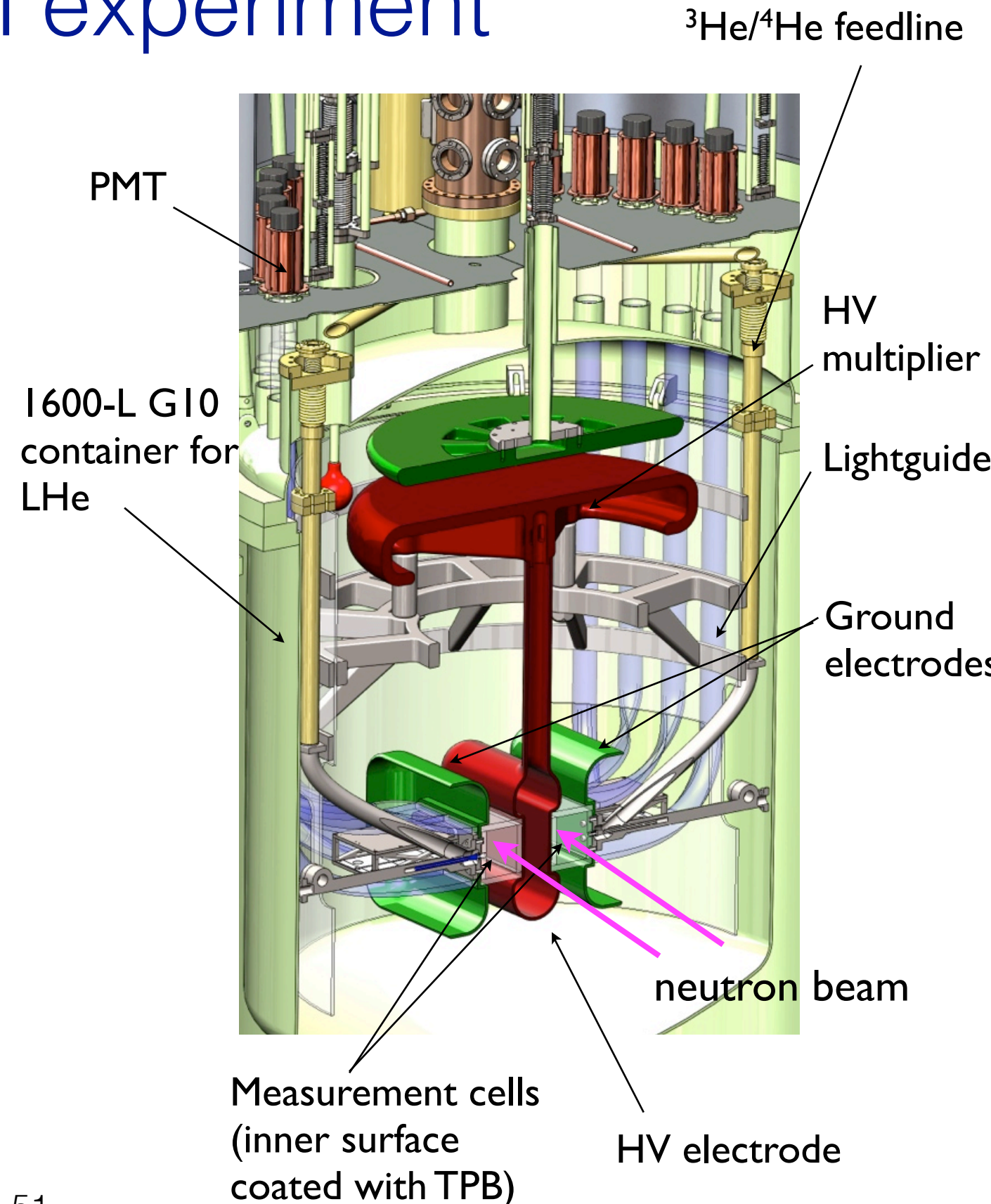
Jan 2015 UCN storage data



Cell fabricated at NSCU

Requirements/goals for HV in the SNS nEDM experiment

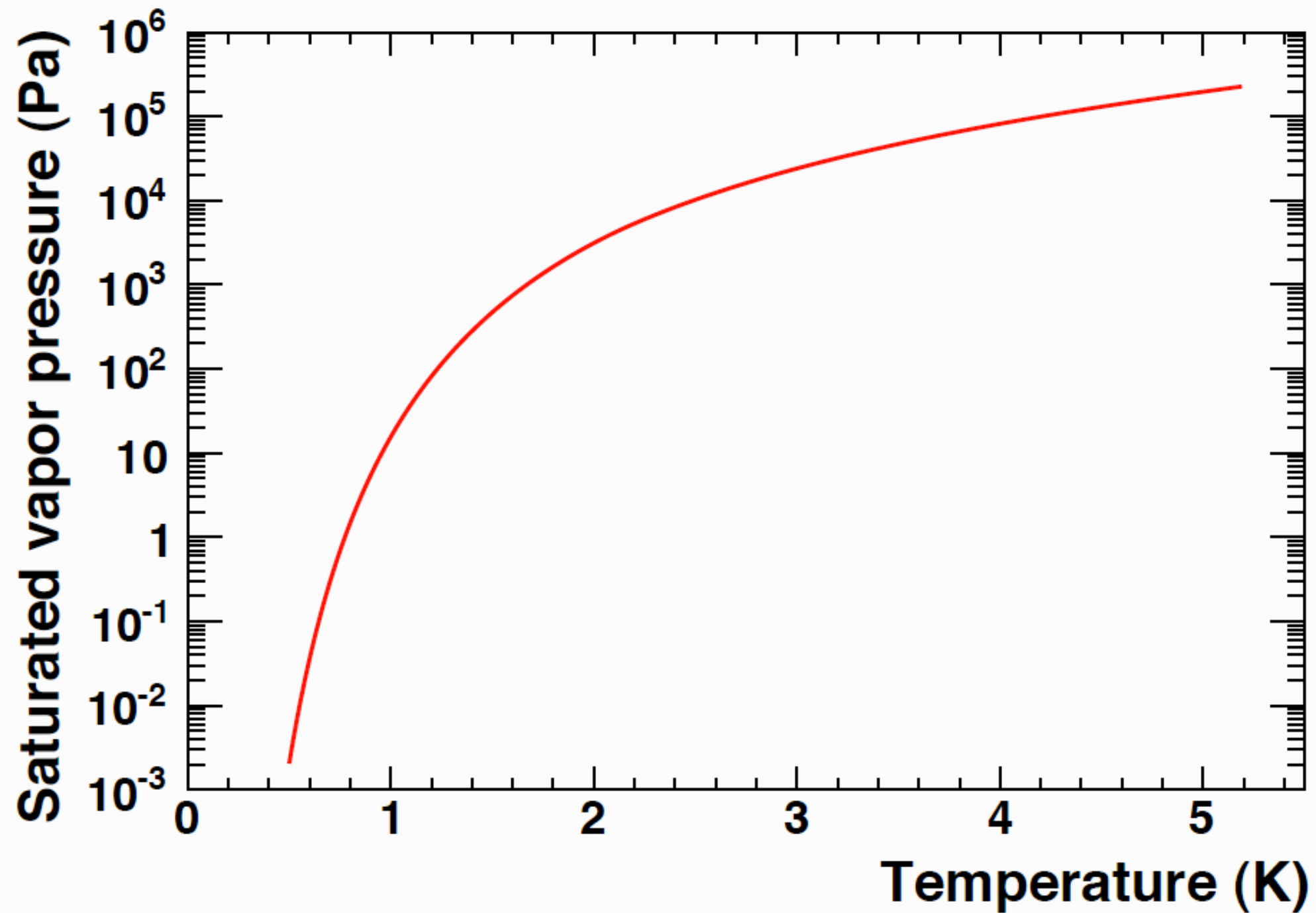
- Electric field goal:
 - 70kV/cm inside the measurement cells
 - Inner dimension: $40 \times 7.62 \times 10.16 \text{ cm}^3$
 - Wall thickness: 1.27 cm
 - Minimum leakage current between the electrodes
- Electrode material requirements:
 - Electrodes made of PMMA coated with conductive material
 - Electrical resistivity: $10^2 \Omega/\square < R_s < 10^8 \Omega/\square$
 - Robust to thermal cycling and sparking
 - Minimal activation due to exposure to neutron beam
 - Non-magnetic
 - Fabrication technique scalable to large ($10 \times 40 \times 80 \text{ cm}^3$) complicated 3D shape



Electrical Breakdown in LHe

- Prior to the Sussex and LANL efforts, data existed for 1.2 - 4.2 K, mostly at SVP (bulk of the data were taken at 4.2 K)
 - For varying geometries (plane-plane, sphere-plane, sphere-sphere)
 - In general, very little consistency
- No satisfactory models or theories
- However, a consideration mean free path of ions in LHe suggests a very high intrinsic breakdown field (> 10 MV/cm)
- Generally accepted picture:
 1. Vapor bubble formation (e.g. field emission from asperities on the cathode)
 2. Growth of bubble
 3. Breakdown through the gas
- Parameters that may affect the breakdown field include:
 - Electrode material and surface quality
 - Electrode area (Weber and Endicott, Trans. AIEE 75, 371 (1956))
 - Gap size
 - Temperature and pressure

LHe saturated vapor pressure

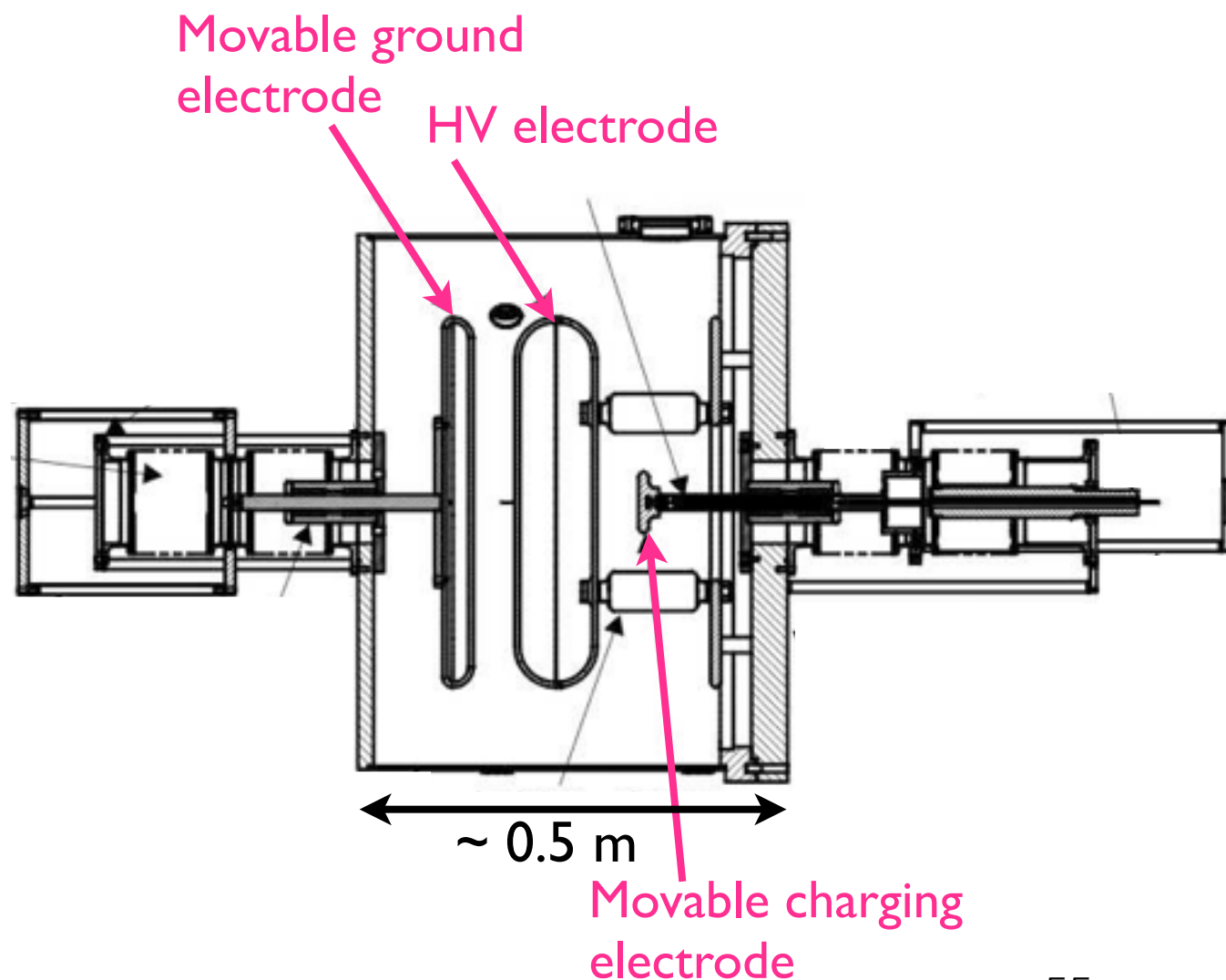


R&D performed so far

- Large Scale HV Test at LANL (electrode size ~ 50 cm in diameter)
 - HV generation
 - Temperature/pressure dependence of breakdown field by evaporative cooling to down to 1.6 K
- Medium Scale HV Test at LANL (electrode size ~ 12 cm in diameter)
 - Temperature dependence down to 0.4 K
 - Pressure dependence between SVP and 1 atm
 - Electrode material dependence
 - Gap dependence
- Electrode material candidate resistivity measurement at LANL
 - Temperature dependence of resistivity down to 1.5 K
- Small Scale HV Test at IU and LANL (electrode size ~ 2 cm in diameter)
 - Temperature dependence down to 1.5 K
 - Pressure dependence between SVP and 1 atm
 - Electrode material dependence

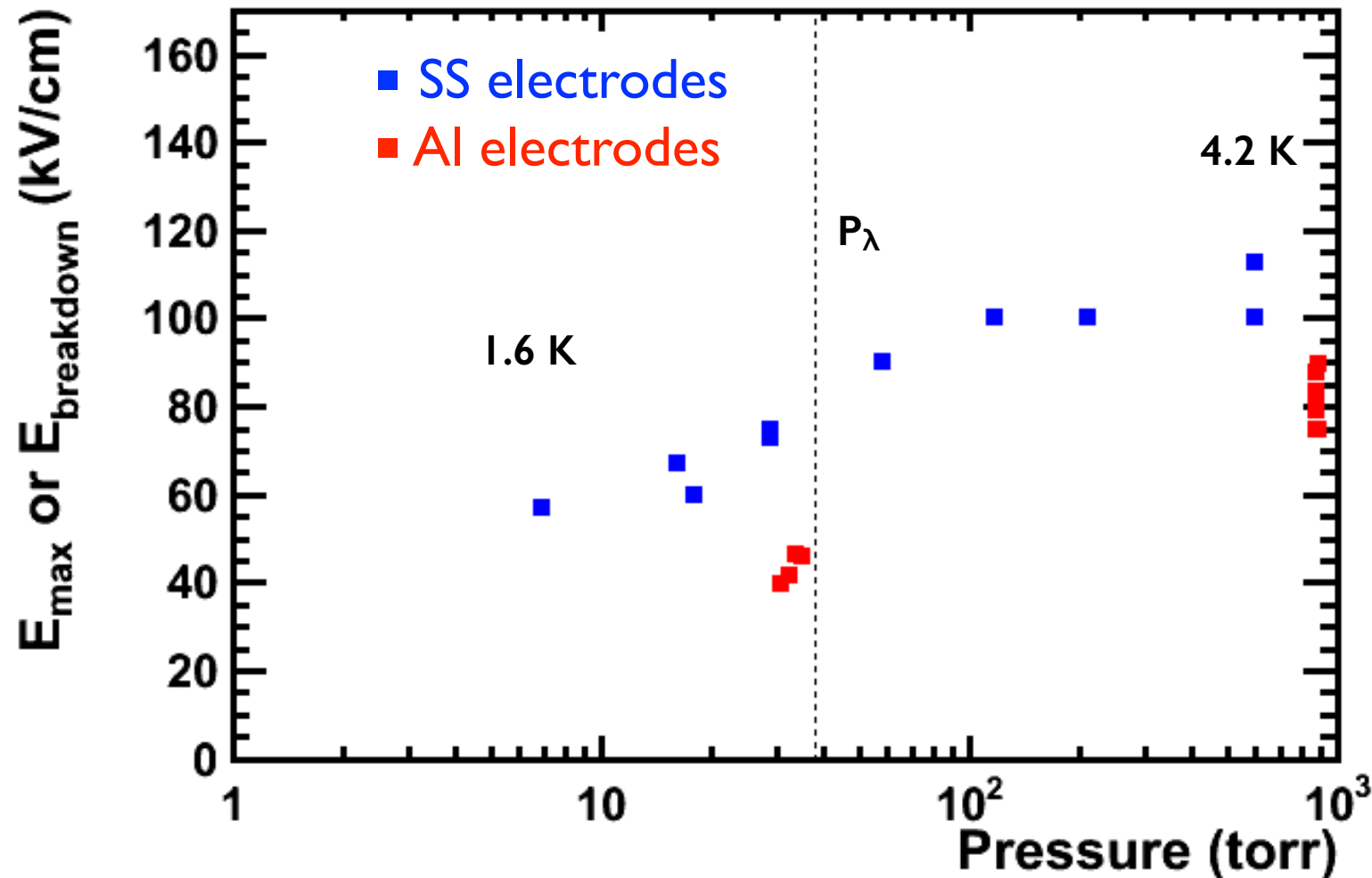
Large Scale HV Test Apparatus

- Need for potentials > 600 kV (75 kV/cm across 7.5 cm plus 2.5 cm cell walls)
- Capacitance multiplier: variable capacitor, potential increases as the spacing
- Demonstrated voltage amplification (~ 600 kV at 4.2 K).



Breakdown field vs pressure?

Old results from the Large Scale Apparatus

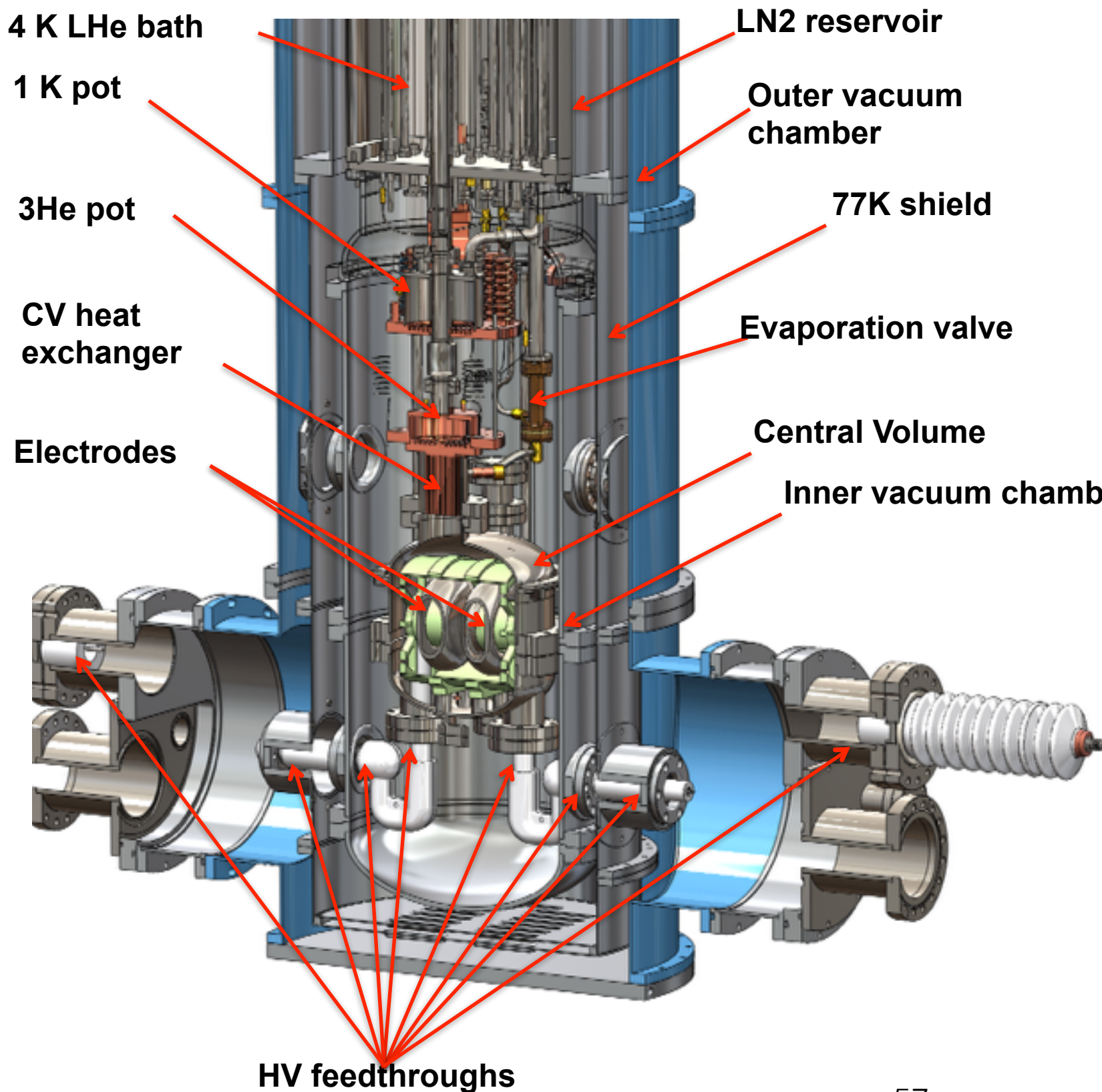


- Electrode size \sim 50 cm in diameter
- Gap \sim 3-4 mm
- Data taken at SVP
- LHe evaporatively cooled

Note: the field strength plotted is simply V/d . The actual highest field in the system is higher because the electrode shape was simply a flat plate with a rounded edge.

Based on our observation made later in other systems, it is possible that the observed pressure dependence was due to bubbles formed on the electrode surface due to heat flowing into the electrodes because of insufficient thermal anchoring.

MSHV system



Features

- 6 liter LHe volume is cooled by a 3He fridge
- Electrodes' size: ~ 12 cm in diameter
- Electric field: up to 75 kV/cm in 2 cm gap
- Lowest temperature: < 0.5 K
- Pressure: variable between SVP and 1 atm
- Turn around time: 2 weeks

MSHV system



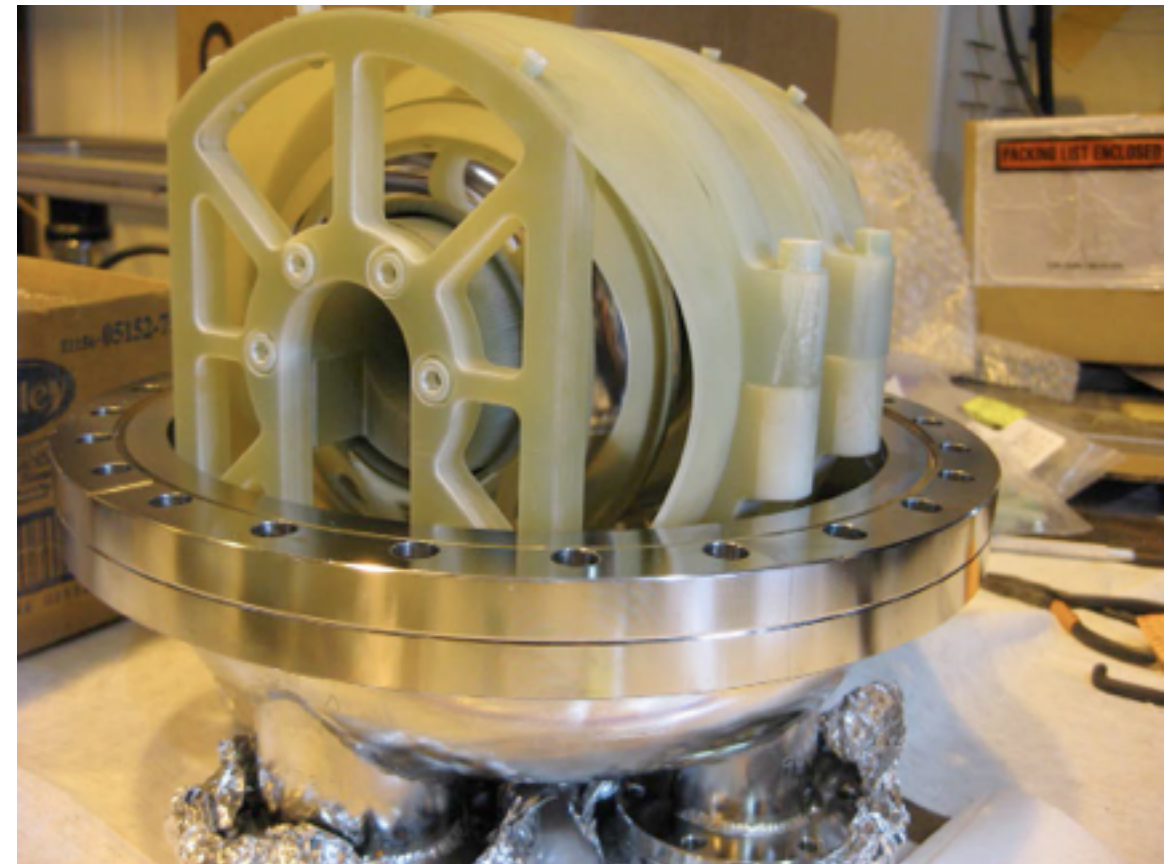
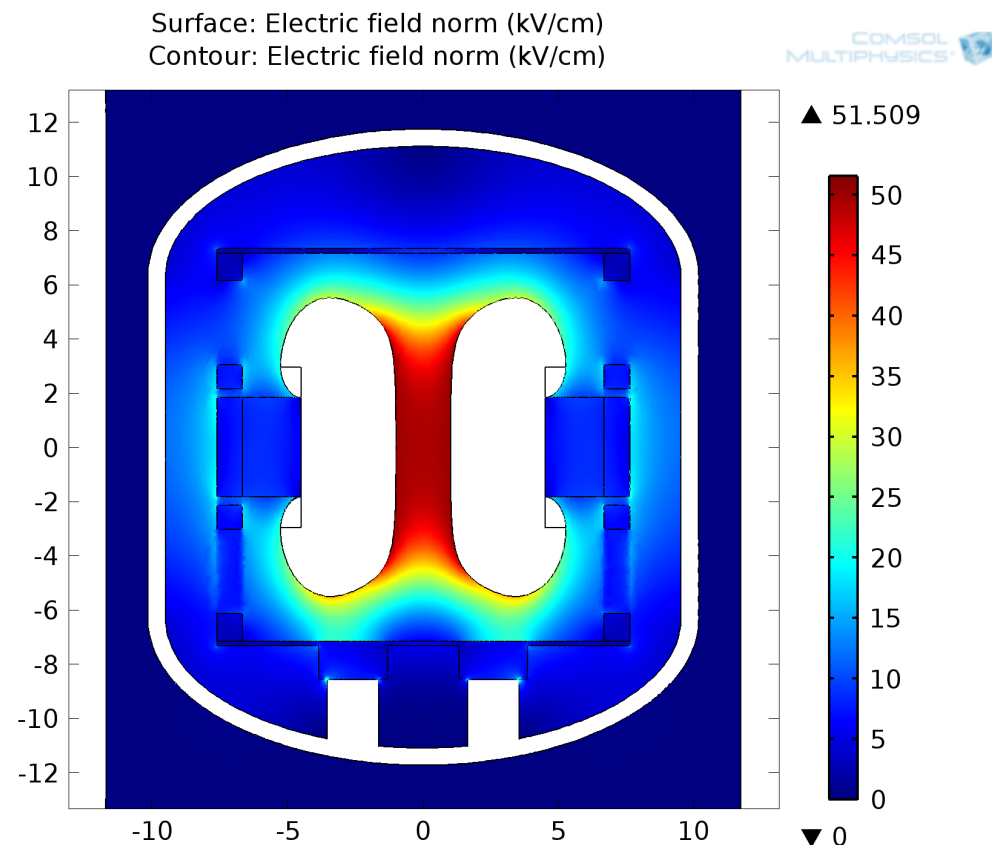
MSHV electrodes fabricated/tested

#	Shape	Material	Results
1	Rogowski	Electropolished SS	E_{BD} wide range of pressures
2	Groove to accept an insulator ring	Electropolished SS	E_{BD} wide range of pressures Leakage current < 5 pA at 40 kV
3	Rogowski	PMMA with copper implantation	E_{BD} wide range of pressures
4	Rogowski	PMMA with carbon paint	Not yet tested
5	Recess to accept a closed PMMA cell	Electropolished SS	Being fabricated
6	Recess to accept a closed PMMA cell	PMMA with copper implantation	Being fabricated

* Achievable electric field was limited by the HV feed line.

Rogowski electrodes

- For the initial test, we used electrodes that have the so-called Rogowski profile.
- The field in the gap is uniform and is the highest in the system.
- Allow us to sample a large area of the electrode surface. Note: breakdown is a random process: ball-plane and ball-ball geometries only sample a very limited surface area.
- For the first test, we used electropolished SS.



Effect of dielectric insulator inserted between electrodes

Field in the gap between the electrode and the insulator

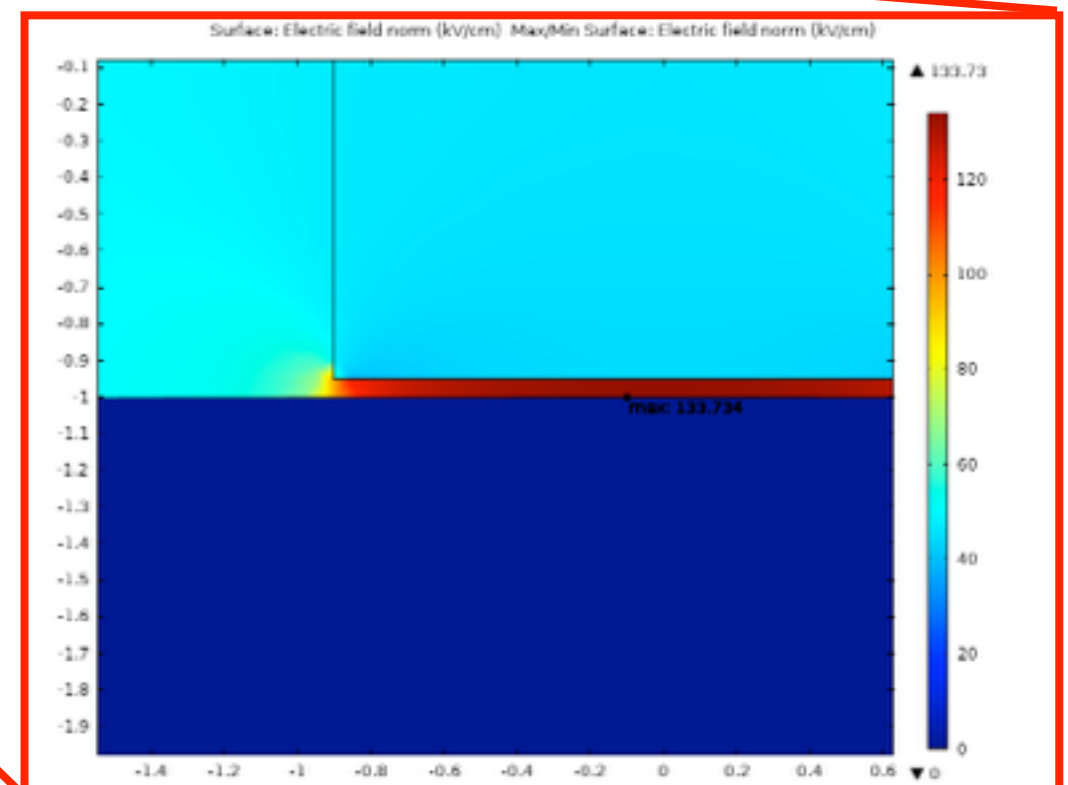
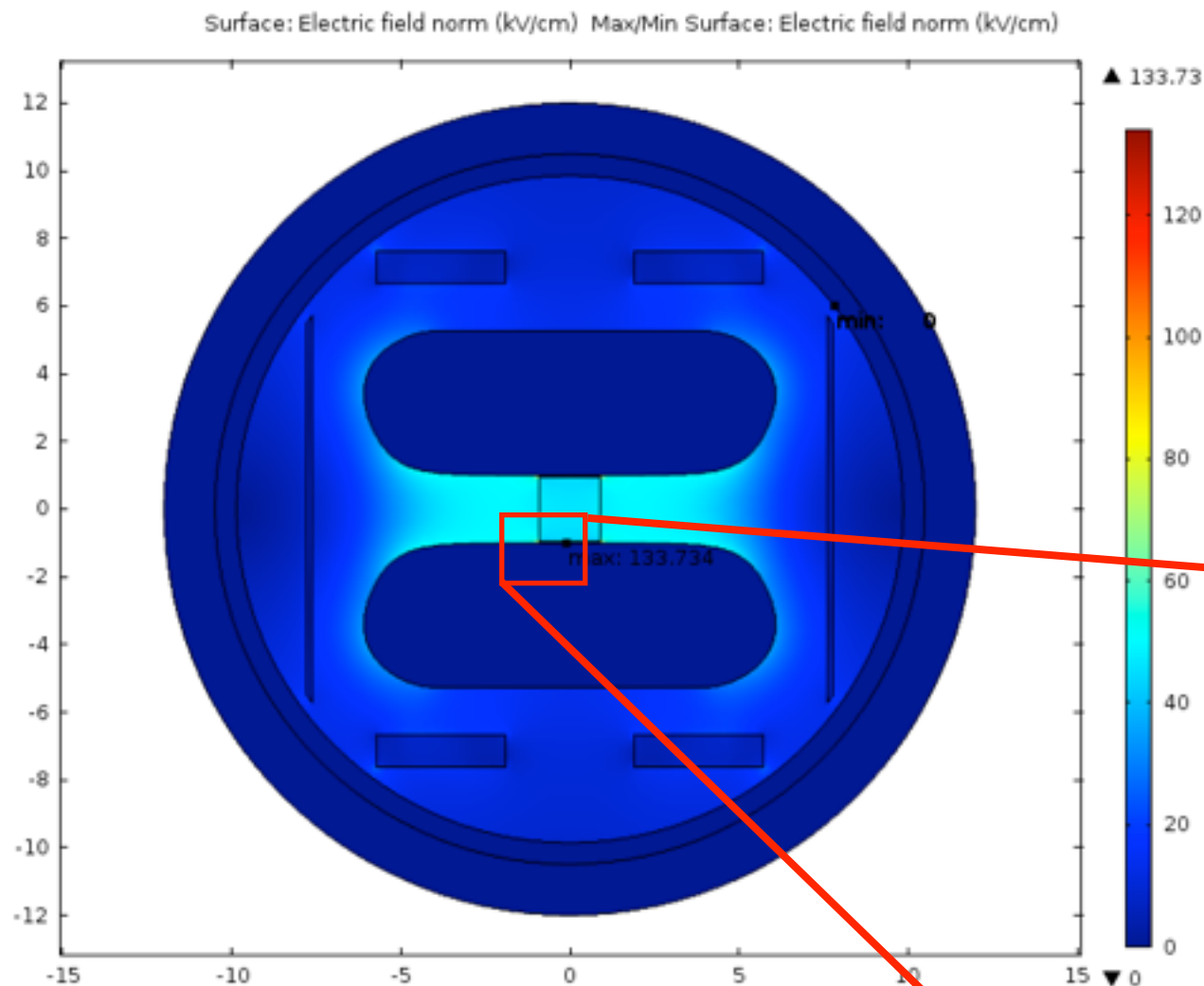
$$E_{gap} = \frac{V}{d + \frac{D-d}{\epsilon_r}} \rightarrow \frac{V}{D} \epsilon_r \quad (\text{when } d \ll D)$$

V : voltage between the electrodes

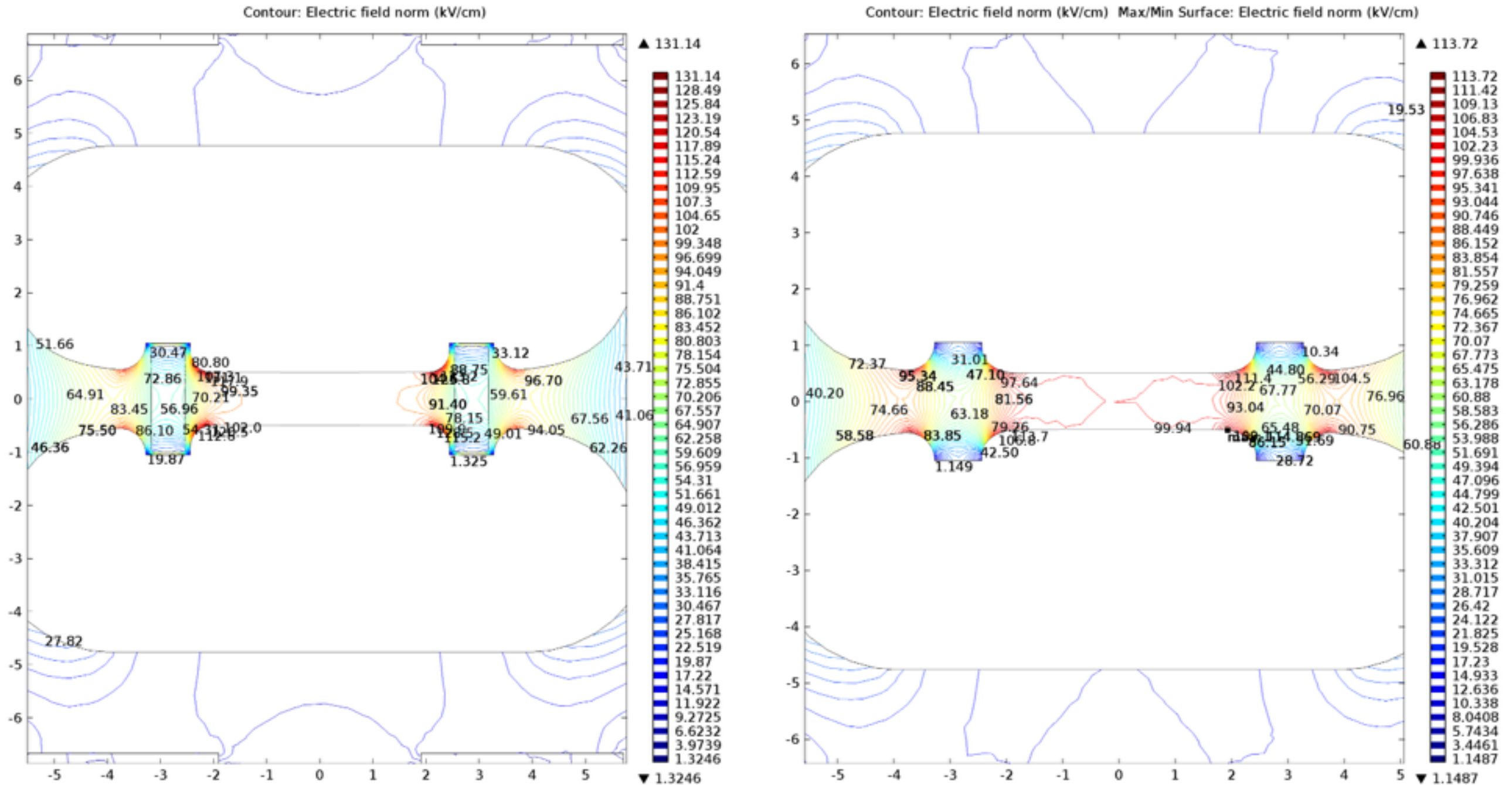
D : gap between the electrodes

d : gap between the insulator and the electrode

ϵ_r : ratio of the dielectric constant $\epsilon_r = \epsilon_{ins}/\epsilon_{He}$

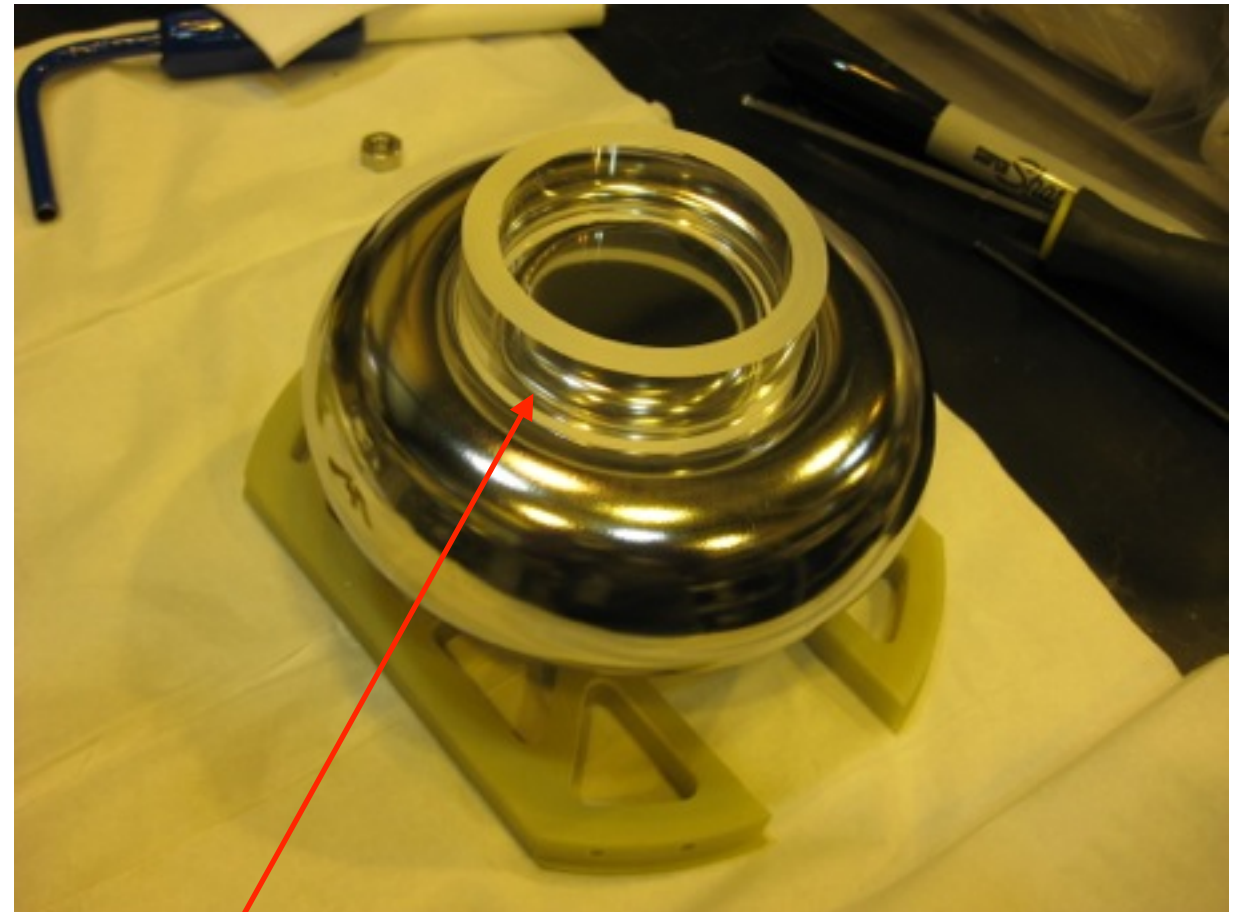


Grooved electrodes



The shape of the groove is designed so that the highest field is 10% or less higher than the uniform field, with and without the PMMA insert, including the region close to where the PMMA insert meets the electrodes.

Grooved electrodes



PMMA cylinder “mockup cell”

PMMA electrodes



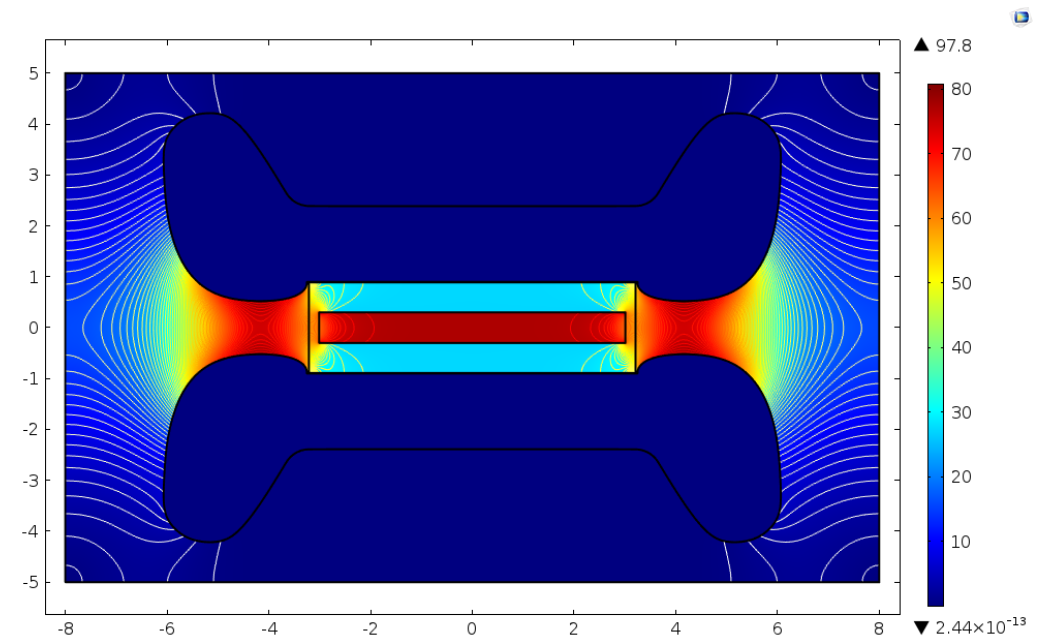
PMMA electrode with carbon paint (made at UT in collaboration with ORNL)



PMMA electrode with copper ion implantation (made by SWRI in collaboration with ORNL)

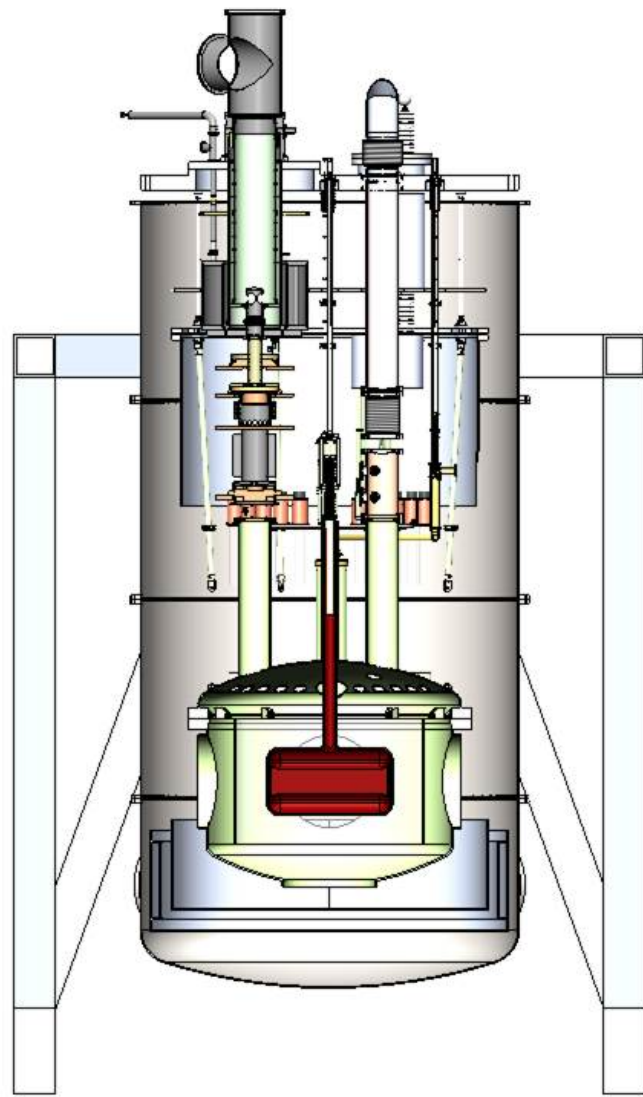
Next steps (I)

We will study the electric breakdown with a closed cell made of dielectric insulator, sandwiched between the electrodes. The electrode shape was optimized to minimize the field strength at “hot spots” at the electrode insulator interface. PMMA will be used as the insulator.

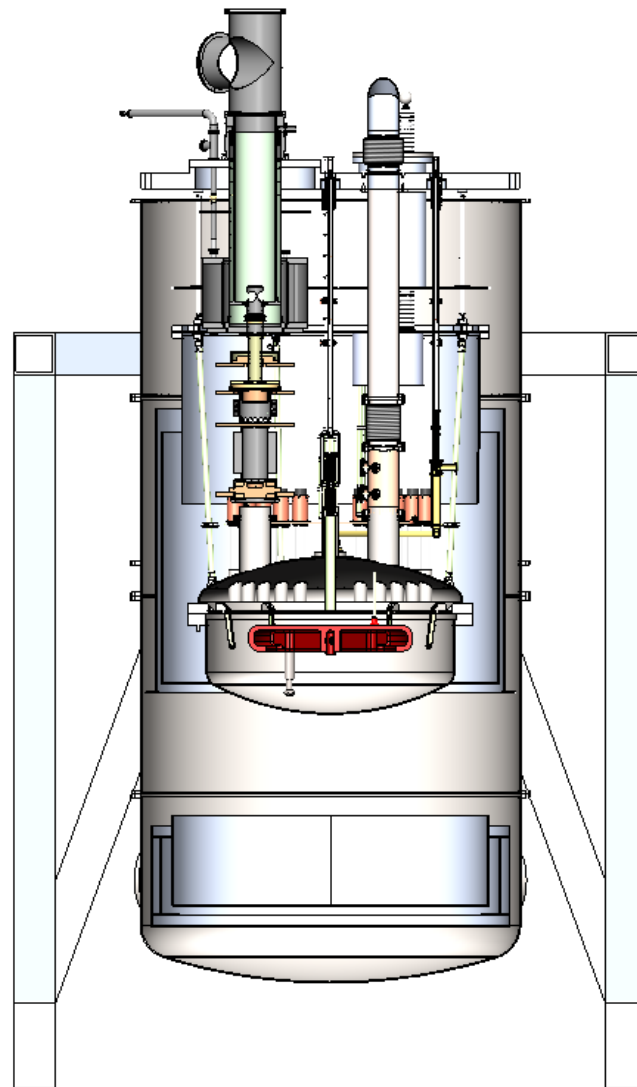


Results of an FEM electrostatic calculation optimizing the shape of the electrode with a closed cell made of dielectric insulator in between.

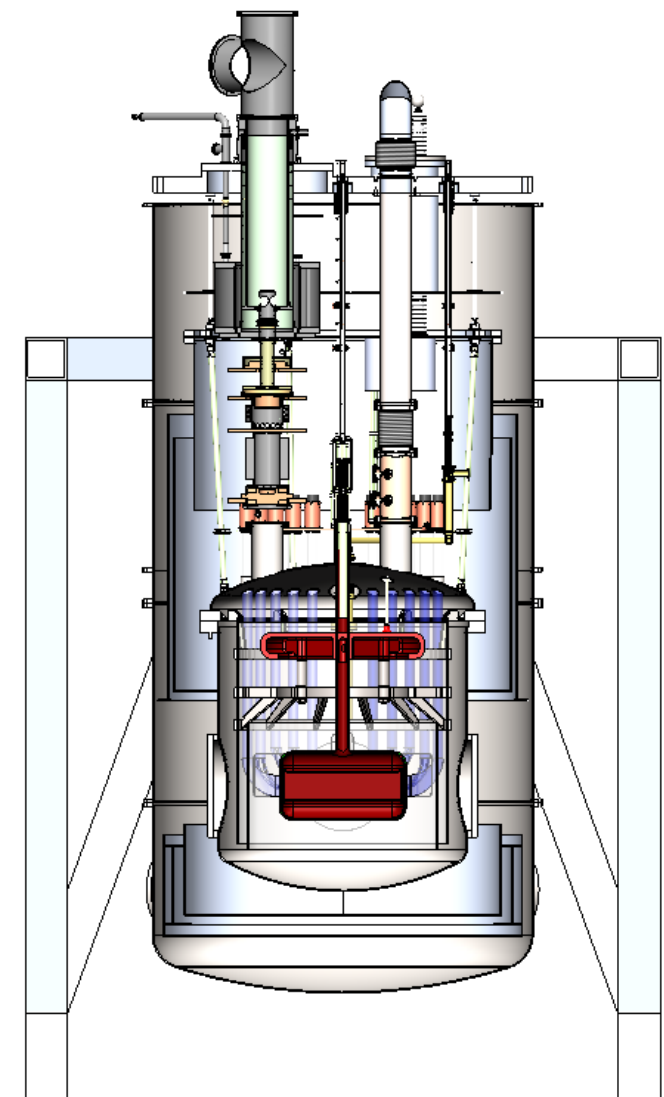
Next steps (II)



Truncated CV
+
cell capacitor



Truncated CV
+
variable capacitor



Full system

Construction of a full size prototype

SNS nEDM experiment time line

- 2012-2013: Critical R&D
- 2014-2017: Critical component demonstration
- 2018-2020: Large scale integration
- 2021-: Assembly and commissioning/Data taking

Summary

- Cryogenic EDM experiments can provide a significant increase in sensitivity, increasing all of E , T , and N significantly.
- Although the realization of such an experiment has its share of challenges, significant progress is being made toward it.